APPENDIX 2. CATIONIC ROMP POLYMERS CONTAINING SUPRAMOLECULAR SELF-ASSOCIATING AMPHIPHILIC (SSA) MOLECULES AND THEIR ANTIMICROBIAL ACTIVITY.

1. NMR spectra

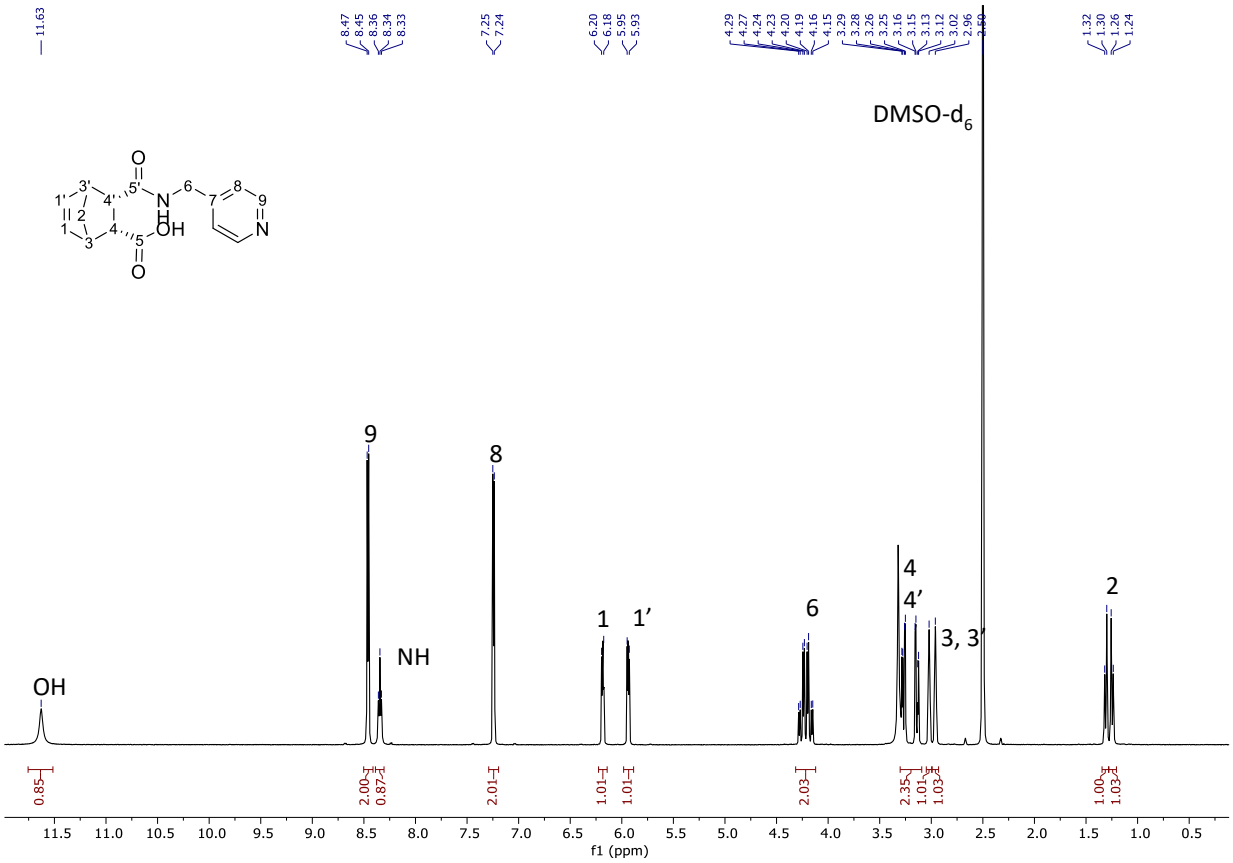

Fig. S1. ^{1}H NMR in dmso-d_6 of compound **3a**

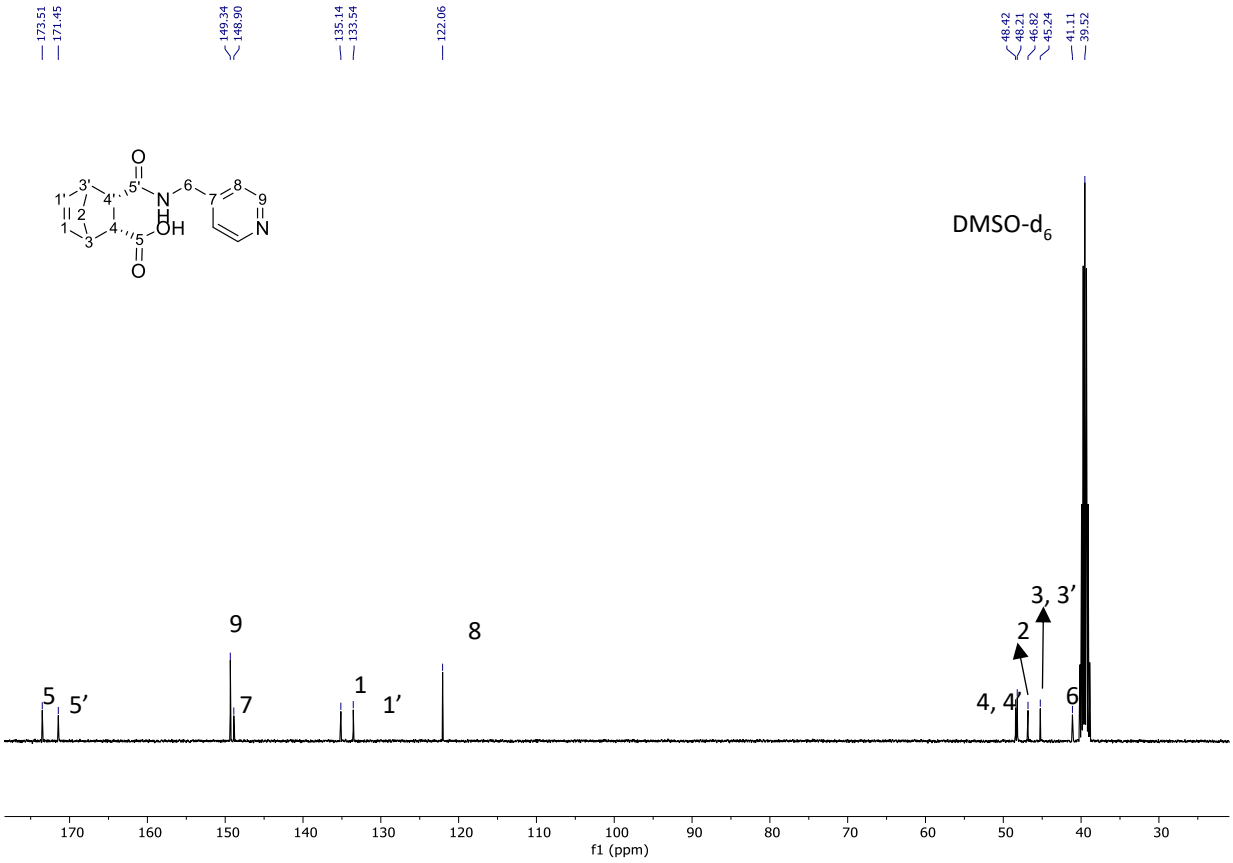

Fig. S2. ^{13}C NMR in dmso-d_6 of compound **3a**

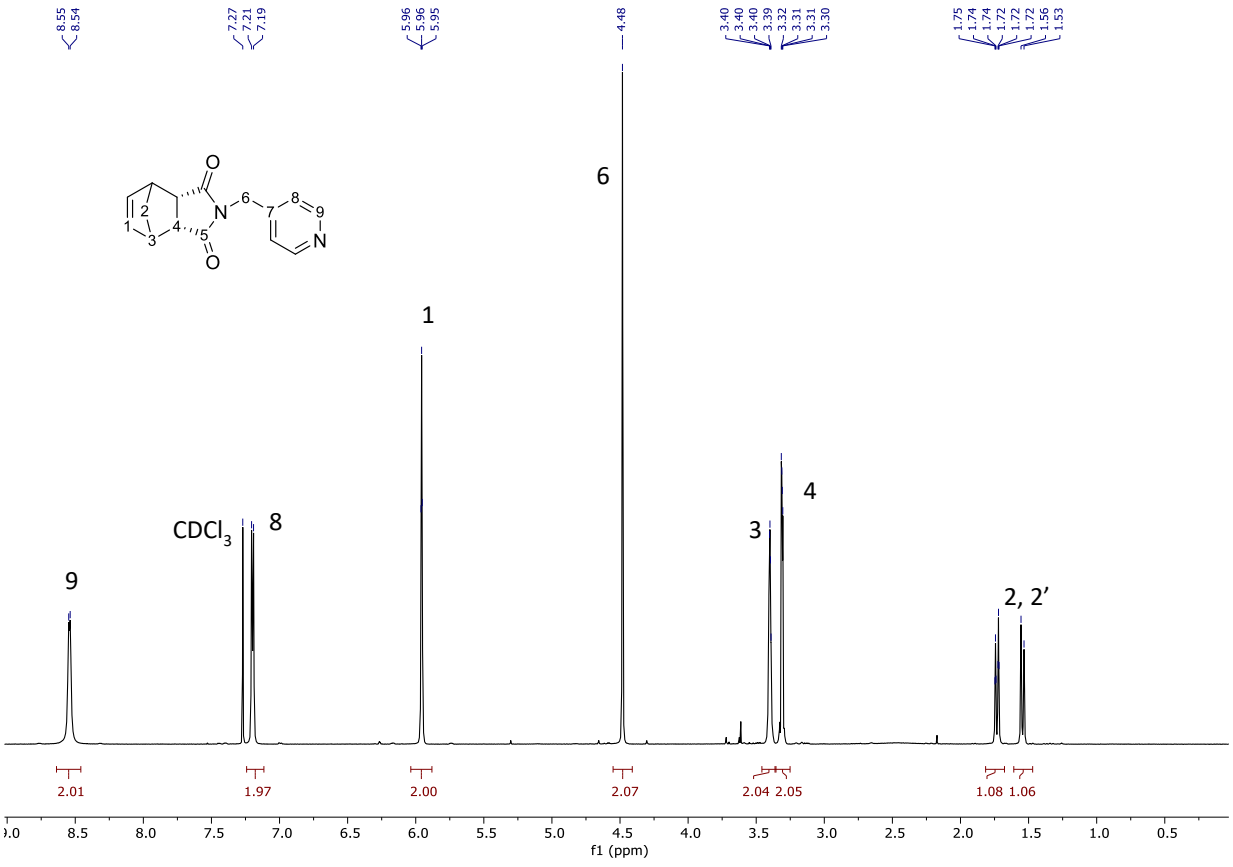

Fig. S3. ^{1}H NMR in $CDCl_3$ of compound **4a**

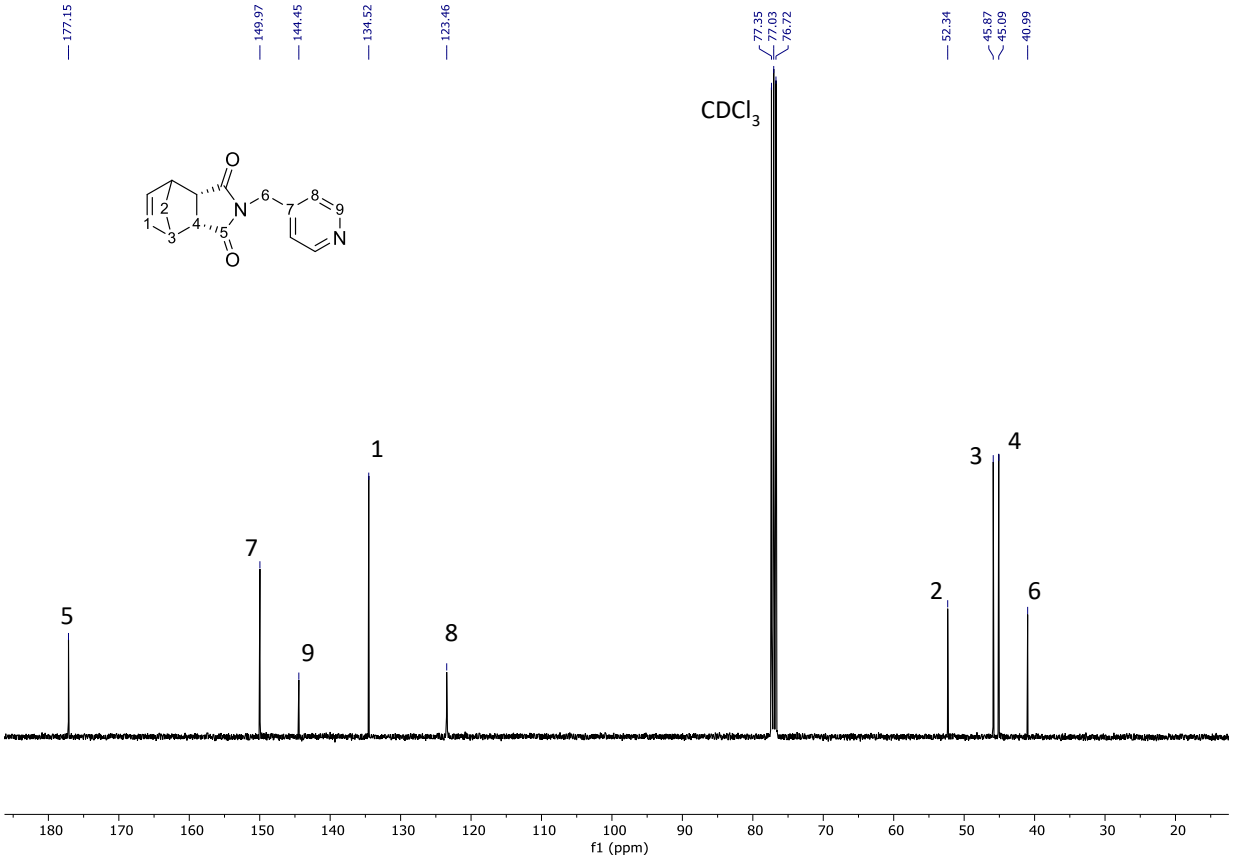

Fig. S4. ^{13}C NMR in $CDCl_3$ of compound **4a**

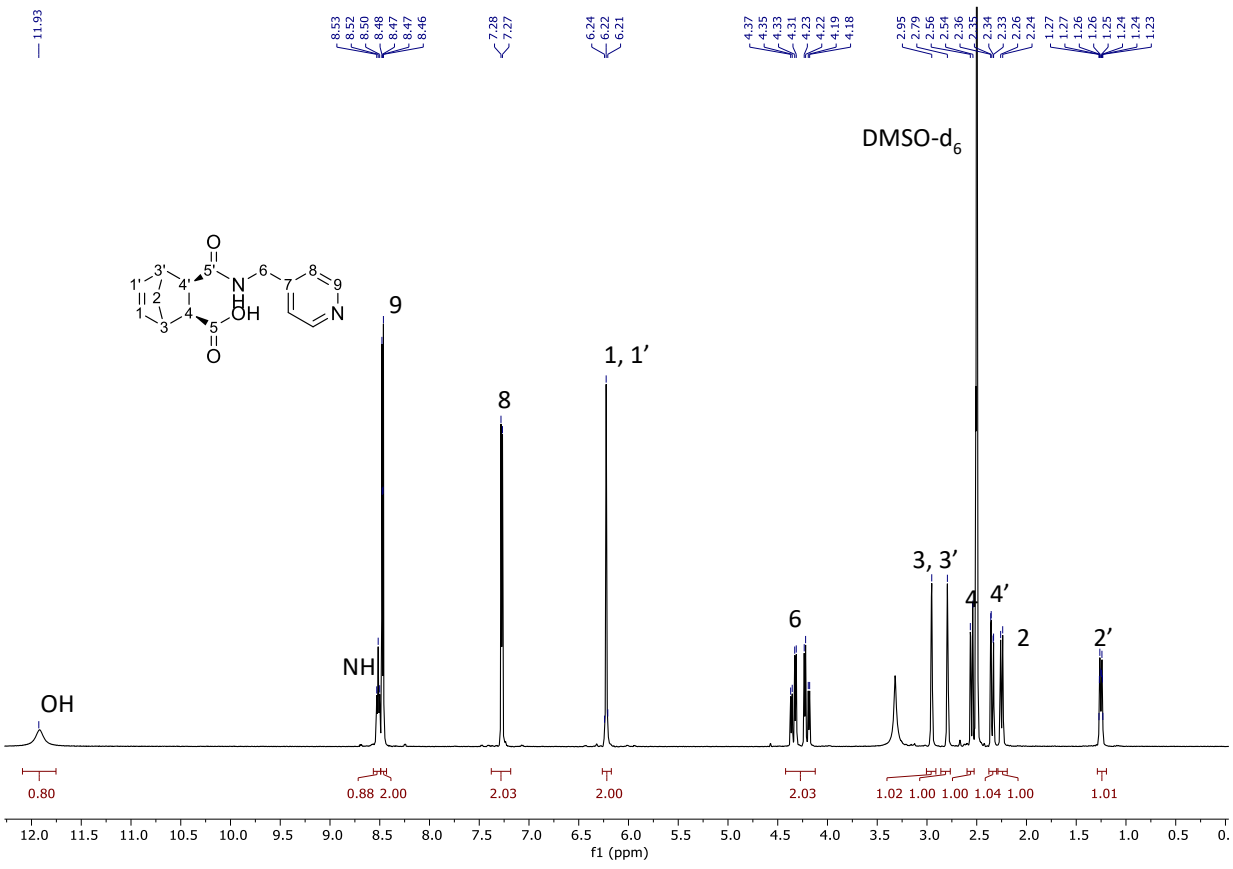

Fig. S5. ^{1}H NMR in dmso-d_6 of compound **3b**

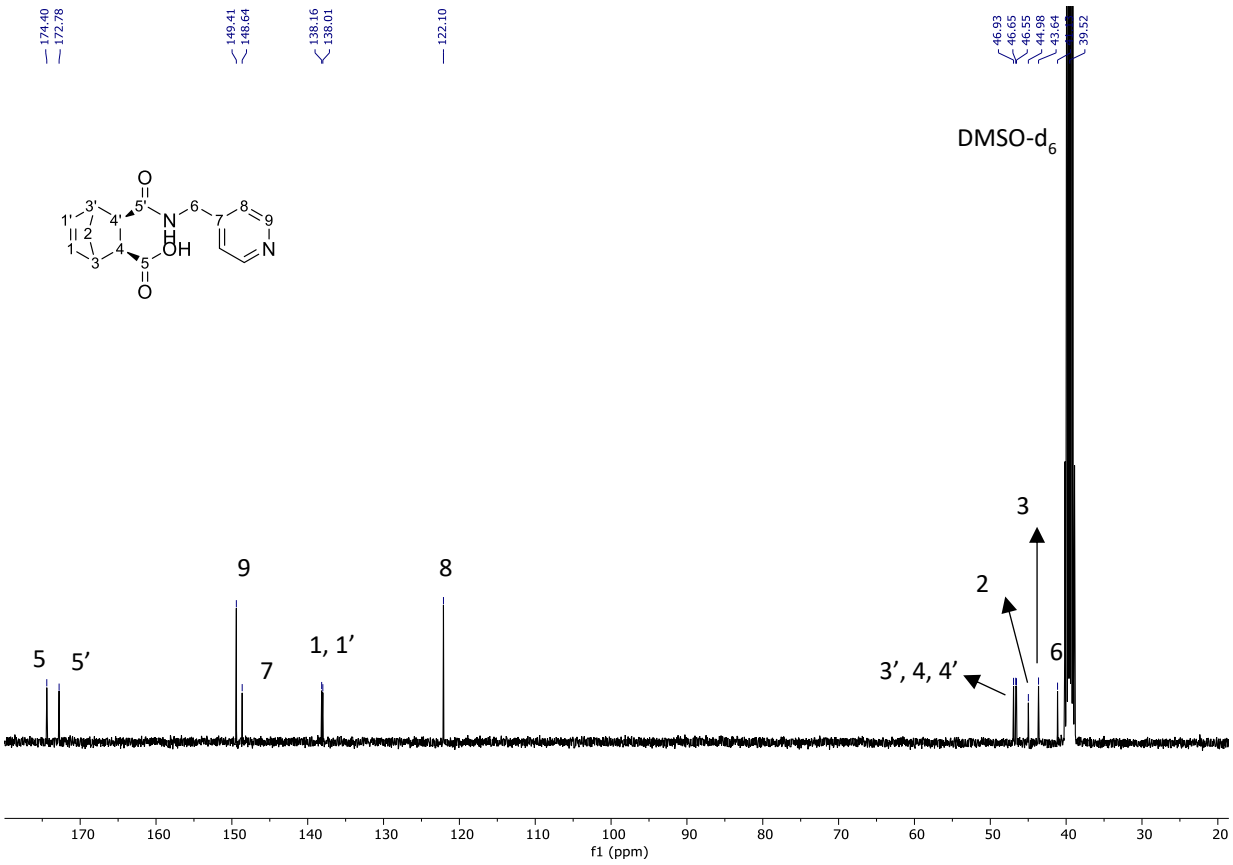

Fig. S6. ^{13}C NMR in dmso-d_6 of compound **3b**

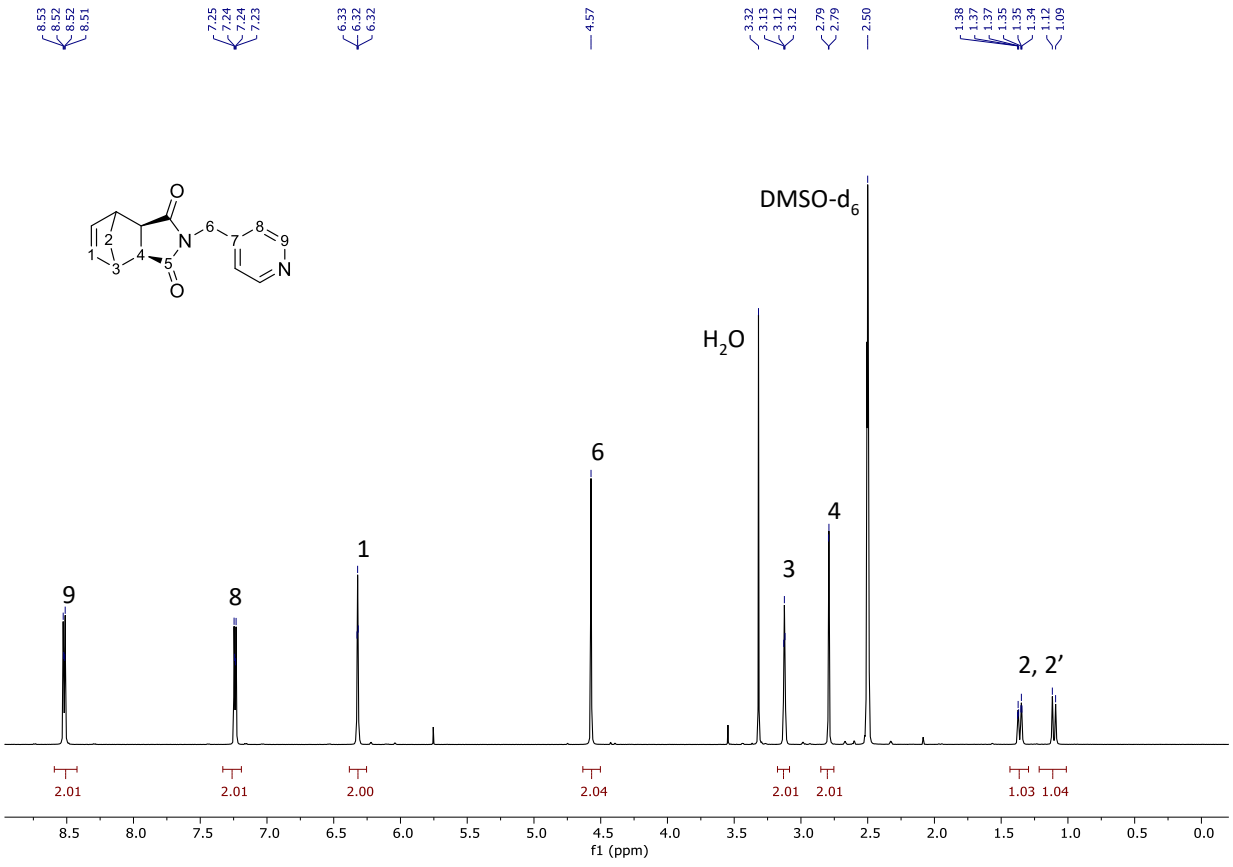

Fig. S7. ^{1}H NMR in dmso-d_6 of compound **4b**

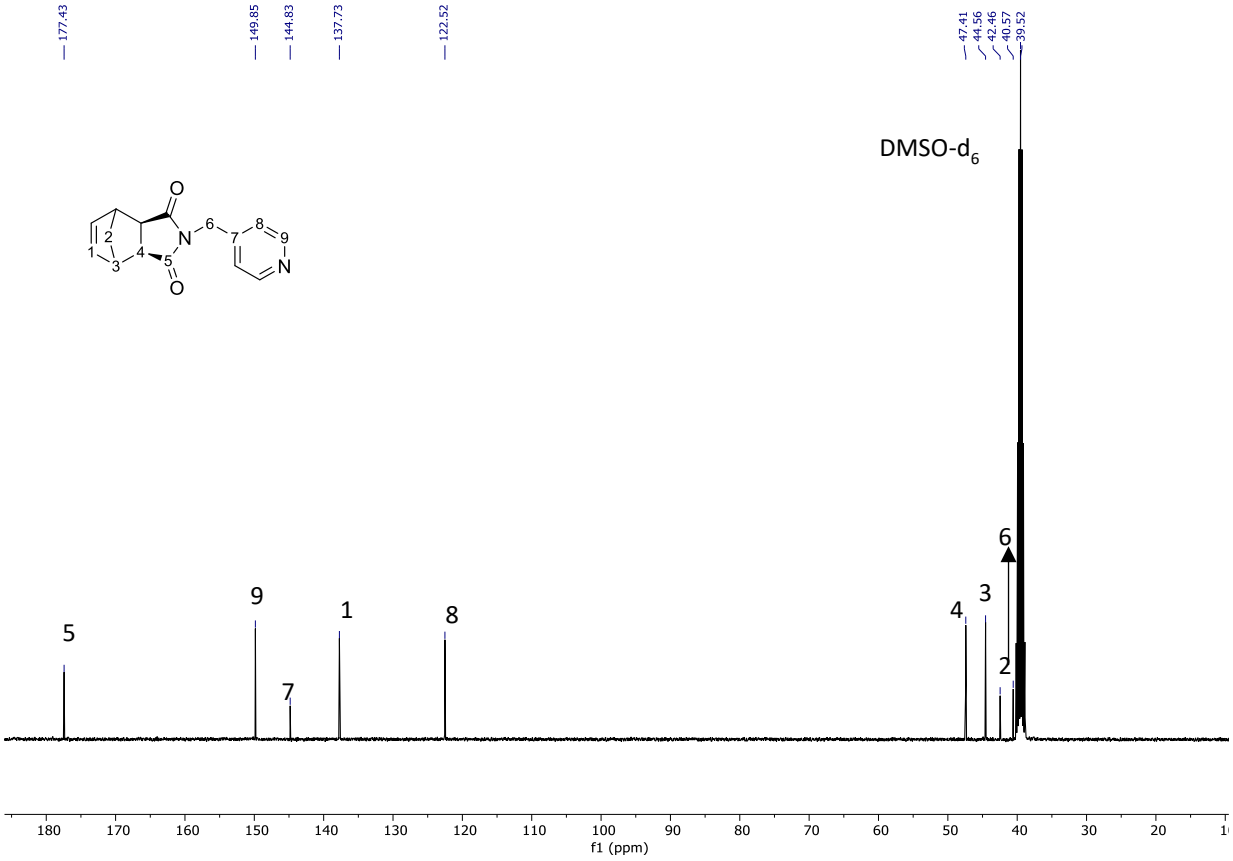

Fig. S8. ^{13}C NMR in dmso-d_6 of compound **4b**

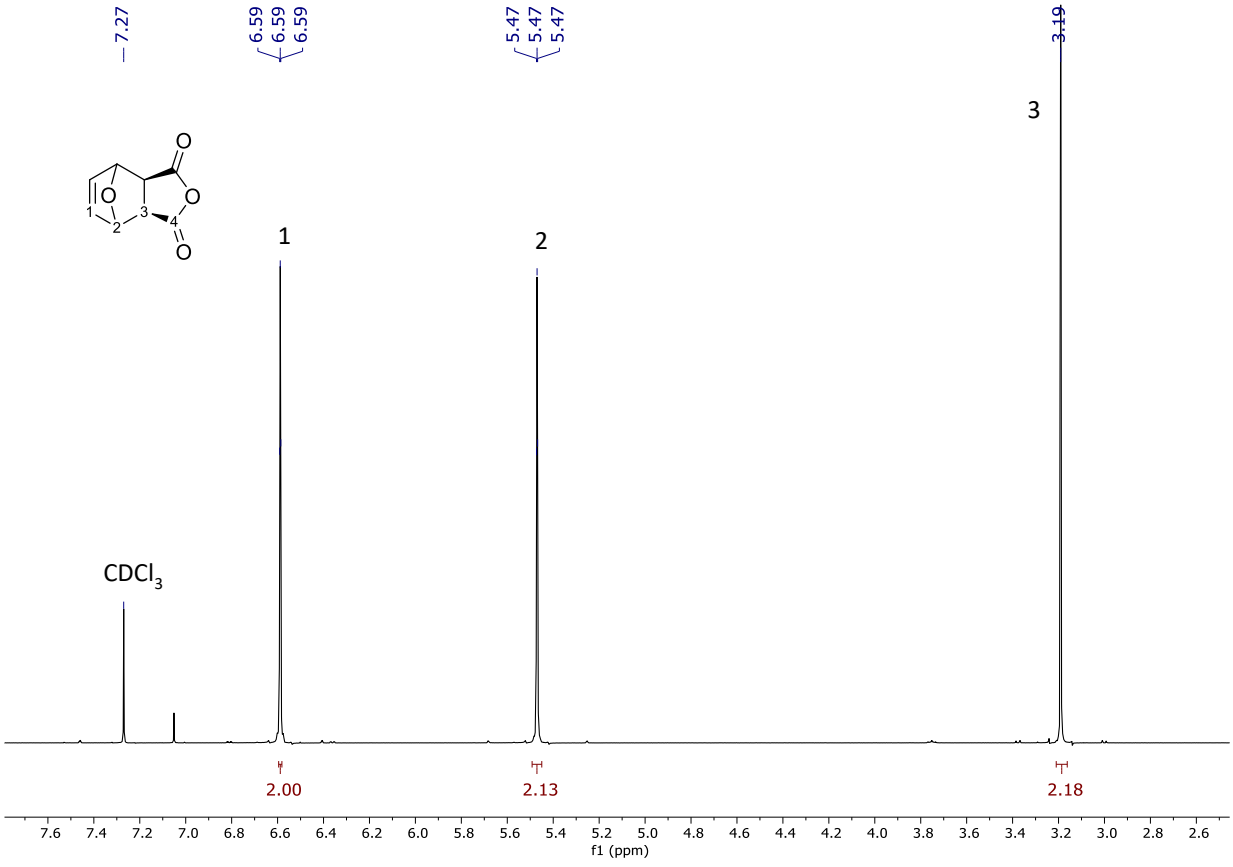

Fig. S9. ^{1}H NMR in $CDCl_3$ of exo-7-oxanorborn-5-ene-2,3-dicarboxylic anhydride, **7**

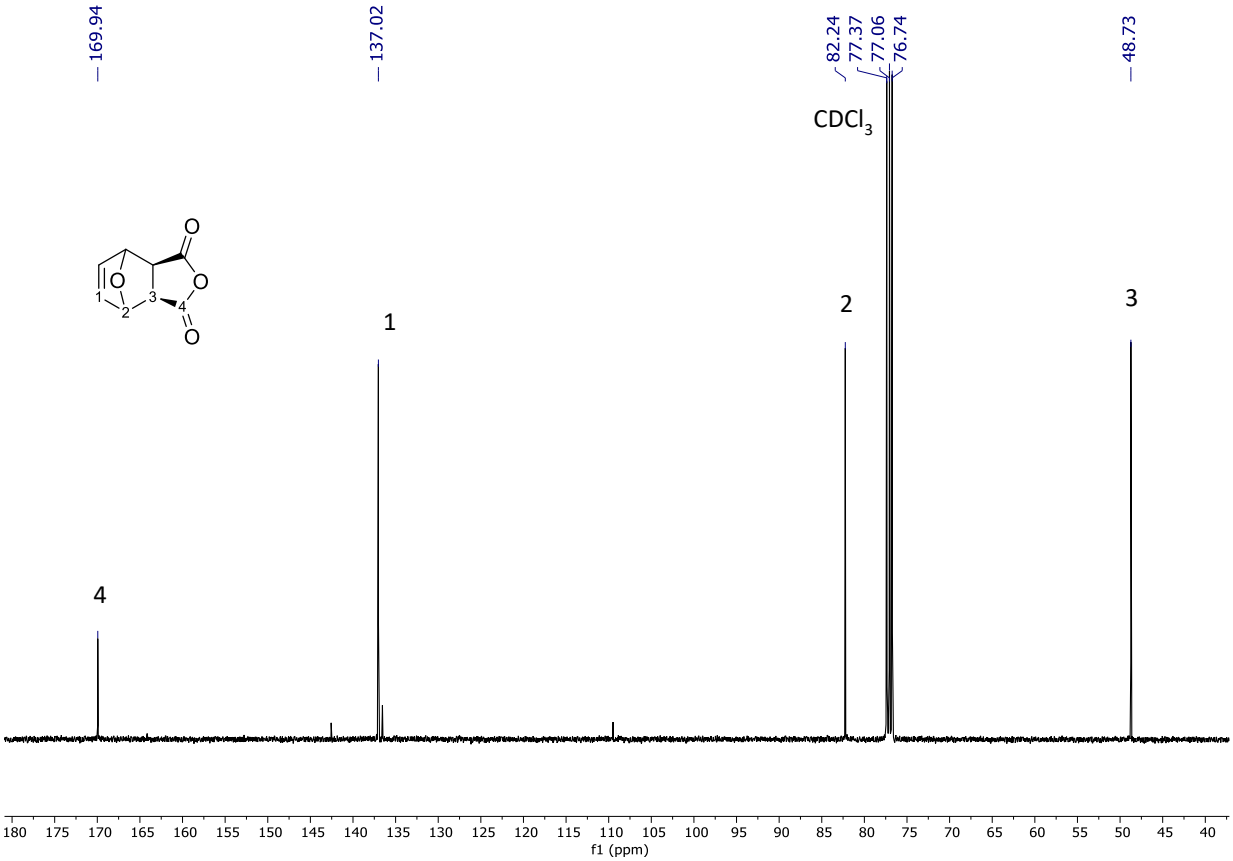

Fig. S10. ^{13}C NMR in $CDCl_3$ of exo-7-oxanorborn-5-ene-2,3-dicarboxylic anhydride, **7**

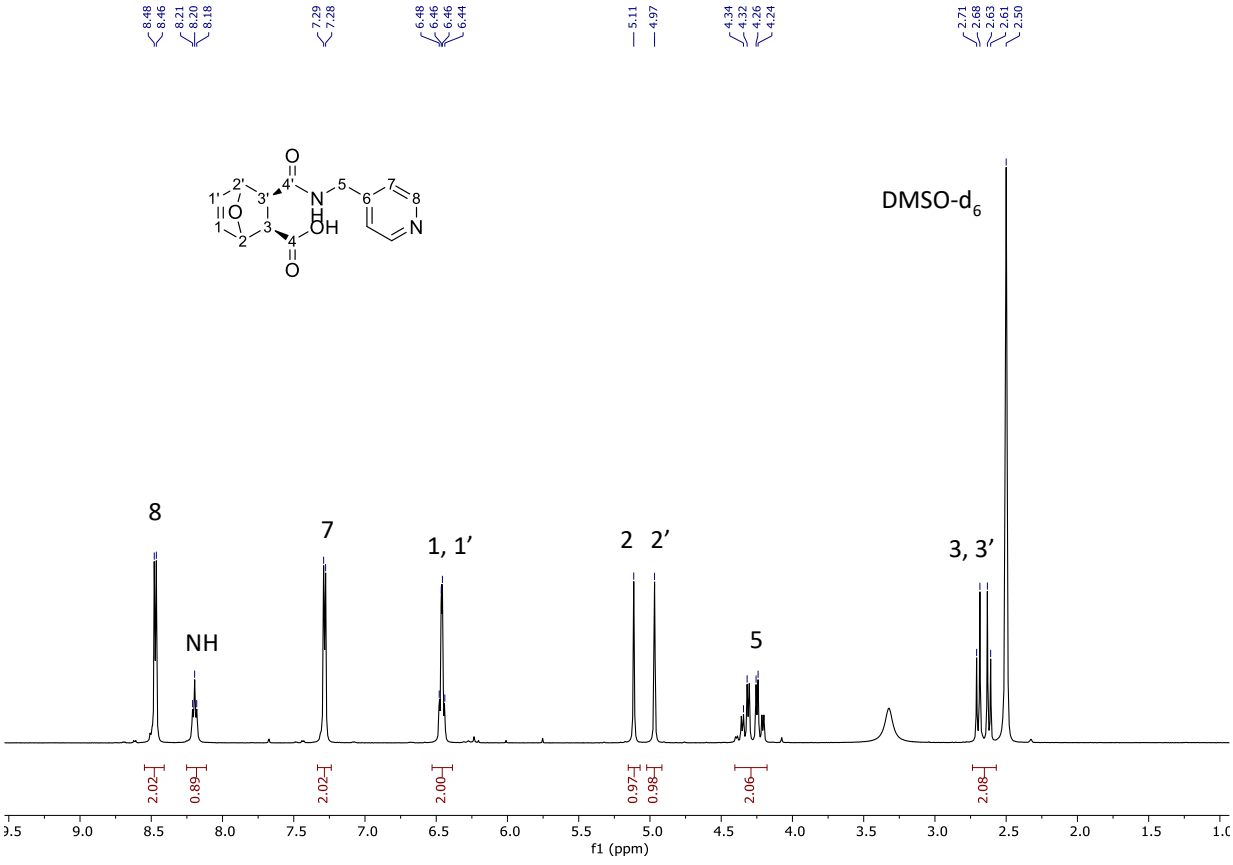

Fig. S11. ^{1}H NMR in dmso-d_6 of compound **8**

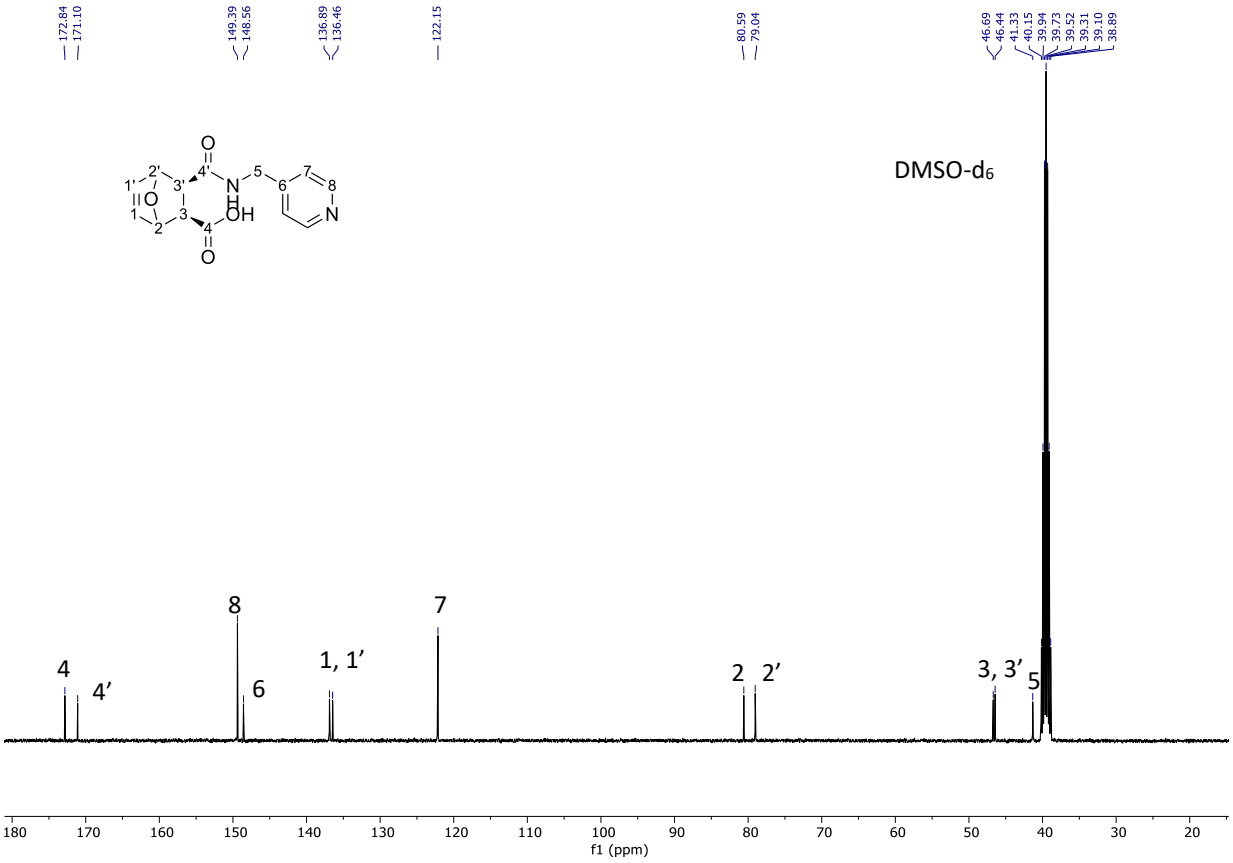

Fig. S12. ^{13}C NMR in dmso-d_6 of compound **8**

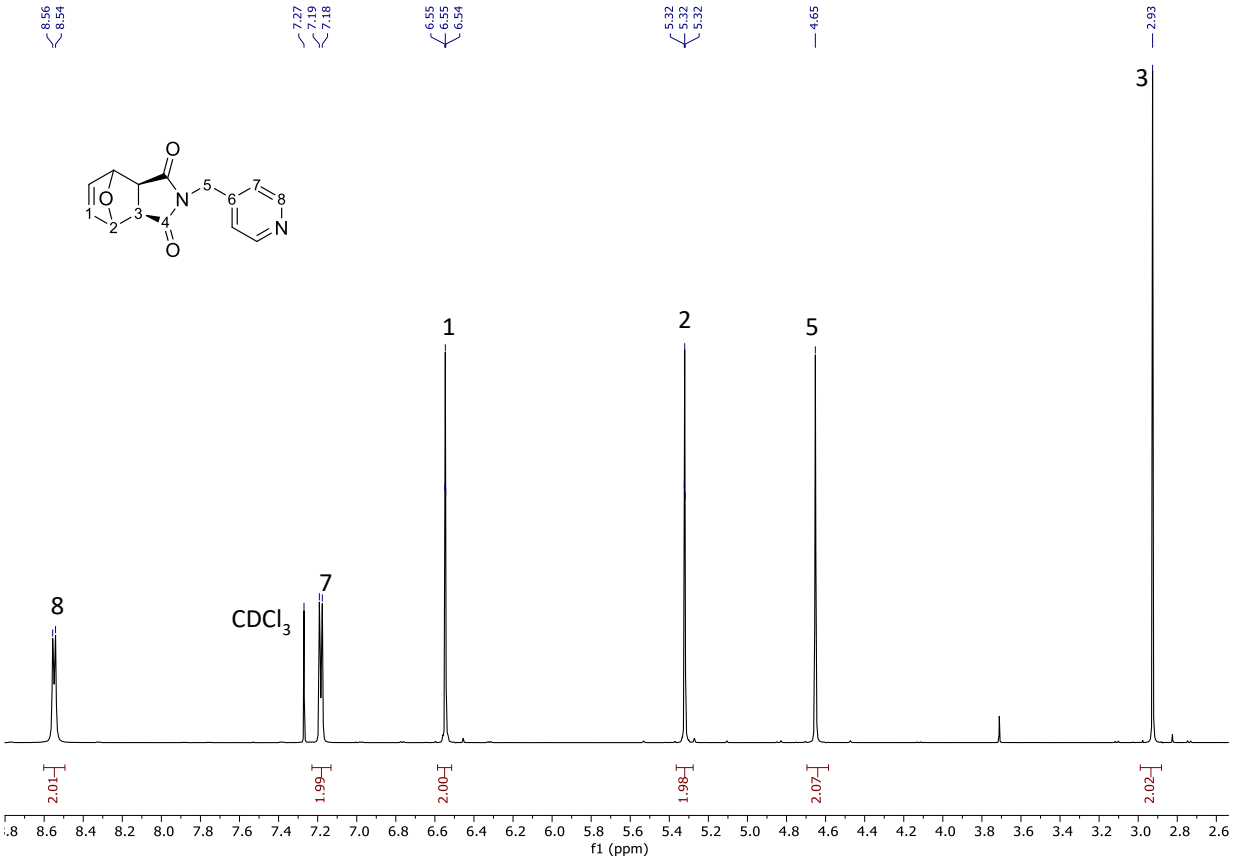

Fig. S13. ^{1}H NMR in $CDCl_3$ of compound **9**

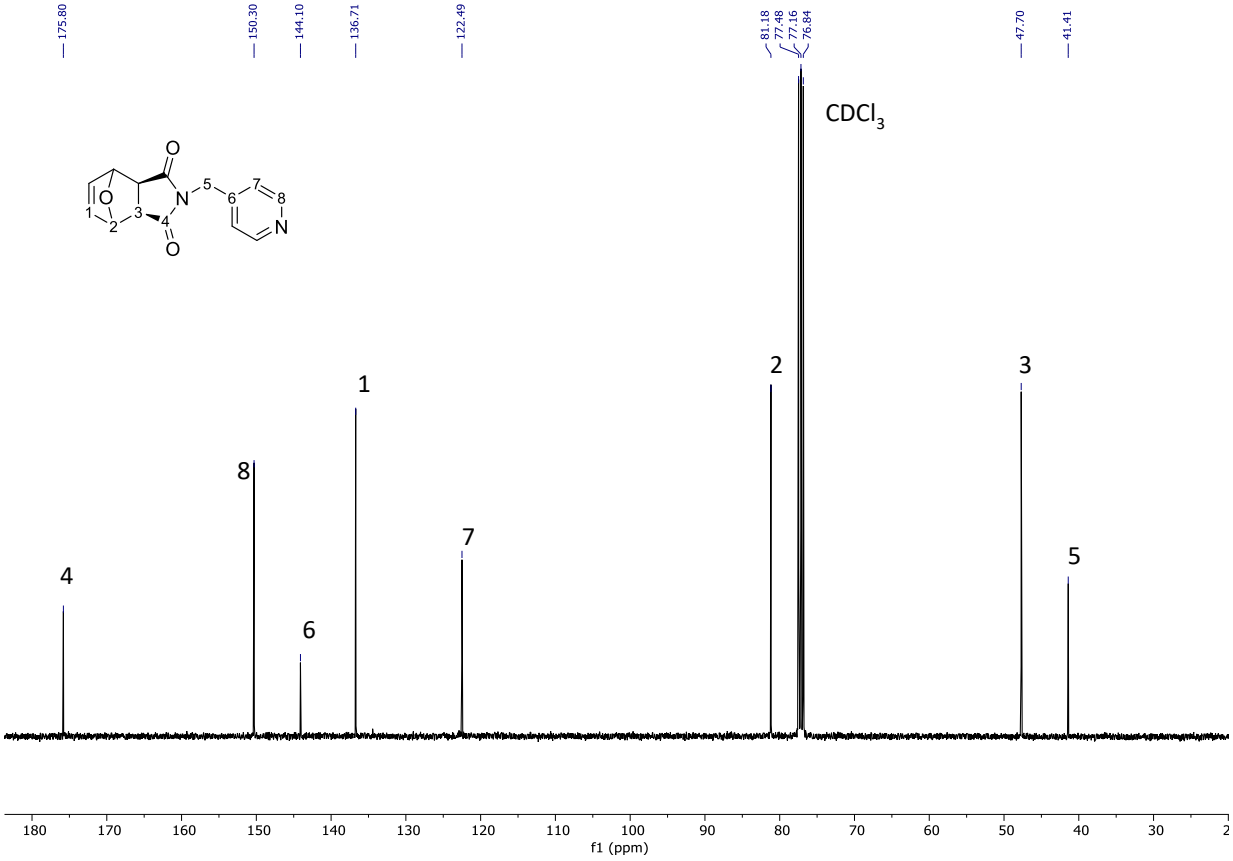

Fig. S14. ^{13}C NMR in $CDCl_3$ of compound **9**

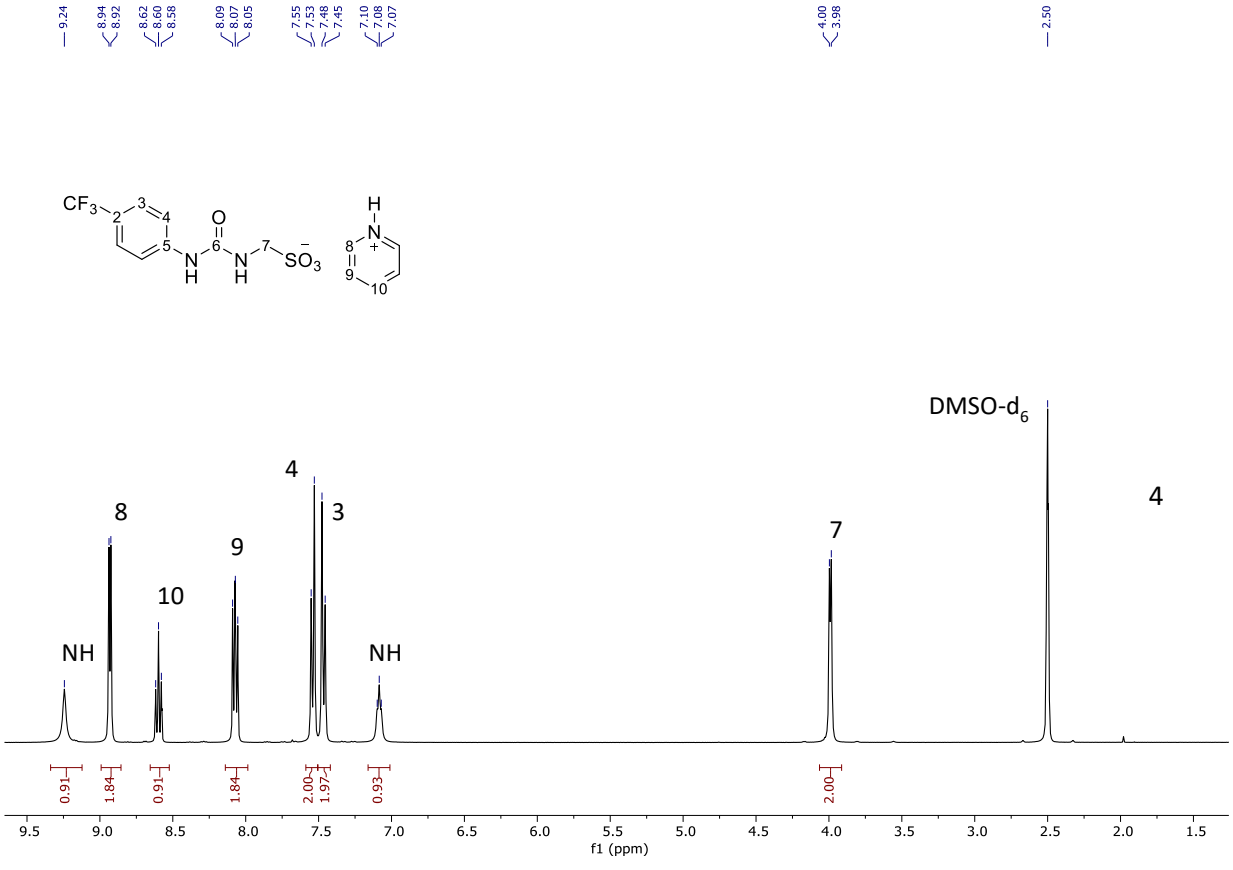

Fig. S15. ^{1}H NMR in dmso-d_6 of compound **10**, **SSA-1**

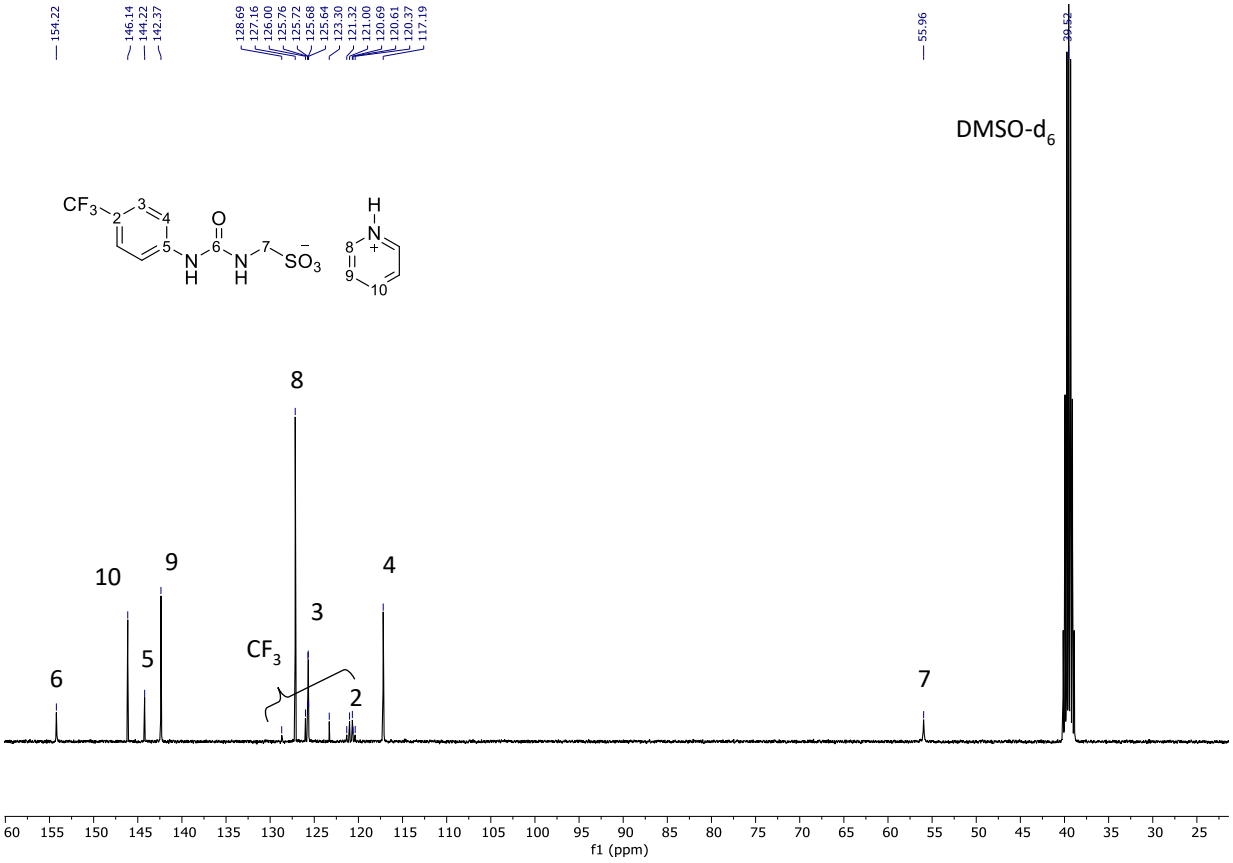

Fig. S16. ^{13}C NMR in dmso-d$_6$ of compound **10**, **SSA-1**

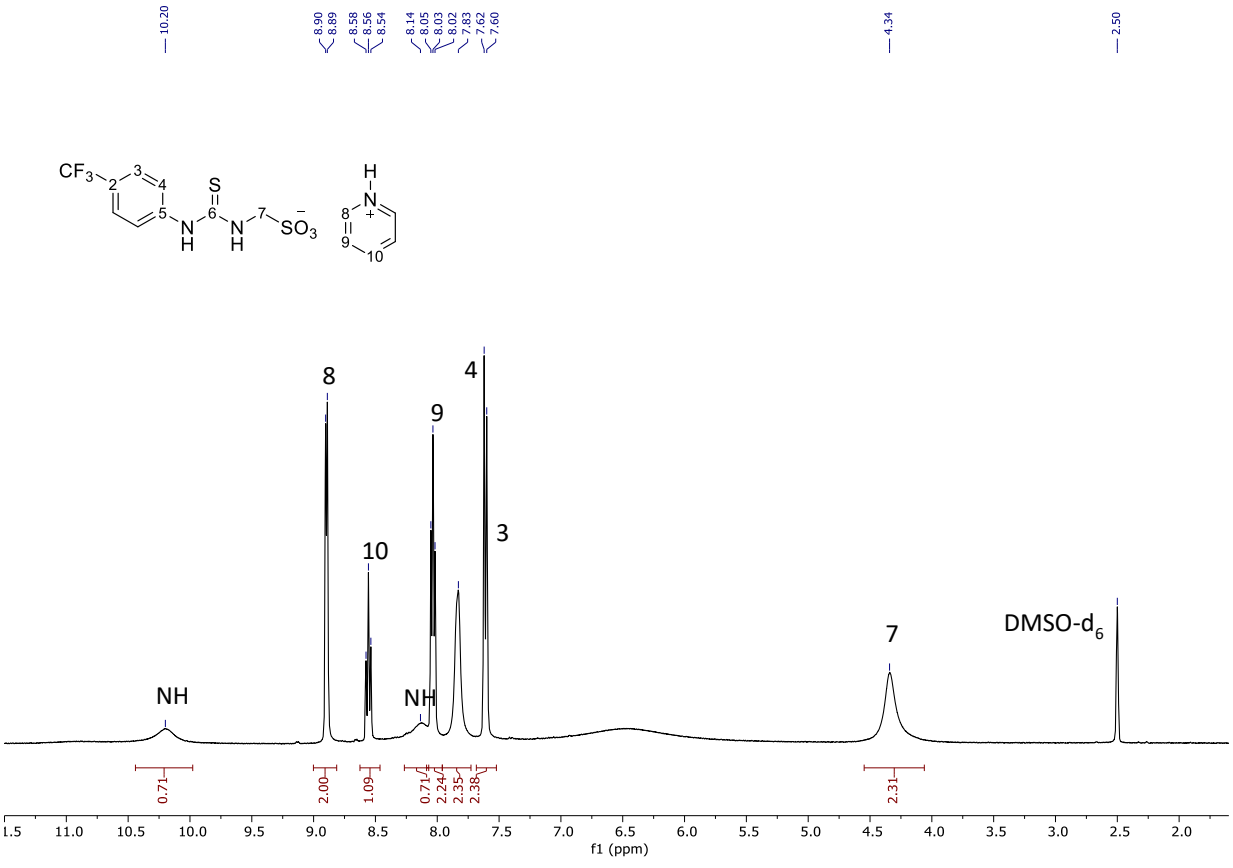

Fig. S17. ^{1}H NMR in dmso-d$_6$ at T = 333 K of compound **11**, **SSA-2**

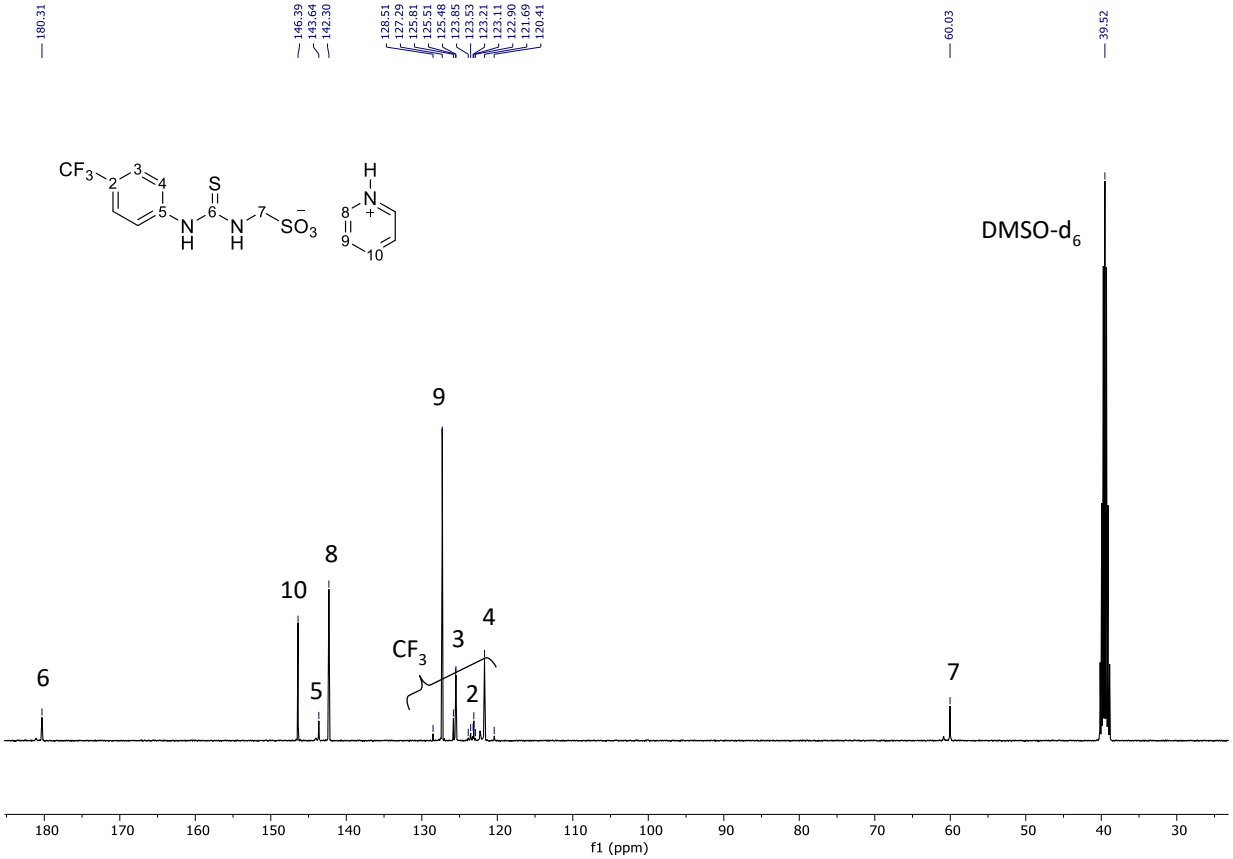

Fig. S18. ^{13}C NMR in dmso-d$_6$ of compound **11**, **SSA-2**

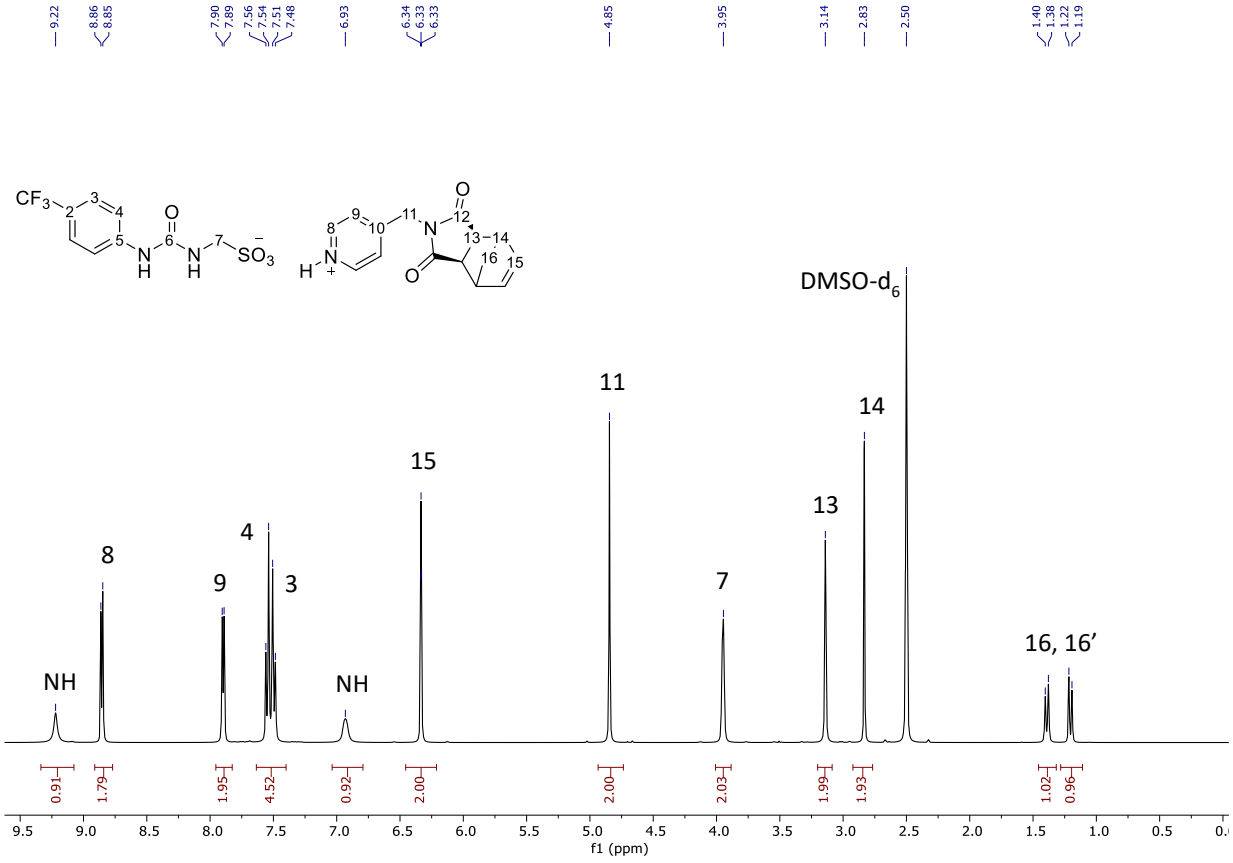

Fig. S19. ^{1}H NMR in dmso-d$_6$ of **mon1**

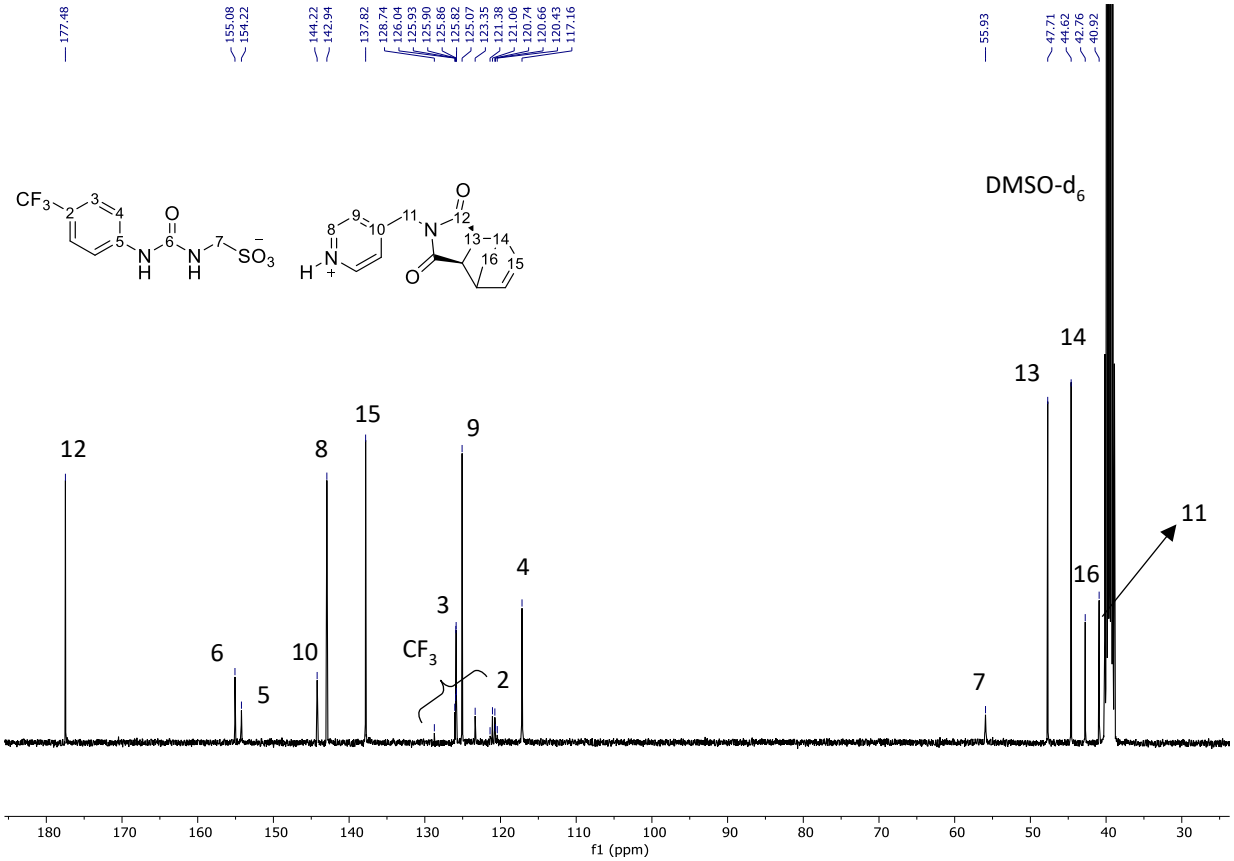

Fig. S20. ^{13}C NMR in dmso-d_6 of **mon1**

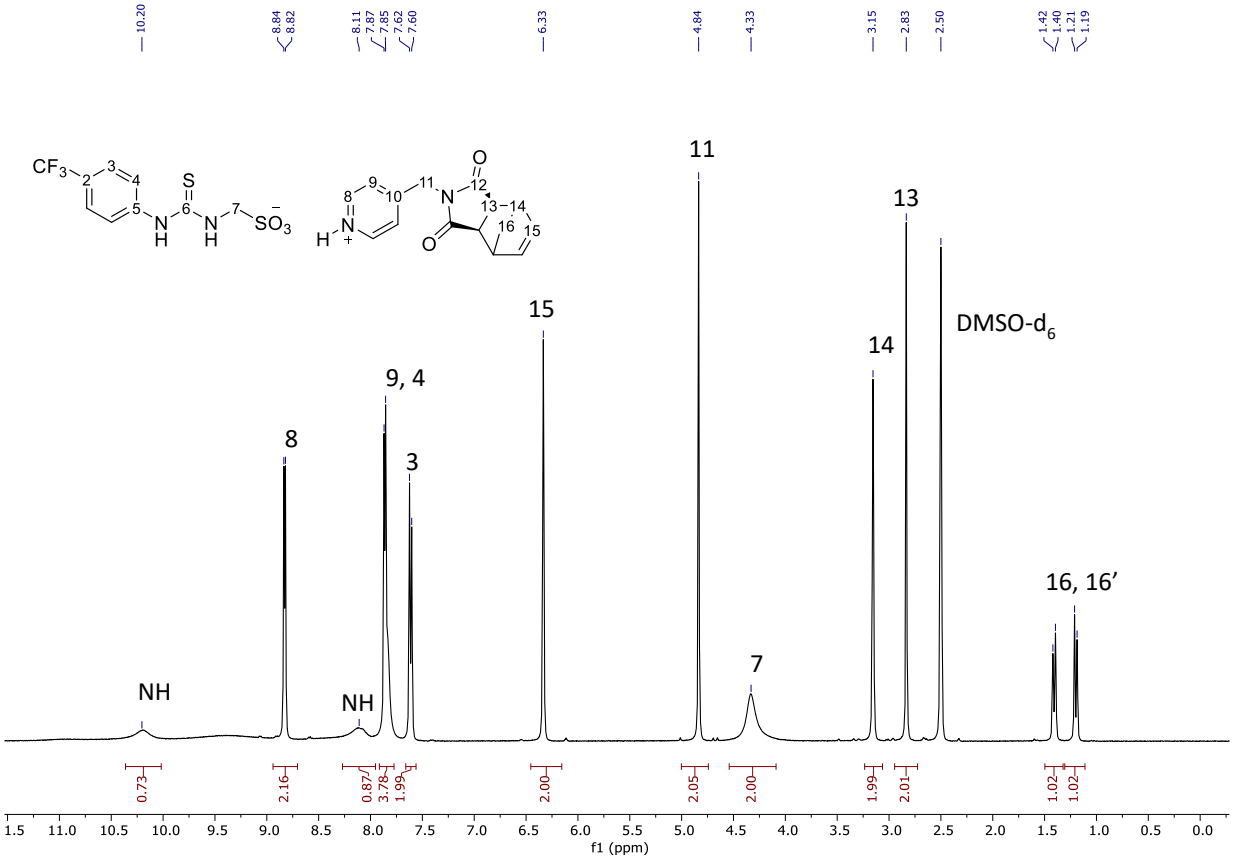

Fig. S21. ^{1}H NMR in dmso-d_6 at T = 333 K of **mon2**

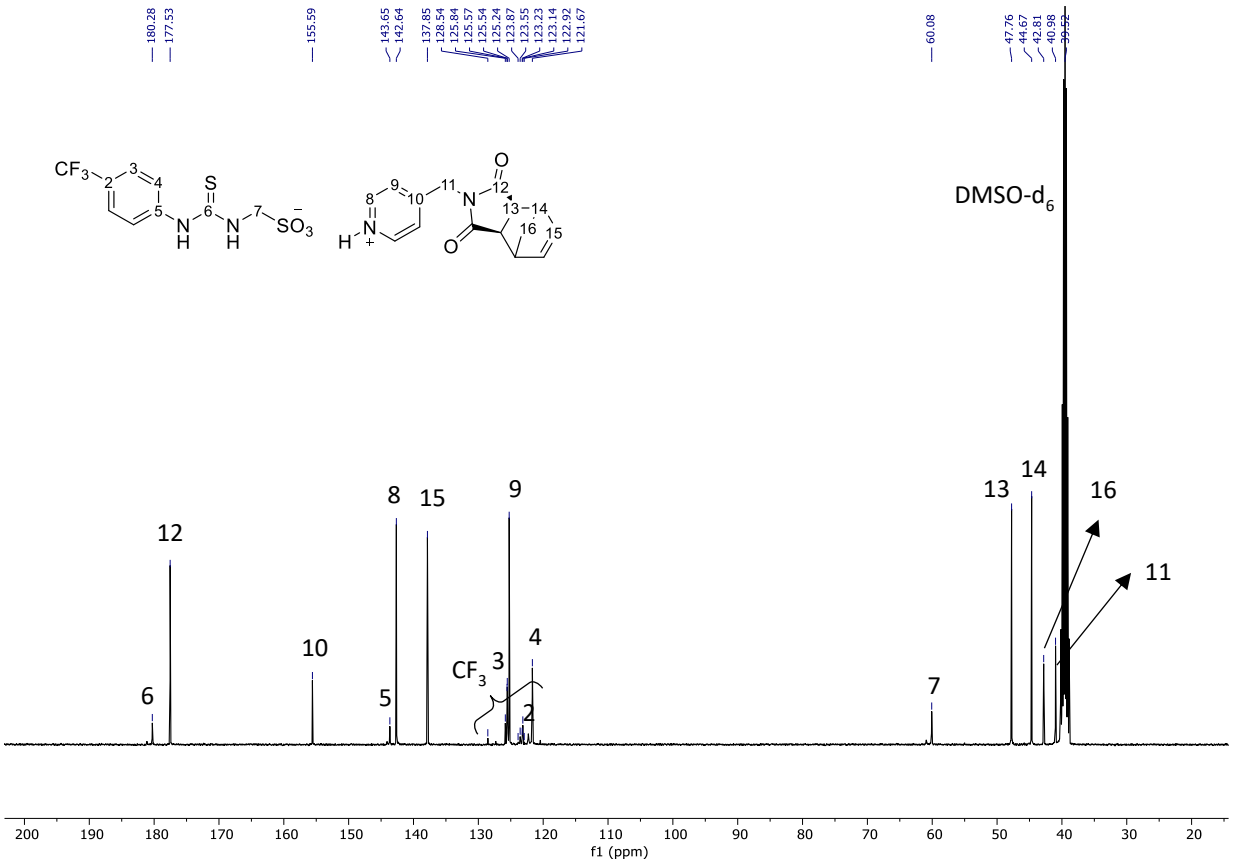

Fig. S22. ^{13}C NMR in dmso-d$_6$ of **mon2**

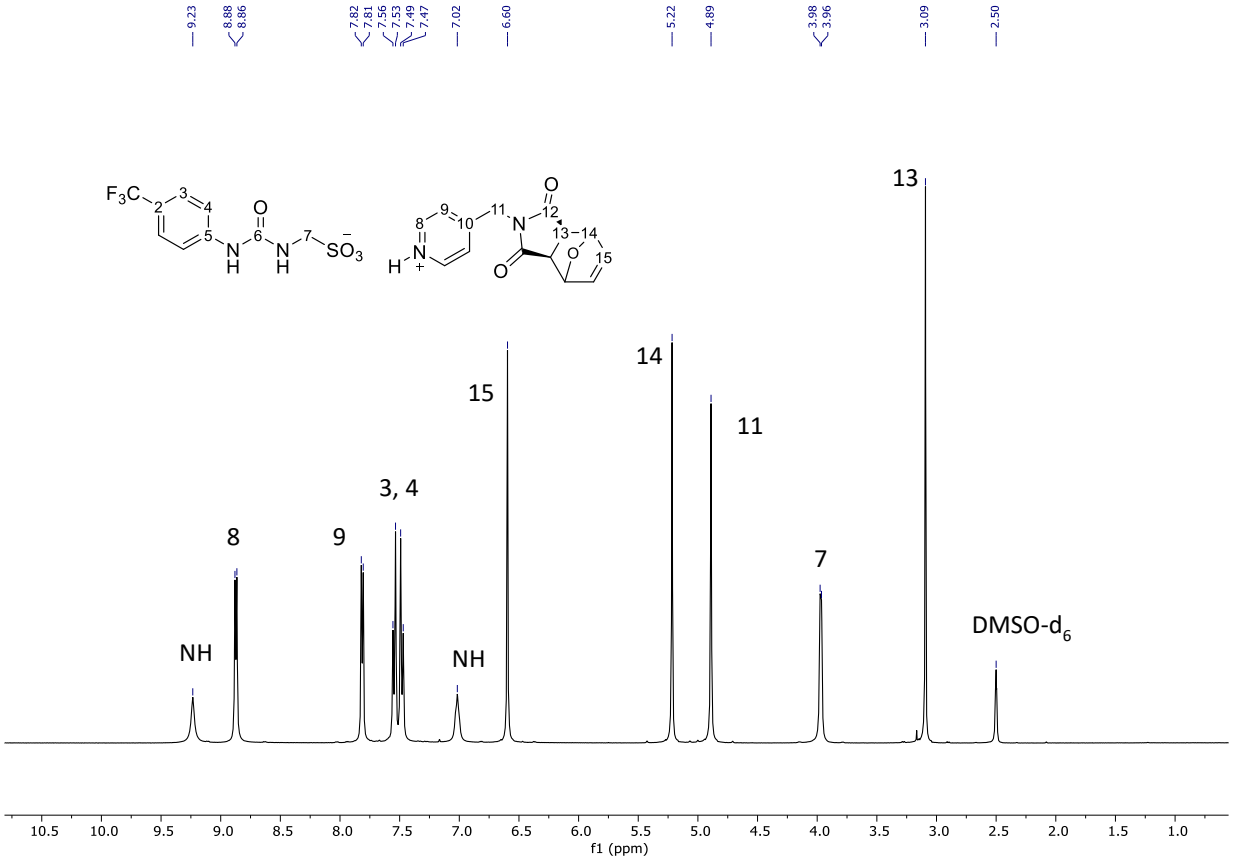

Fig. S23. ^{1}H NMR in dmso-d$_6$ of **mon3** with MeOH

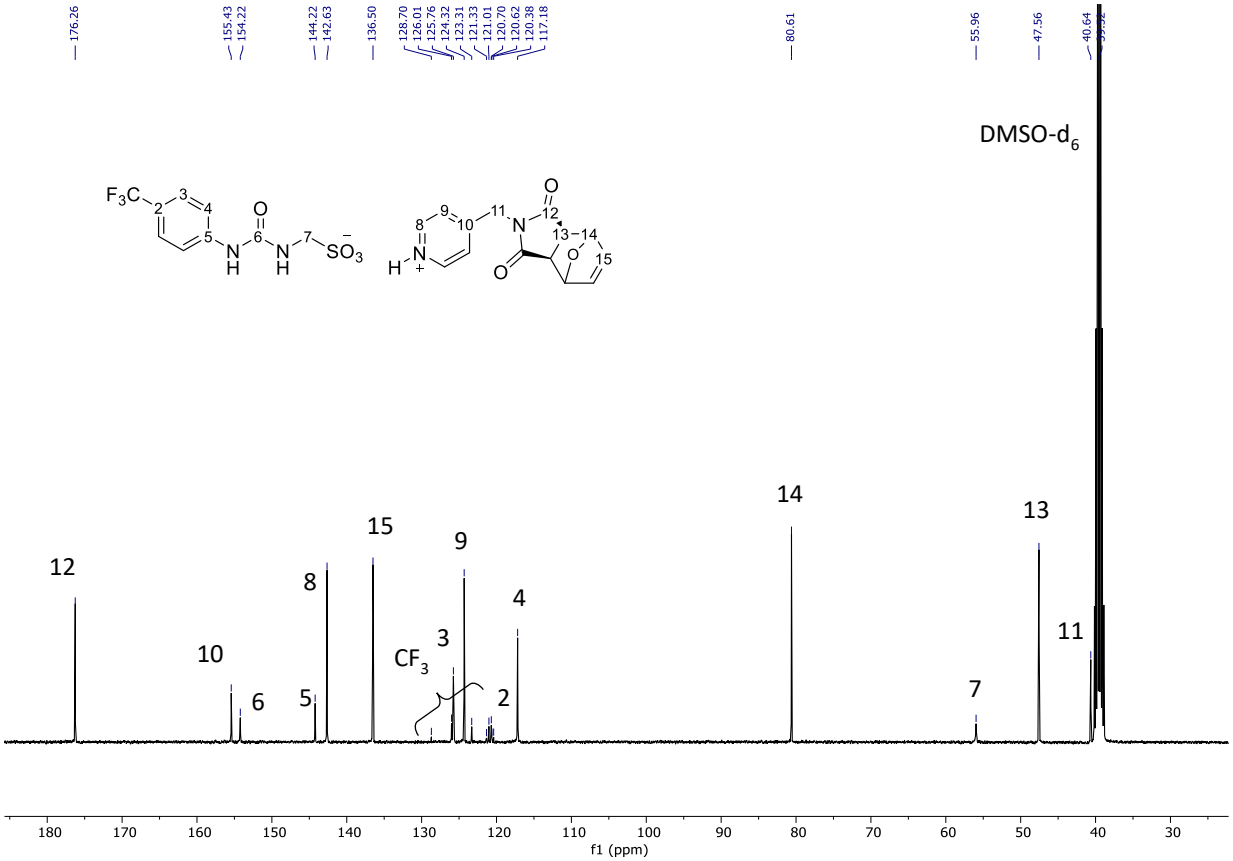

Fig. S24. ^{13}C NMR in dmso-d$_6$ of **mon3**

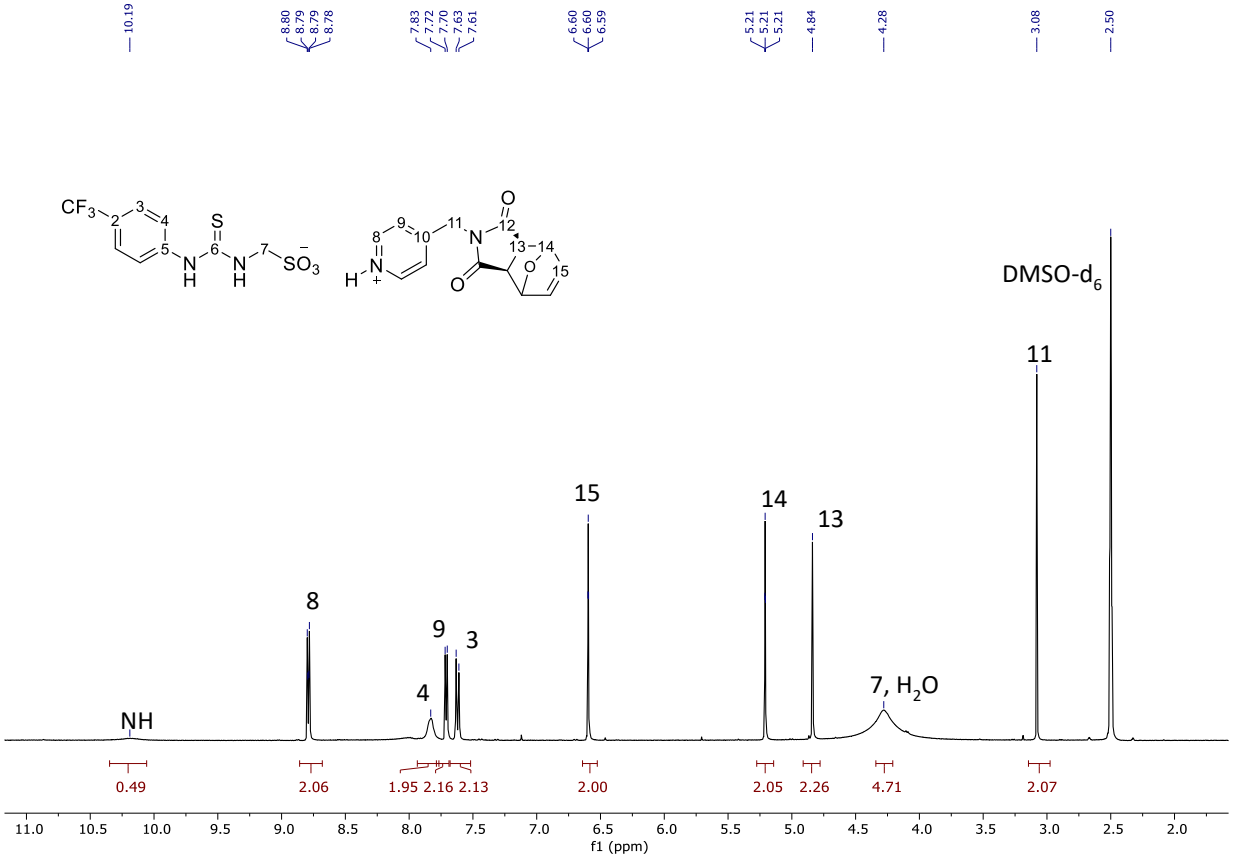

Fig. S25. ^{1}H NMR in dmso-d$_6$ at T = 333 K of **mon4**

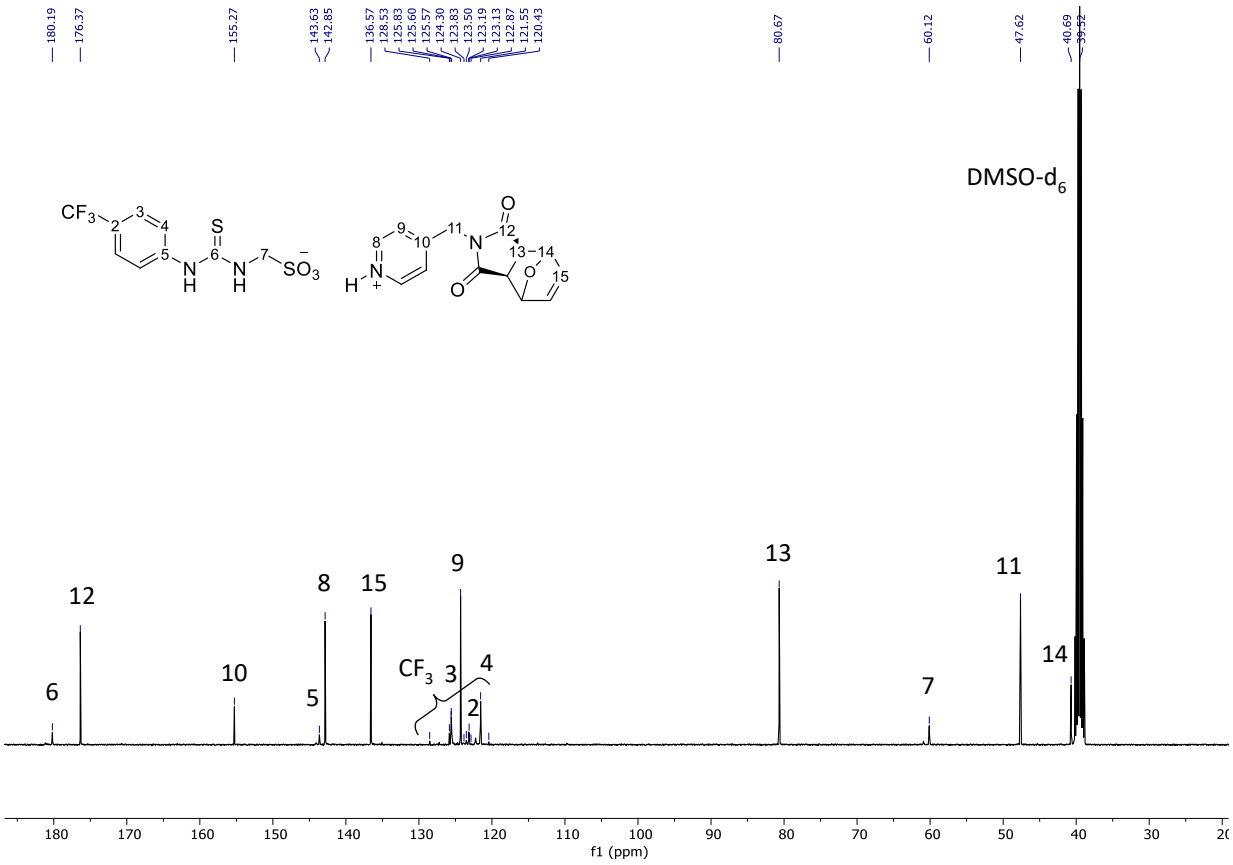

Fig. S26. ^{13}C NMR in dmso-d$_6$ of **mon4**

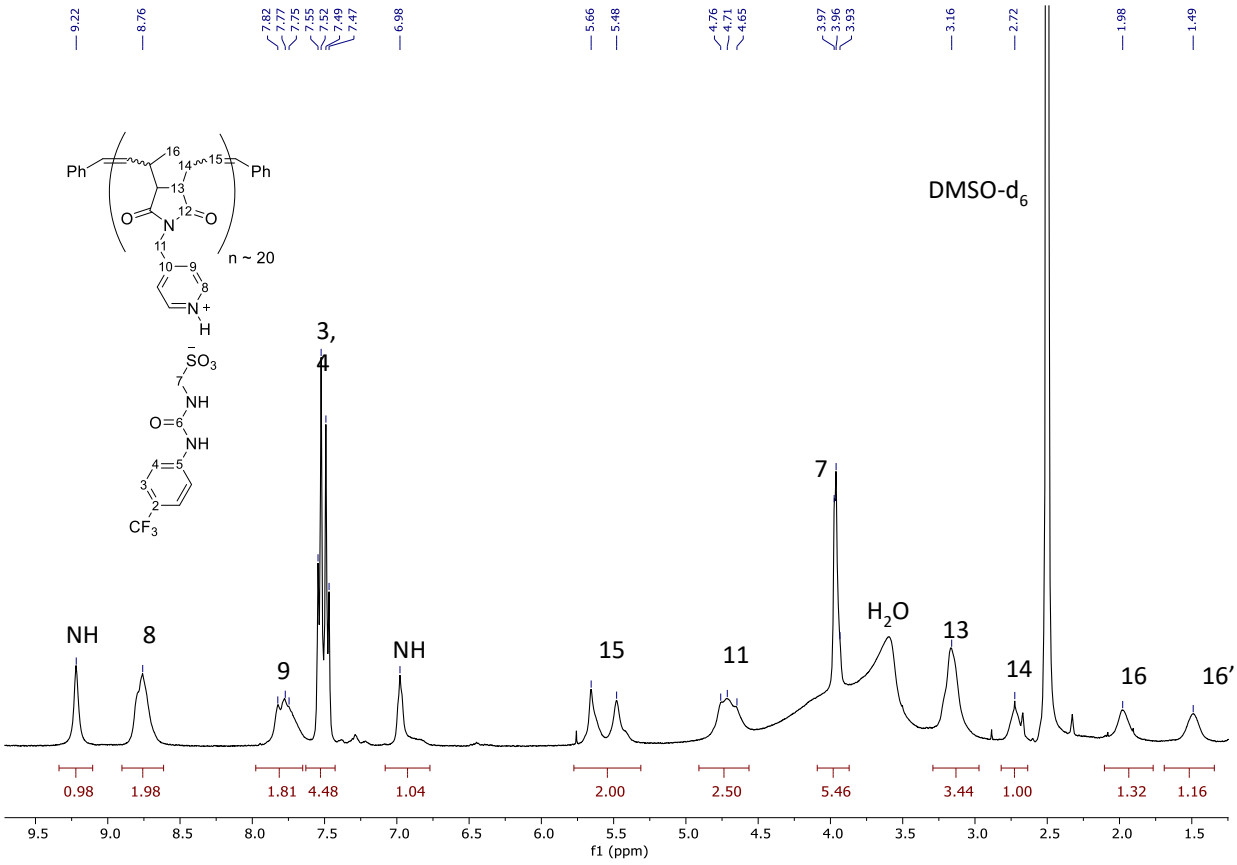

Fig. S27. ^{1}H NMR in dmso-d$_6$ of **poly1**

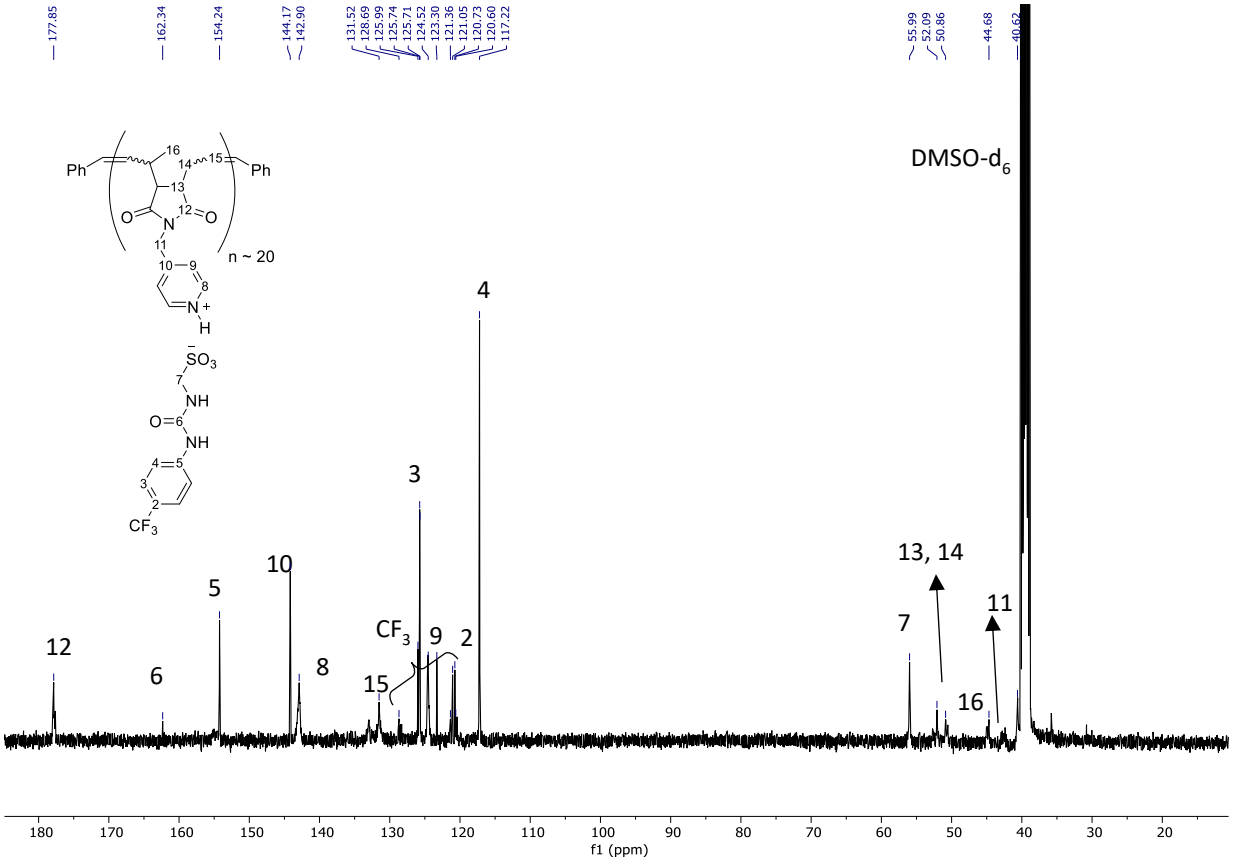

Fig. S28. ^{13}C NMR in dmso-d$_6$ of **poly1**

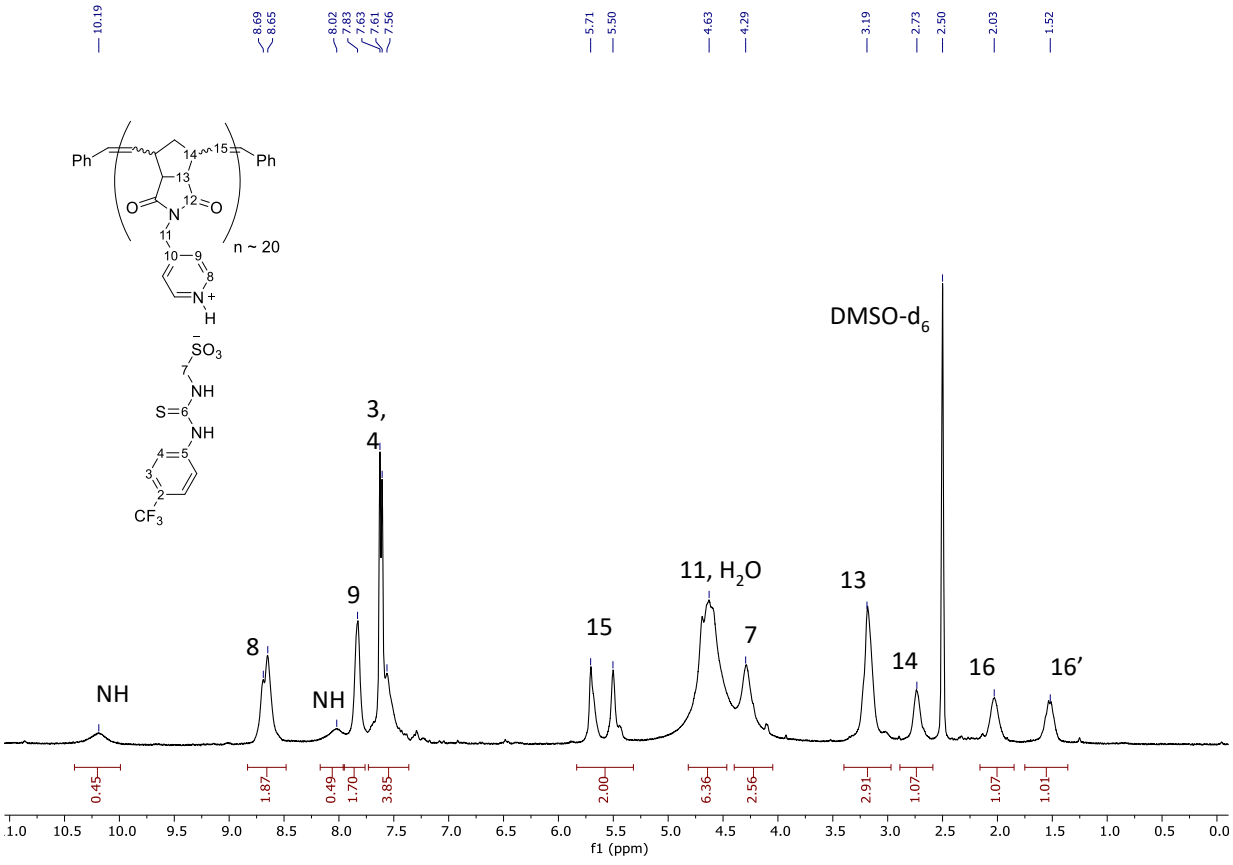

Fig. S29. ^{1}H NMR in dmso-d$_6$ at 333 K of **poly2**

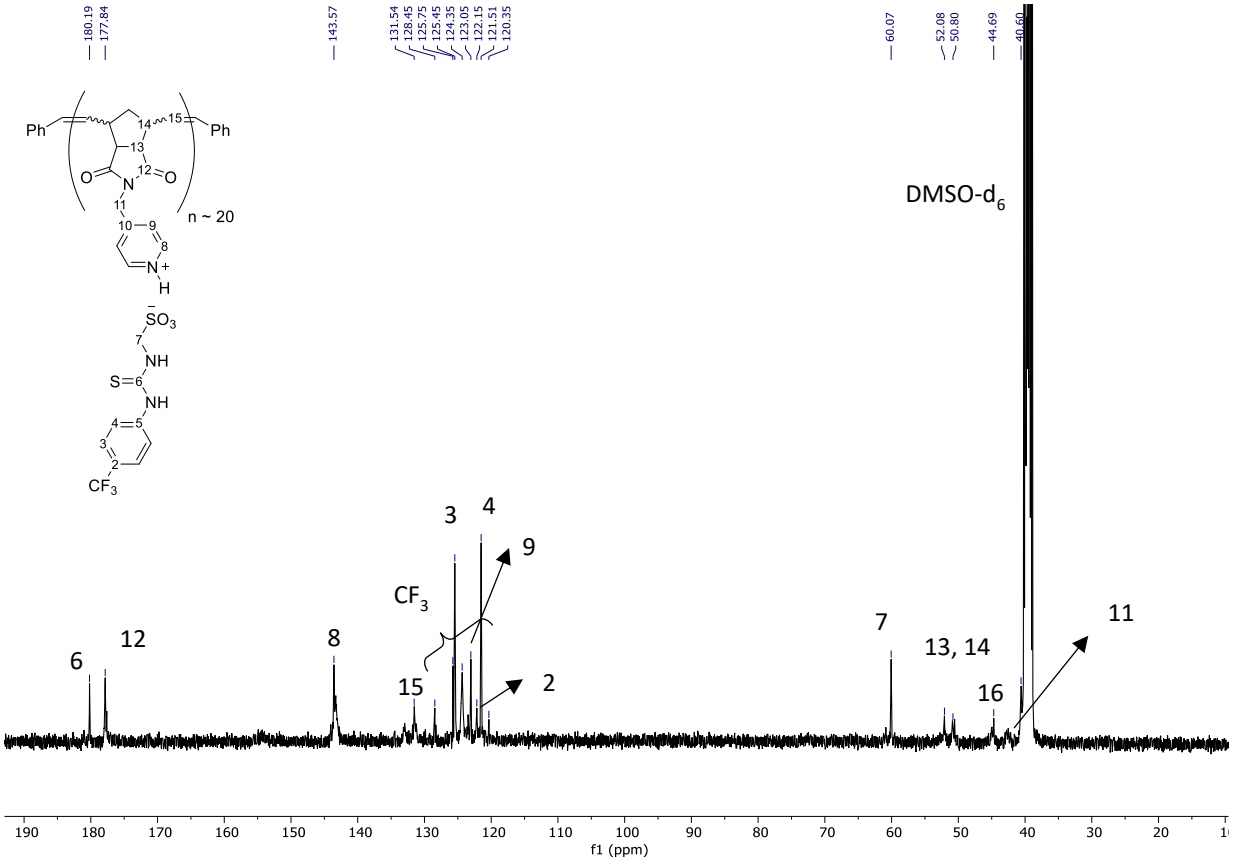

Fig. S30. ^{13}C NMR in dmso-d$_6$ of **poly2**

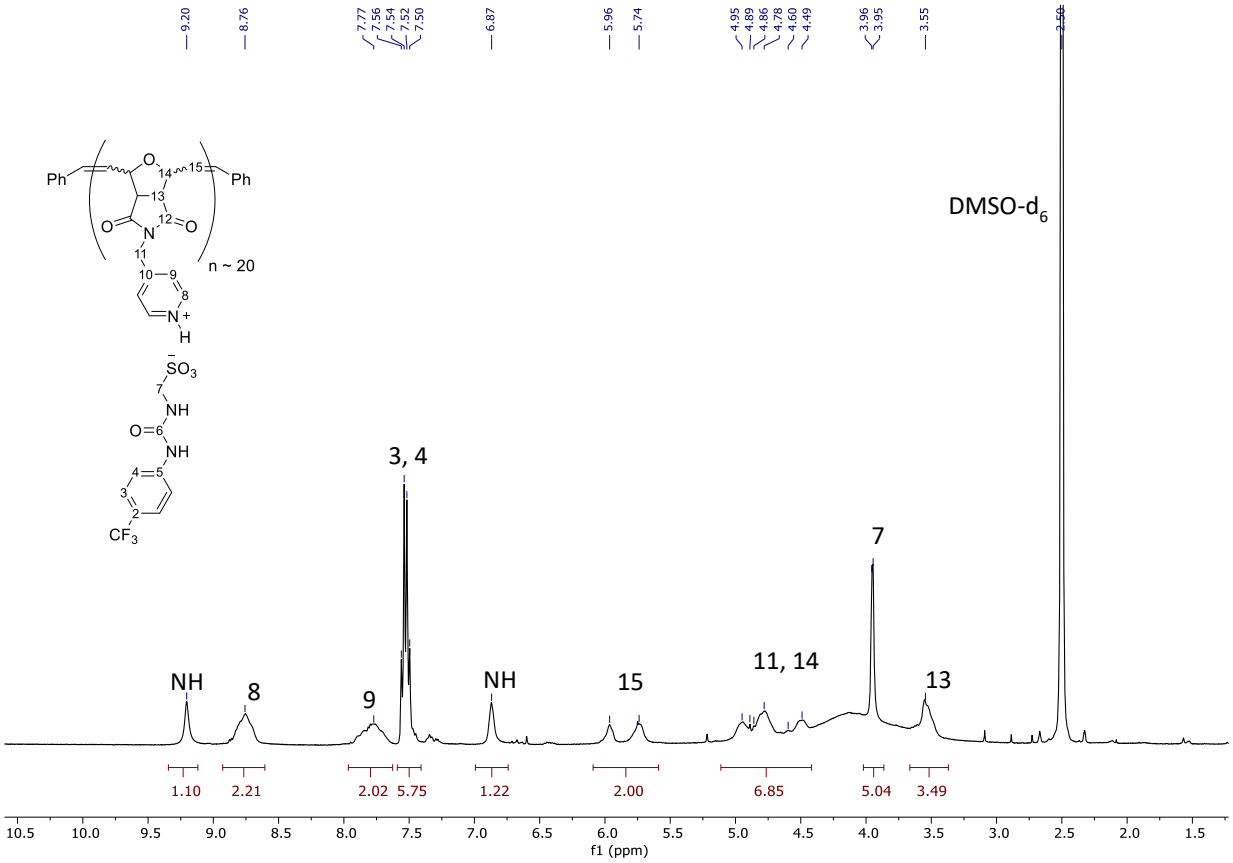

Fig. S31. ^{1}H NMR in dmso-d$_6$ of **poly3**

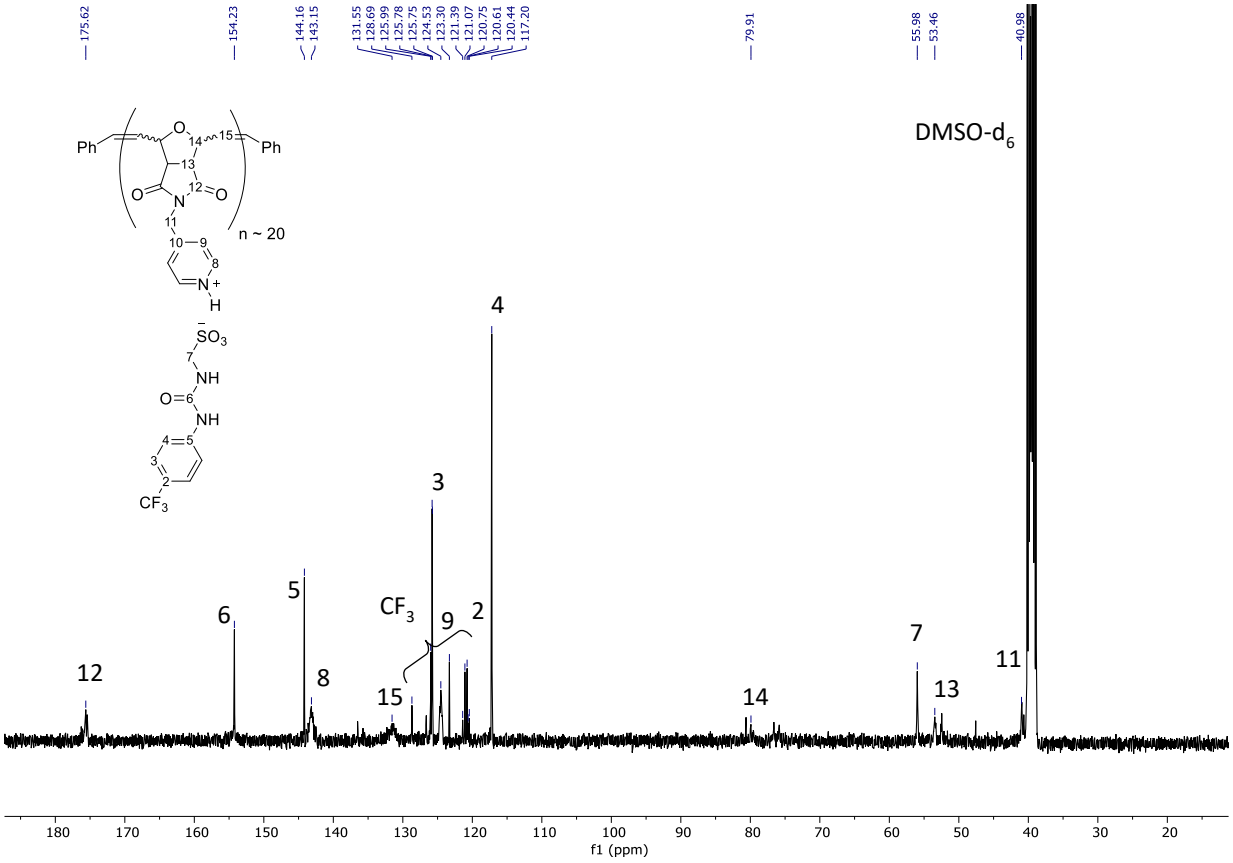

Fig. S32. ^{13}C NMR in dmso-d$_6$ of **poly3**

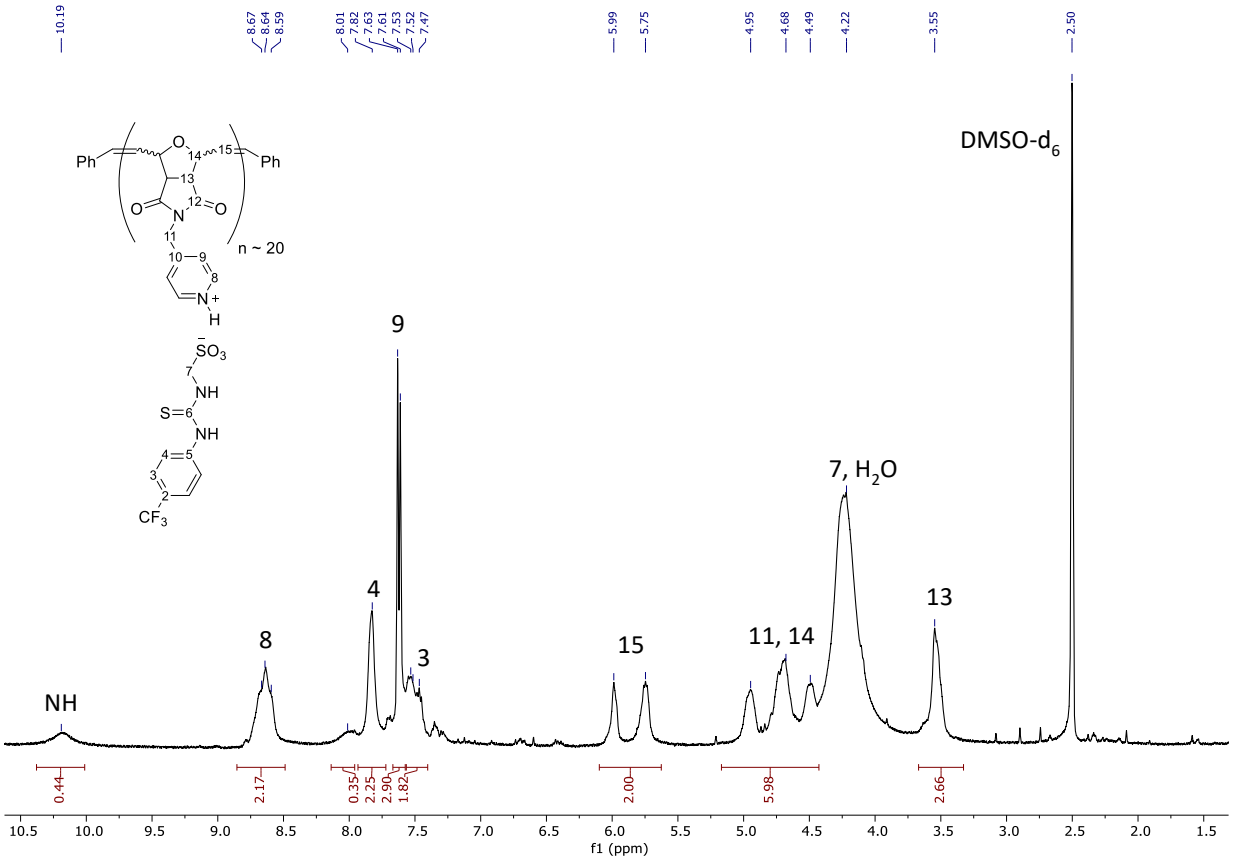

Fig. S33. ^{1}H NMR in dmso-d$_6$ at 333 K of **poly4**

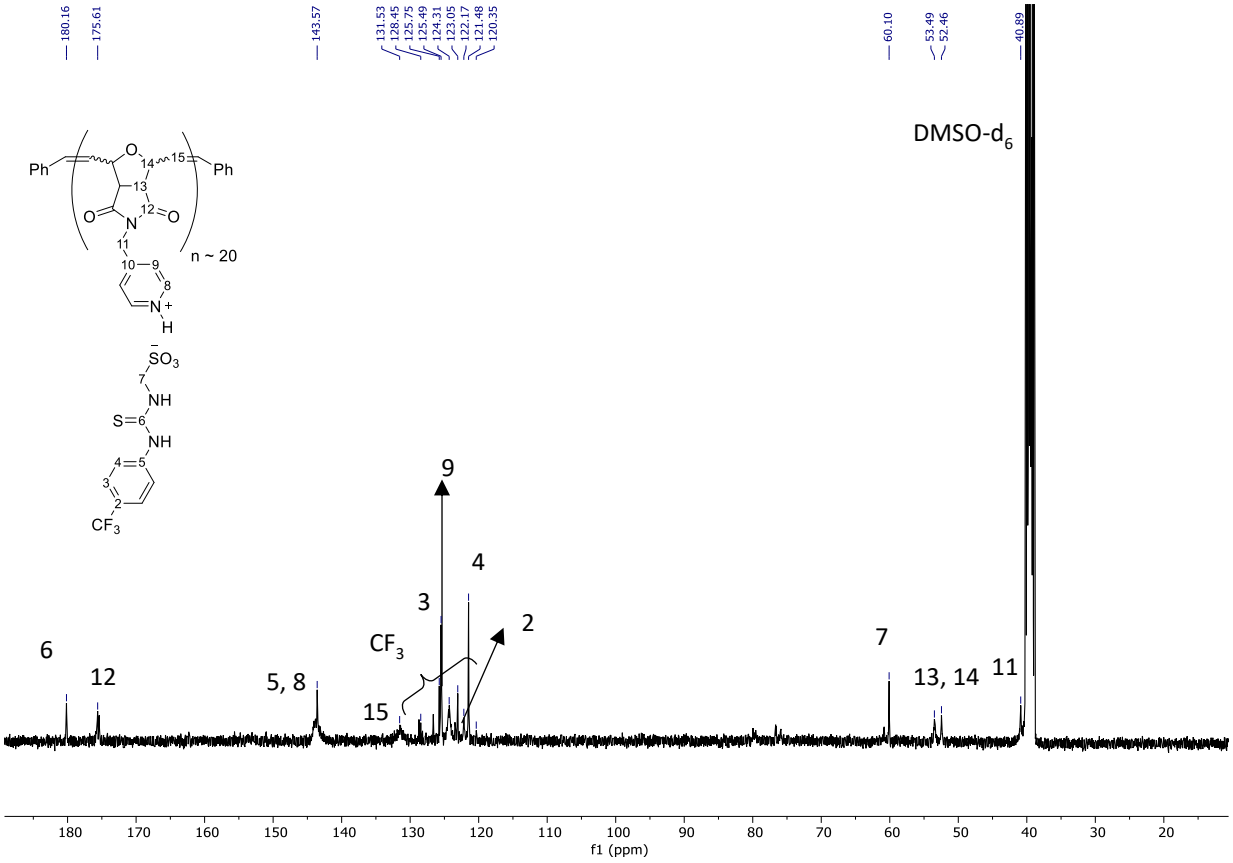

Fig. S34. ^{13}C NMR in dmso-d_6 of **poly4**

2. LC-MS spectra

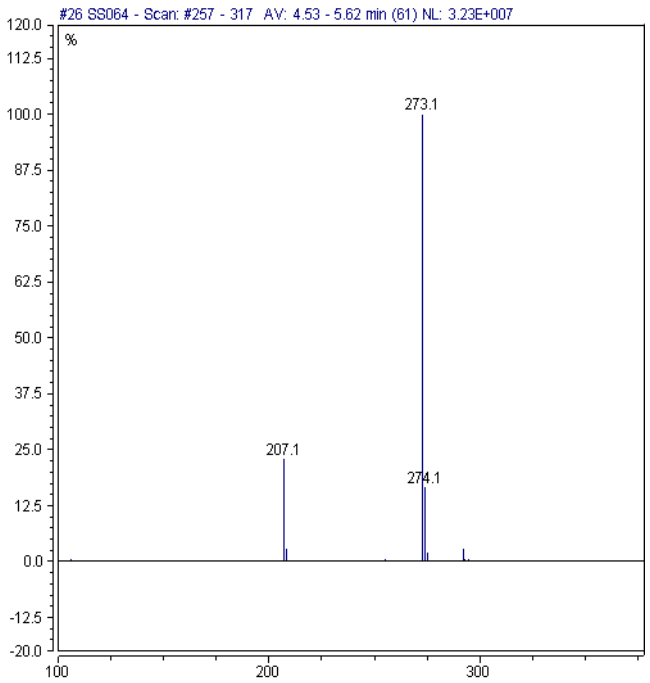

Fig. S35. LC-MS spectra of compound **3b.** Here the $[M+H]^+$ value of 273.1 is identified.

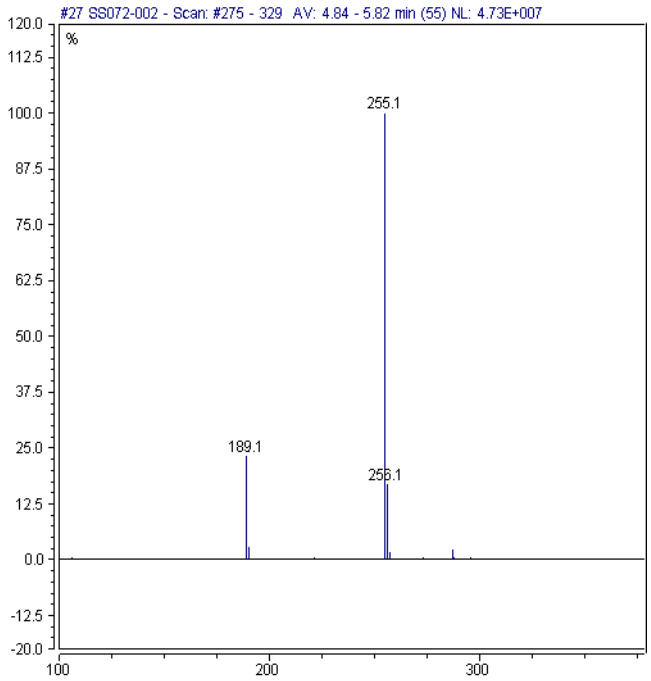

Fig. S36. LC-MS spectra of compound **4b.** Here the $[M+H]^+$ value of 255.1 is identified.

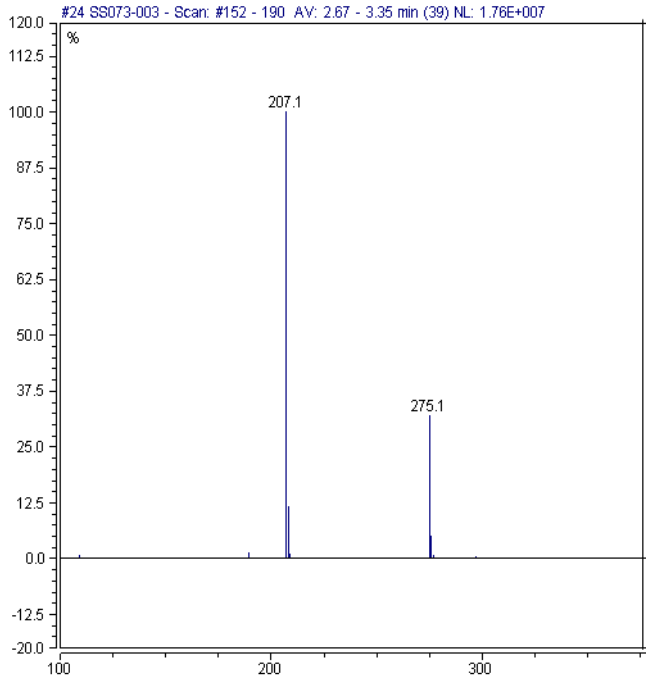

Fig. S37. LC-MS spectra of compound **8.** Here the $[M+H]^+$ value of 275.1 is identified.

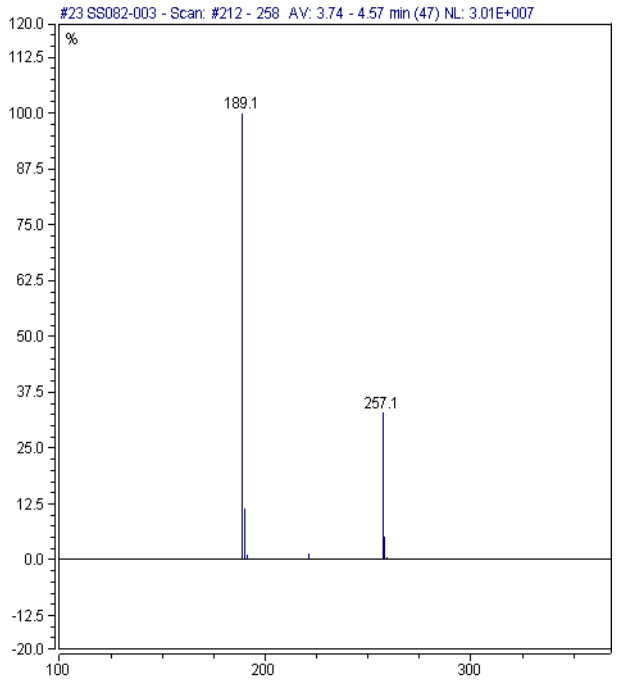

Fig. S38. LC-MS spectra of compound **9.** Here the $[M+H]^+$ value of 257.1 is identified.

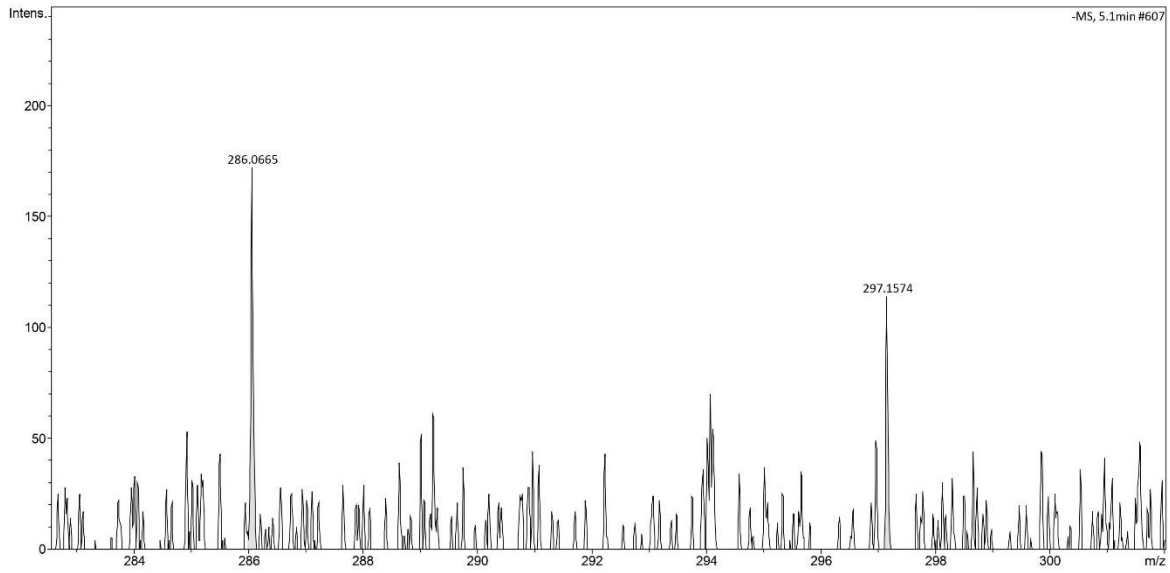

Fig. S39. High resolution LC-MS spectra of anionic component of **mon1** obtained using ESI-. Here the $[M]^-$ of 297.1574 value is identified.

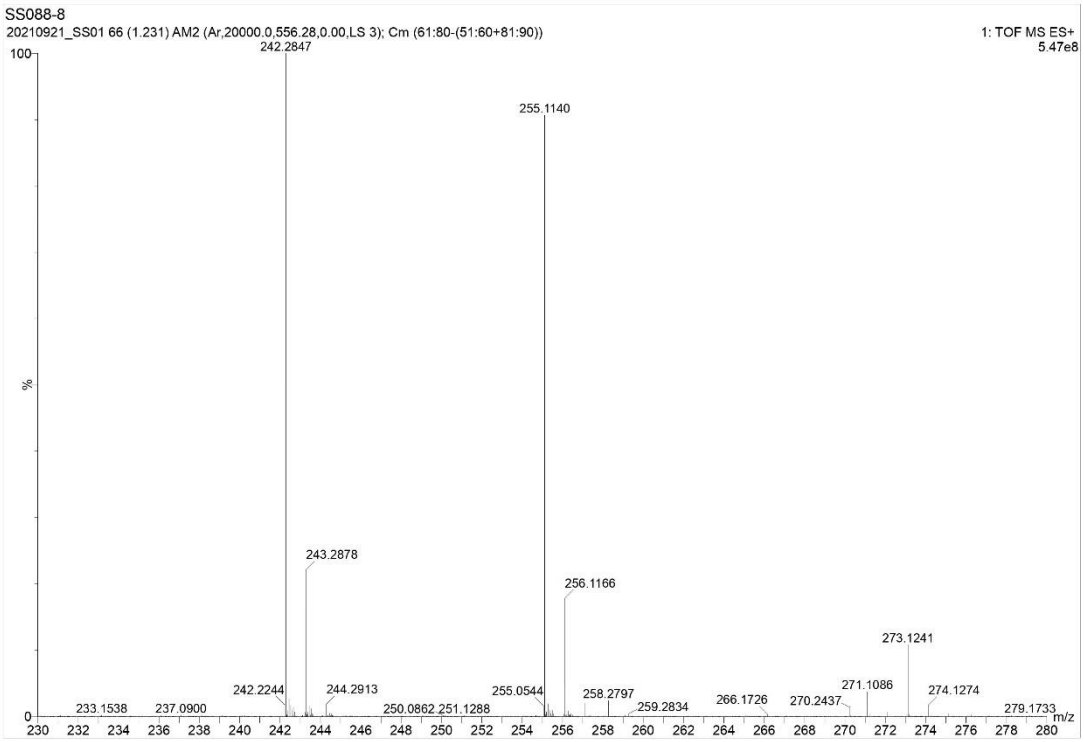

Fig. S40. High resolution LC-MS spectra of cationic component of **mon1** obtained using ESI+. Here the $[M+H]^+$ of 255.1140 value is identified.

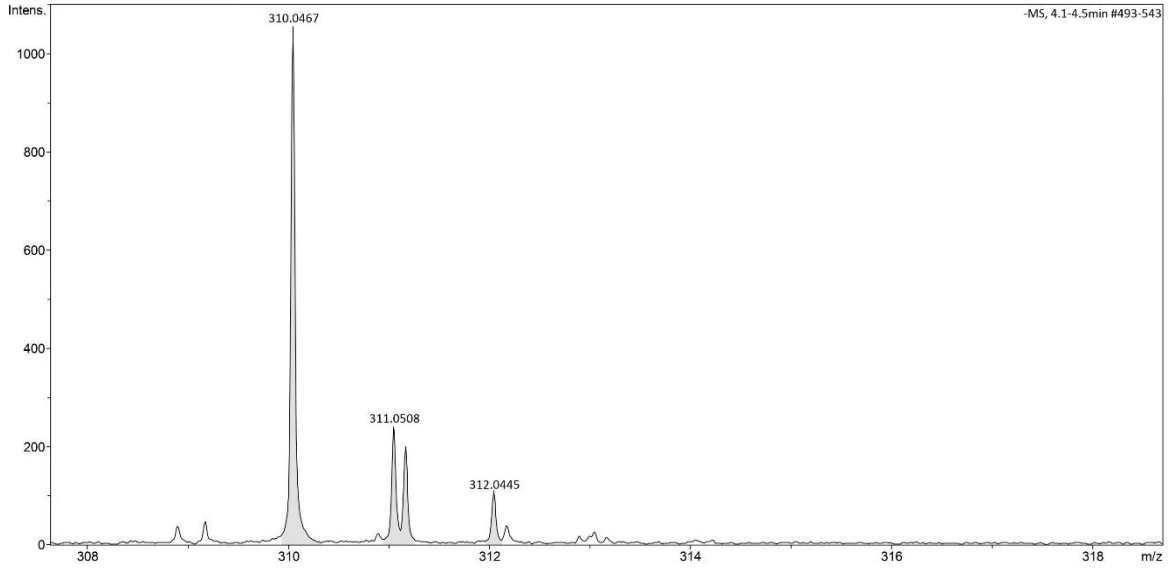

Fig. 41. High resolution LC-MS spectra of anionic component of **mon2** obtained using ESI-. Here the $[M]^-$ of 312.0445 value is identified.

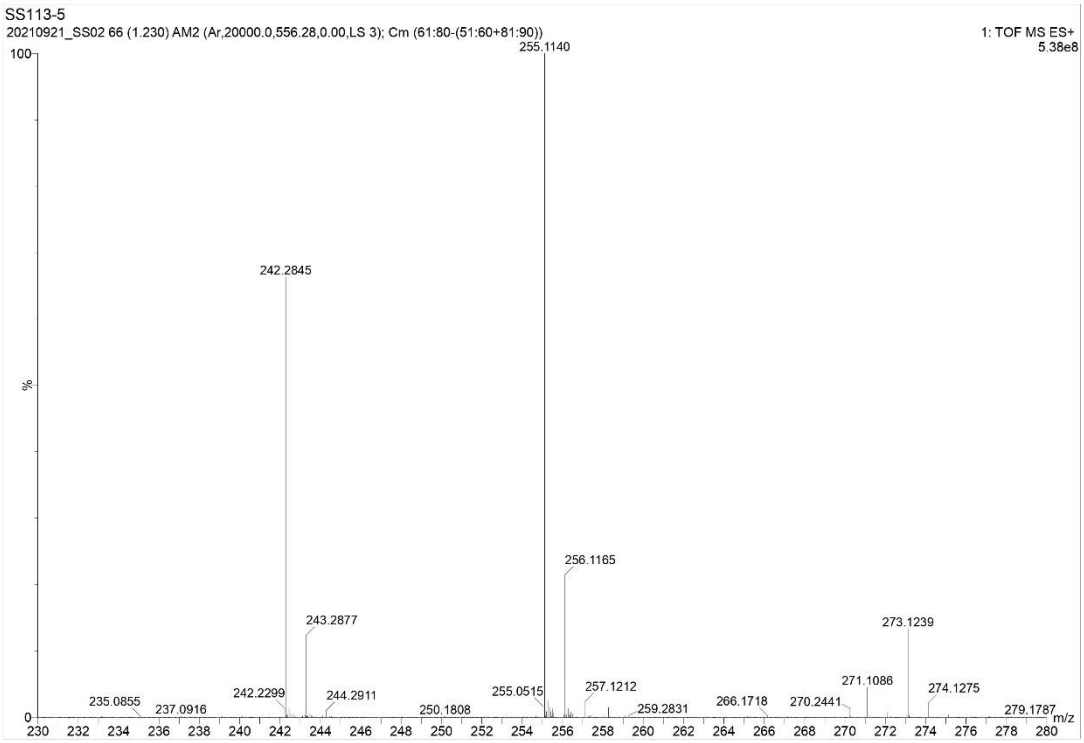

Fig. S42. High resolution LC-MS spectra of cationic component of **mon2** obtained using ESI+. Here the $[M+H]^+$ of 255.1140 value is identified.

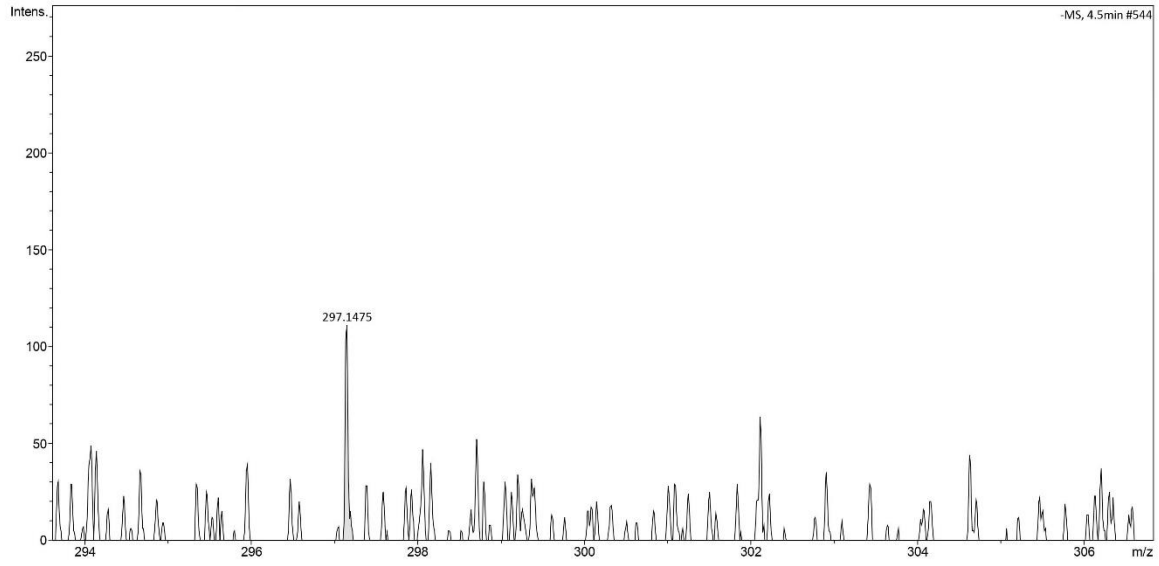

Figure 43. High resolution LC-MS spectra of anionic component of **mon3** obtained using ESI-. Here the $[M]^-$ of 297.1475 value is identified.

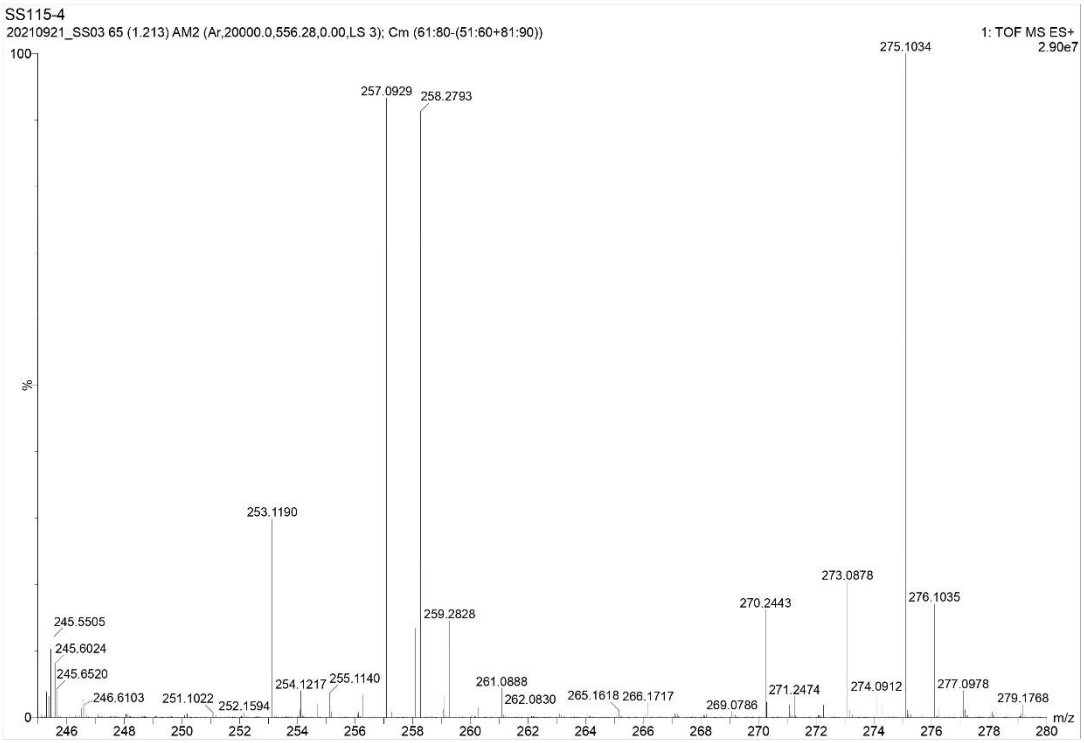

Fig. S44. High resolution LC-MS spectra of cationic component of **mon3** obtained using ESI+. Here the $[M+H]^+$ of 257.0929 value is identified.

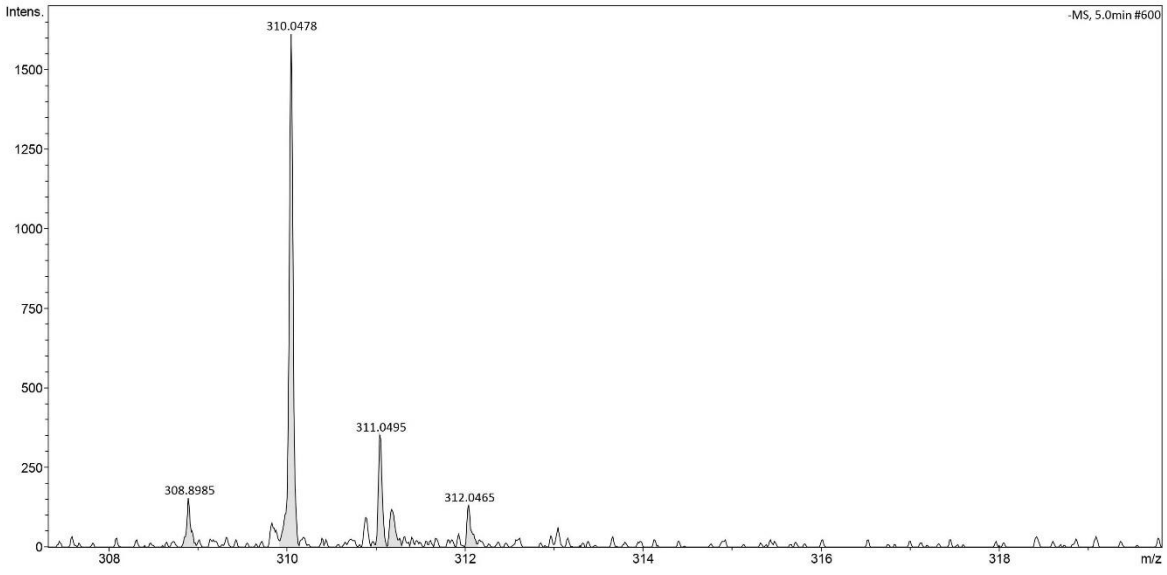

Fig. S45. High resolution LC-MS spectra of anionic component of **mon4** obtained using ESI-. Here the $[M]^-$ of 312.0445 value is identified.

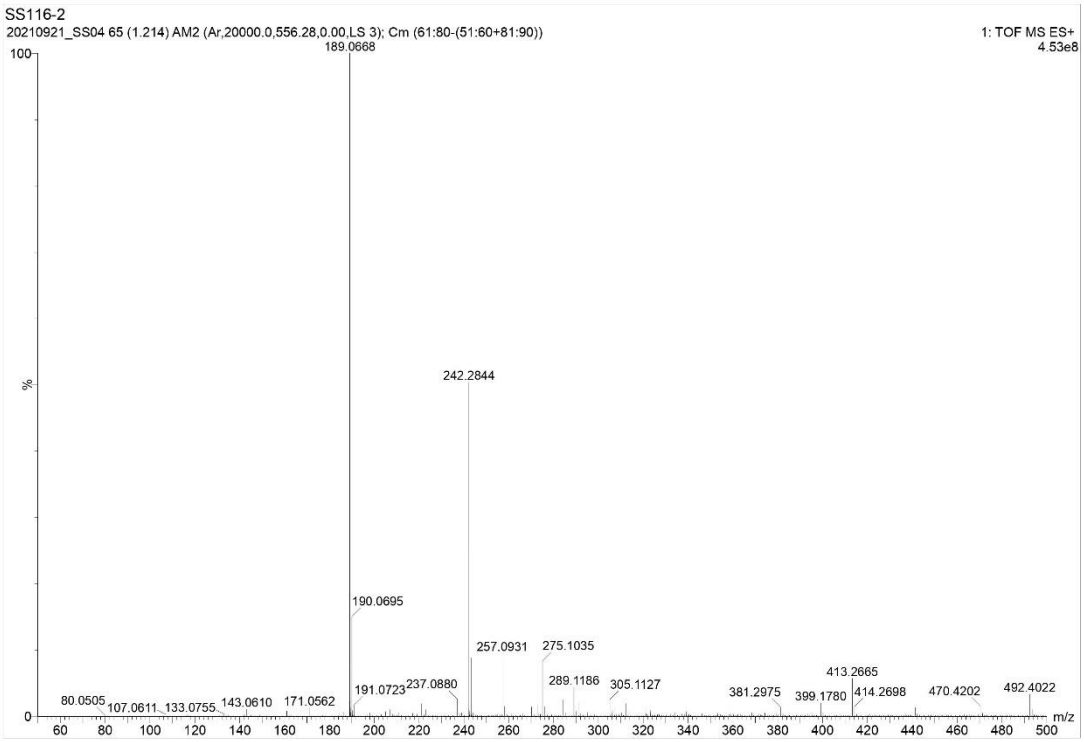

Fig. S46. High resolution LC-MS spectra of cationic component of **mon4** obtained using ESI+. Here the $[M+H]^+$ of 257.0931 value is identified.

3. IR spectra

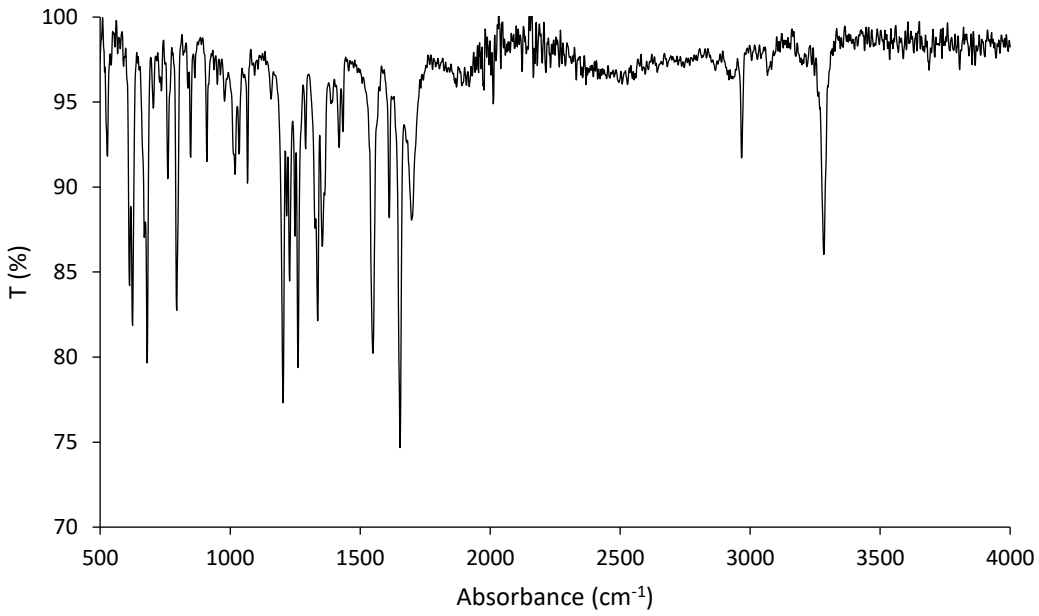

Fig. S47. IR spectra of compound **3a**

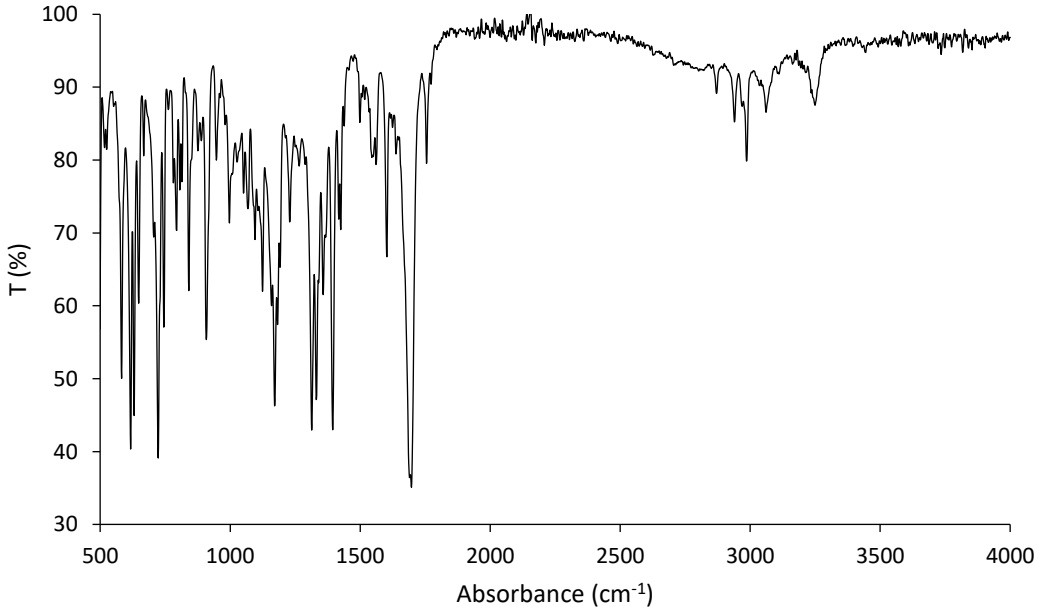

Fig. S48. IR spectra of compound **4a**

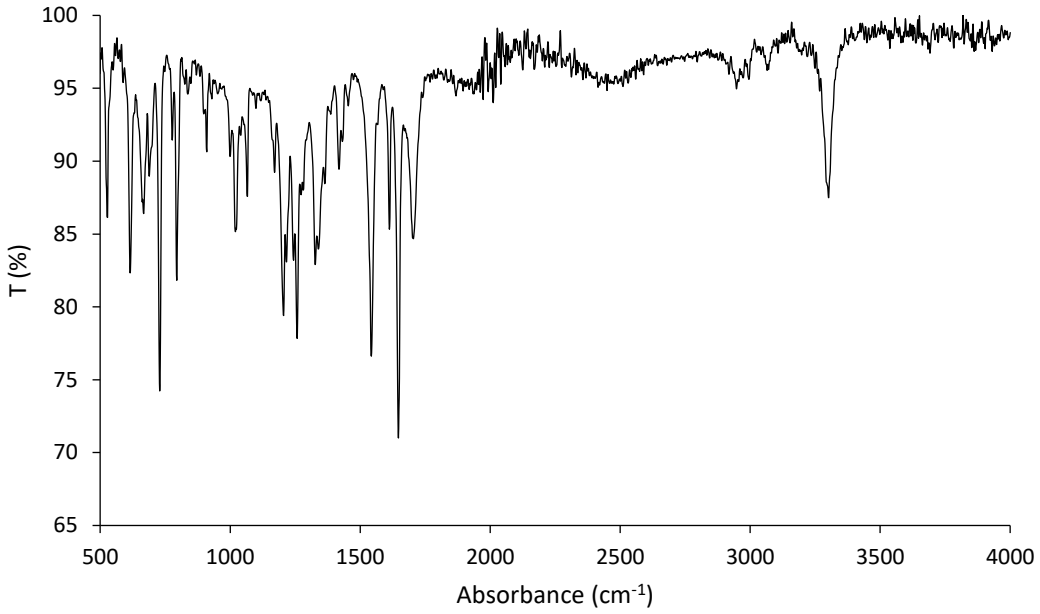

Fig. S49. IR spectra of compound **3b**

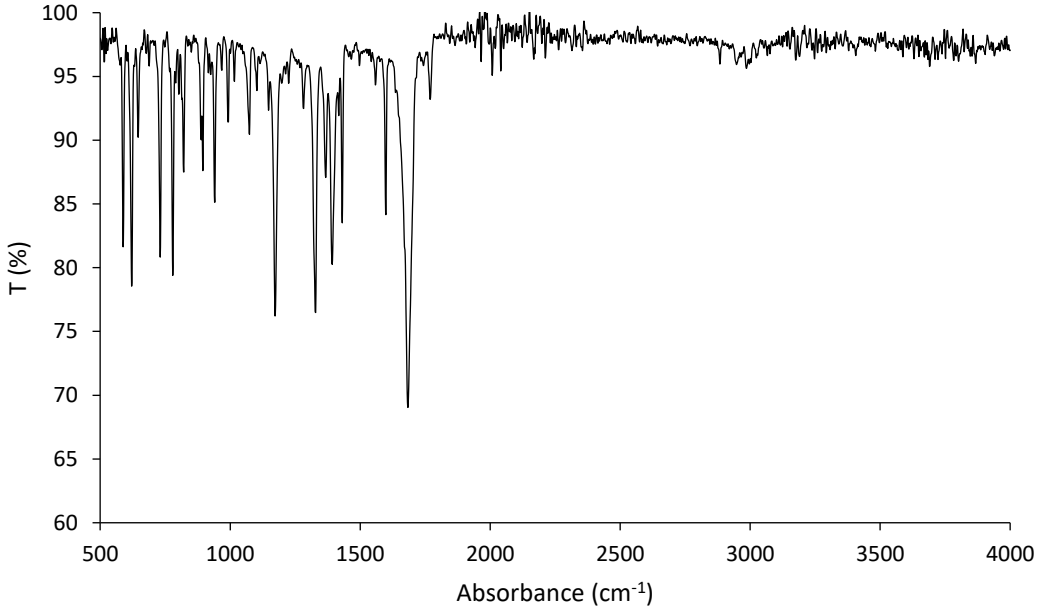

Fig. S50. IR spectra of compound **4b**

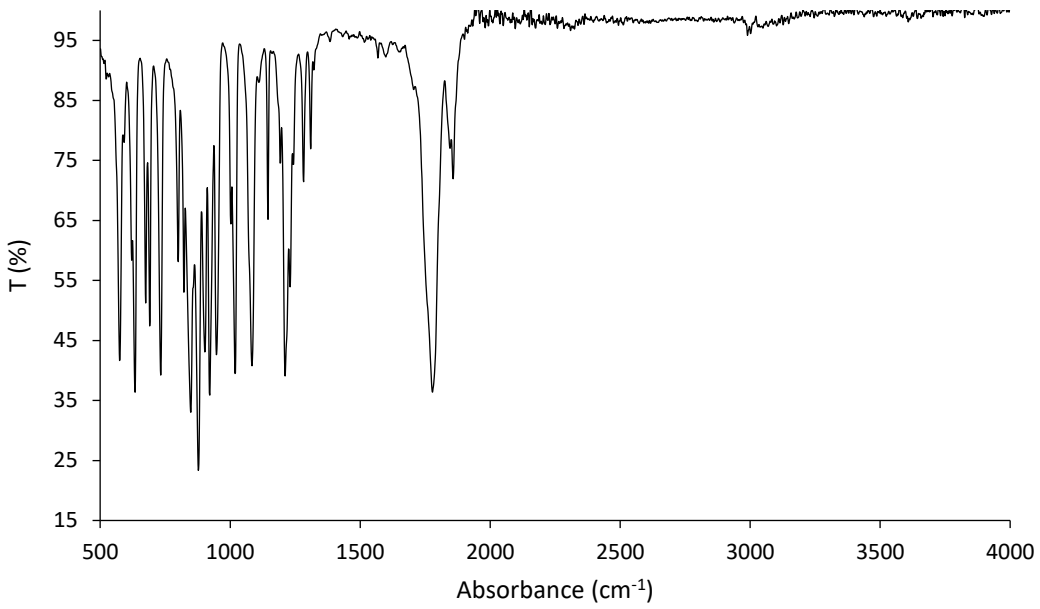

Fig. S51. IR spectra of compound **7**

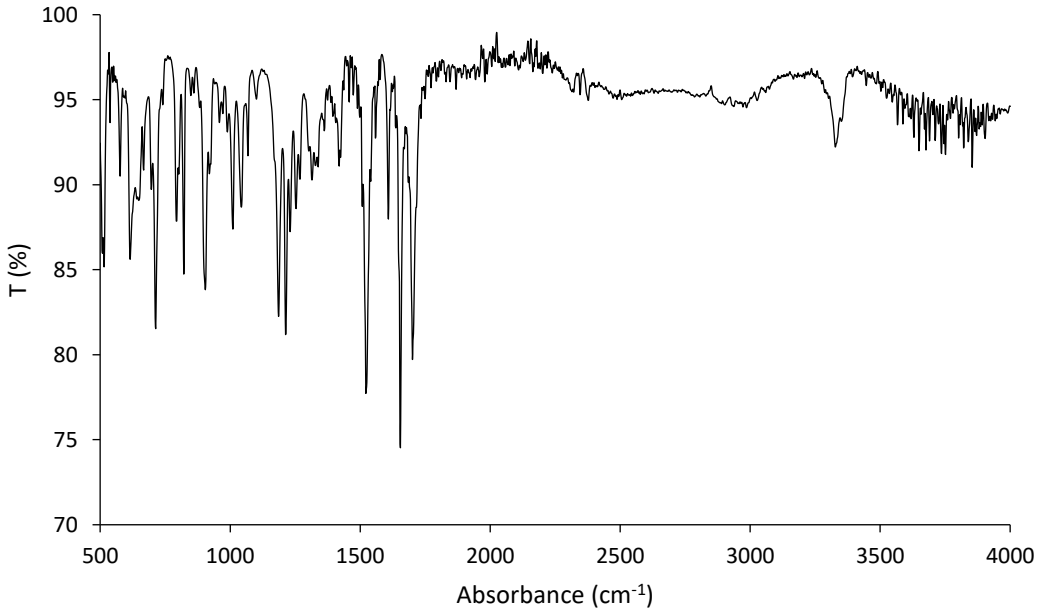

Fig. S52. IR spectra of compound **8**

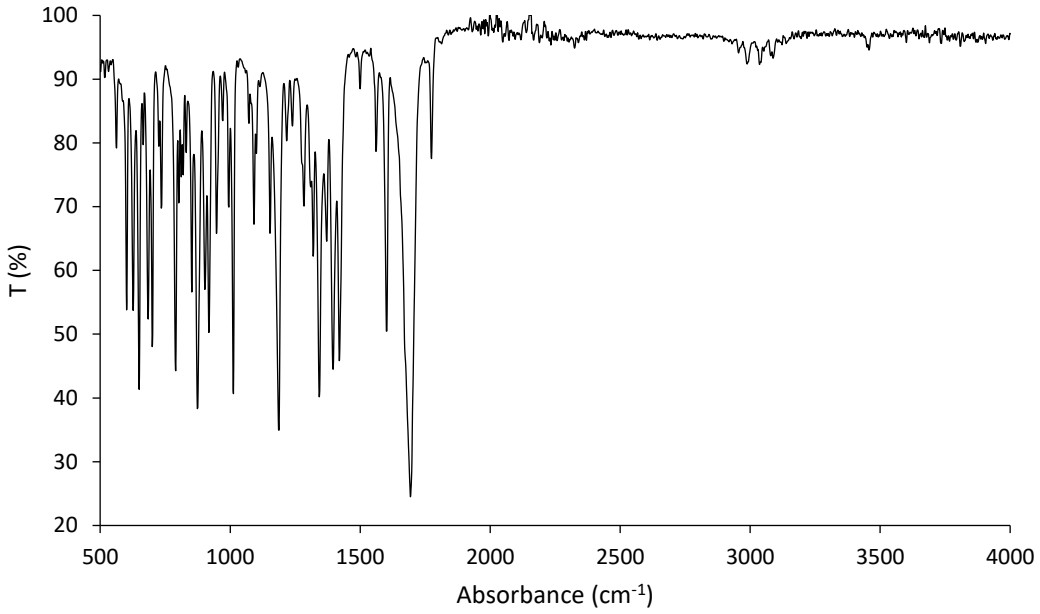

Fig. S53. IR spectra of compound **9**

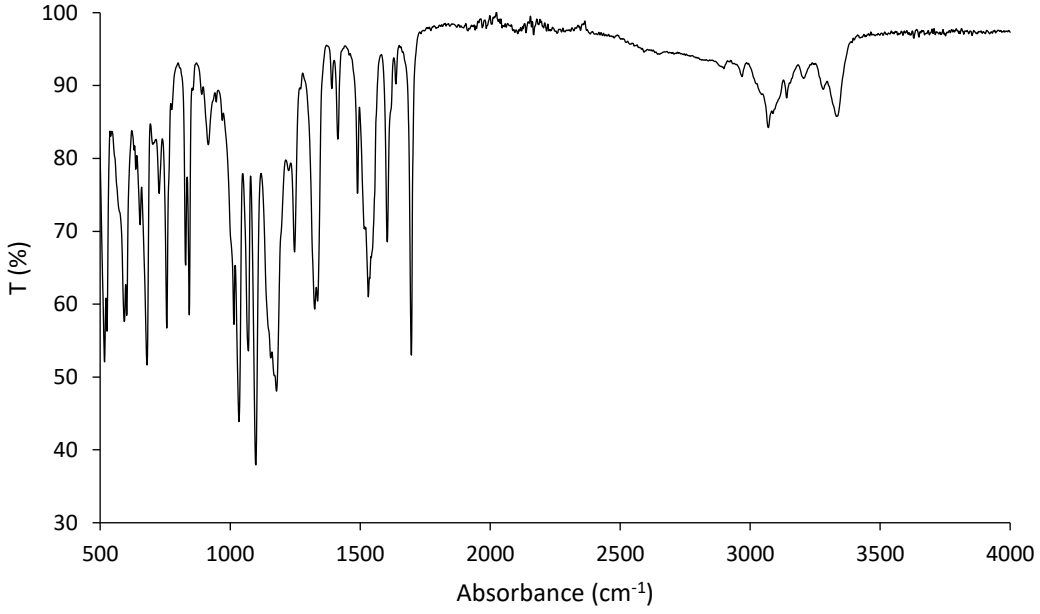

Fig. S54. IR spectra of compound **SSA-1**

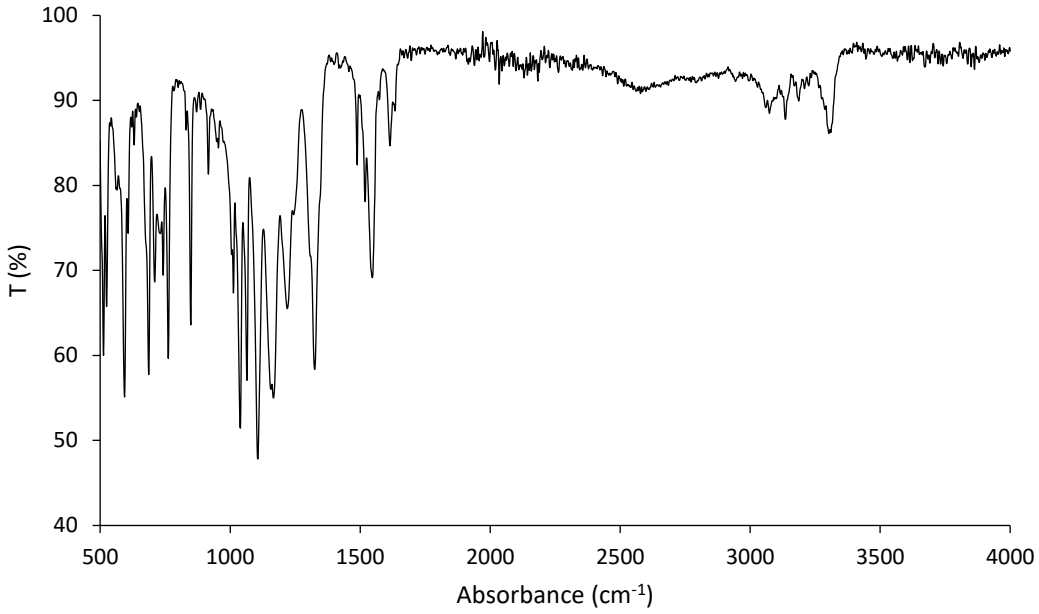

Fig. S55. IR spectra of compound **SSA-2**

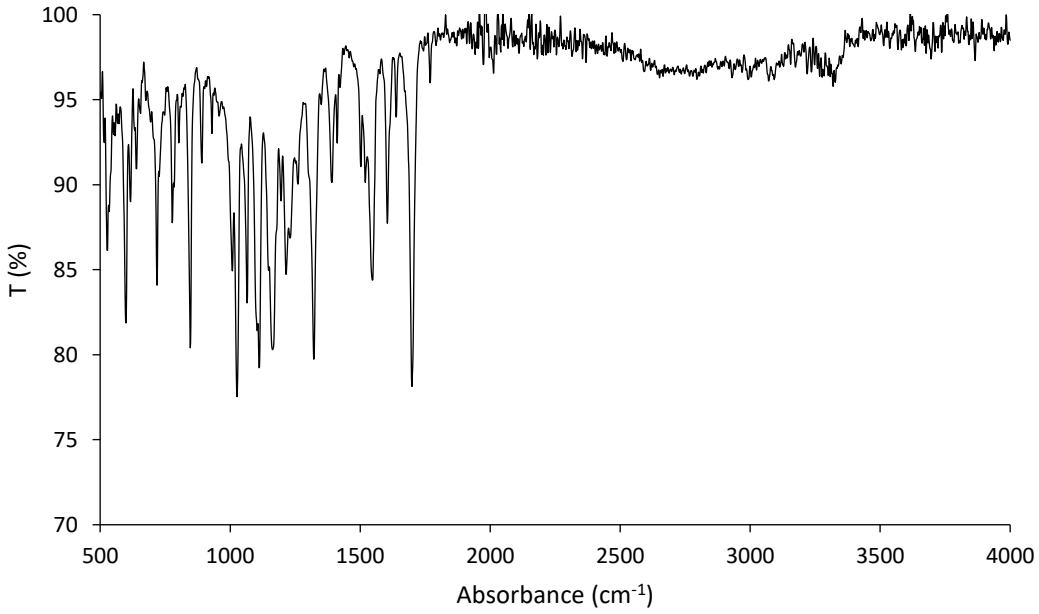

Fig. S56. IR spectra of monomer **mon1**

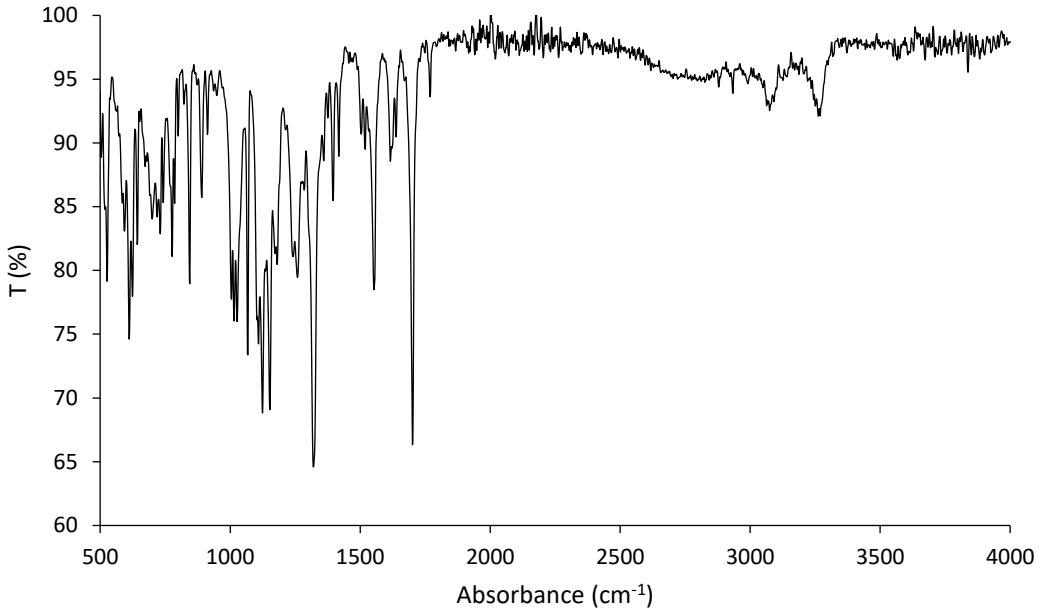

Fig. S57. IR spectra of monomer **mon2**

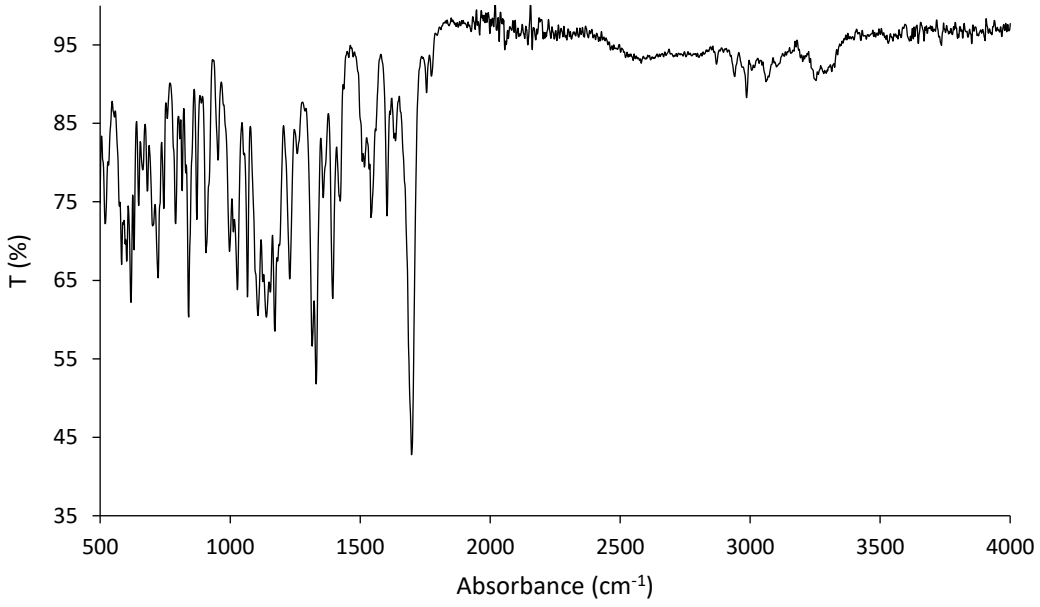

Fig. S58. IR spectra of monomer **mon3**

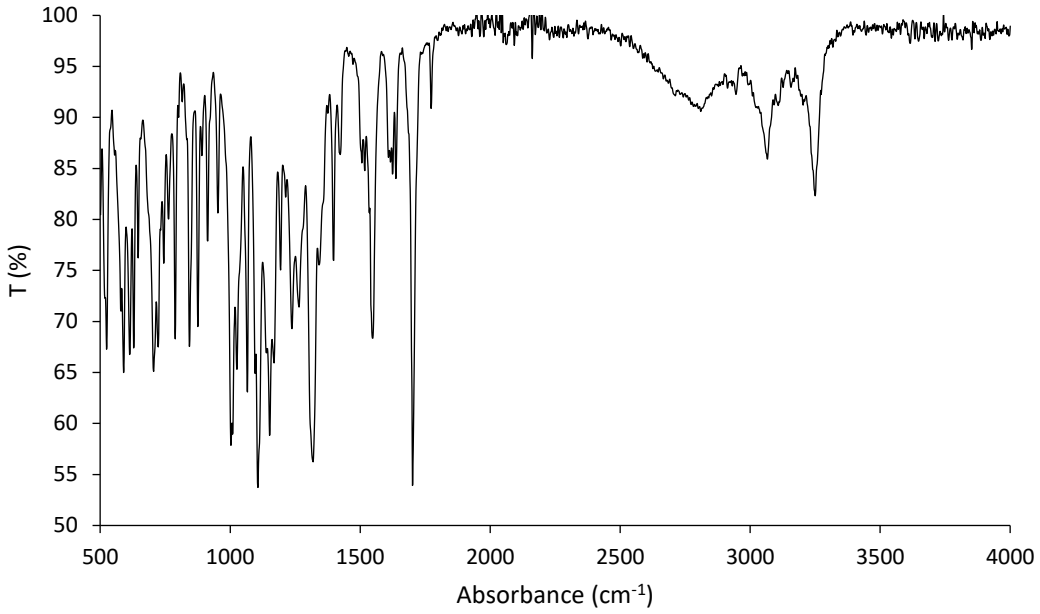

Fig. S59. IR spectra of monomer **mon4**

4. ^{1}H DOSY NMR experiments on monomers **mon1 – mon4**

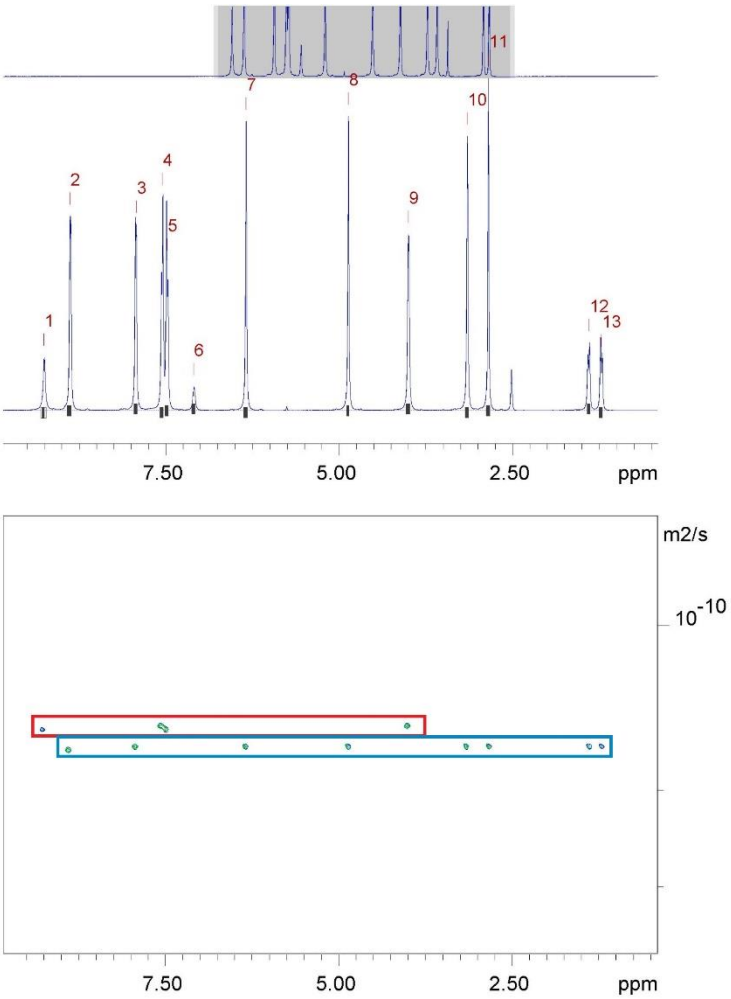

Peak name	F2 [ppm]	Io	error	D [m2/s]	error
1	9.258	7.60e+09	6.042e+05	1.55e-10	2.737e-14
2	8.885	2.33e+10	5.688e+05	1.68e-10	9.030e-15
3	7.927	2.26e+10	5.138e+05	1.67e-10	8.410e-15
4	7.554	2.31e+10	5.022e+05	1.54e-10	7.457e-15
5	7.482	2.34e+10	5.042e+05	1.54e-10	7.406e-15
6	7.096	3.15e+09	5.091e+05	1.60e-10	5.740e-14
7	6.344	2.30e+10	5.153e+05	1.67e-10	8.283e-15
8	4.868	2.00e+10	4.517e+05	1.66e-10	8.314e-15
9	3.998	2.08e+10	5.304e+05	1.54e-10	8.725e-15
10	3.152	2.33e+10	5.137e+05	1.67e-10	8.147e-15
11	2.845	2.34e+10	5.155e+05	1.68e-10	8.138e-15
12	1.397	8.72e+09	4.842e+05	1.66e-10	2.042e-14
13	1.219	8.99e+09	5.137e+05	1.67e-10	2.111e-14

Fig. S60. ^{1}H DOSY NMR spectrum of **mon1** (112 mM) in DMSO-d_6 at 298 K and a table exporting the diffusion constants calculated for each peak used to determine the hydrodynamic diameter of the anionic (dH = 1.41 nm) and cationic (dH = 1.31 nm) components of **mon 1**. Peaks 1, 4-6 and 9 correspond to the anionic component of monomer **1** while peaks 2, 3, 7, 8, 10-13 correspond to the cationic component of **mon1**.

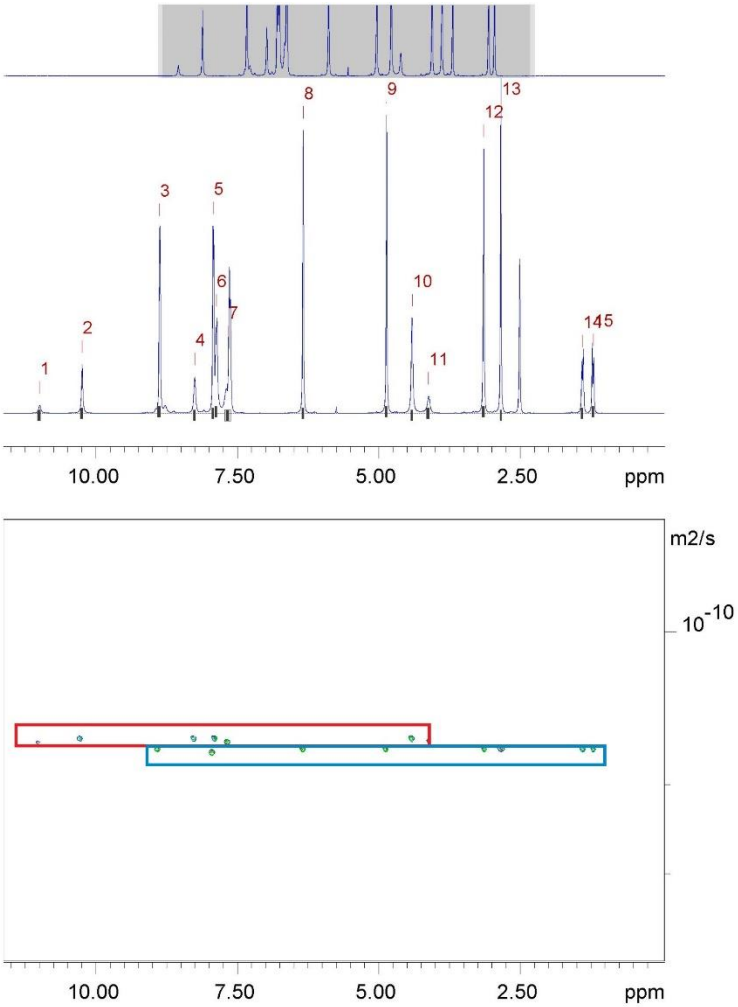

Peak name	F2 [ppm]	Io	error	D [m2/s]	error
1	11.002	1.34e+09	5.292e+05	1.65e-10	1.438e-13
2	10.250	5.71e+09	5.060e+05	1.63e-10	3.190e-14
3	8.881	2.29e+10	5.127e+05	1.71e-10	8.419e-15
4	8.255	4.84e+09	4.327e+05	1.63e-10	3.221e-14
5	7.931	2.12e+10	4.389e+05	1.72e-10	7.797e-15
6	7.873	1.35e+10	4.310e+05	1.64e-10	1.148e-14
7	7.670	2.68e+10	7.150e+05	1.64e-10	9.630e-15
8	6.340	2.24e+10	4.377e+05	1.71e-10	7.293e-15
9	4.867	2.11e+10	4.652e+05	1.71e-10	8.263e-15
10	4.413	1.30e+10	4.576e+05	1.63e-10	1.261e-14
11	4.127	3.04e+09	5.070e+05	1.65e-10	6.042e-14
12	3.148	2.37e+10	4.879e+05	1.71e-10	7.724e-15
13	2.841	2.24e+10	4.107e+05	1.71e-10	6.861e-15
14	1.402	7.02e+09	4.377e+05	1.70e-10	2.329e-14
15	1.209	7.94e+09	4.381e+05	1.71e-10	2.067e-14

Fig. S61. ^{1}H DOSY NMR spectrum of **mon2** (112 mM) in DMSO-d_6 at 298 K and a table exporting the diffusion constants calculated for each peak used to determine the hydrodynamic diameter of the anionic (dH = 1.34 nm) and cationic (dH = 1.28 nm) components of **mon2**. Peaks 1, 2, 4, 6, 7, 10, 11 correspond to the anionic component of monomer **2** while peaks 3, 5, 8, 9, 12-15 correspond to the cationic component of **mon2**.

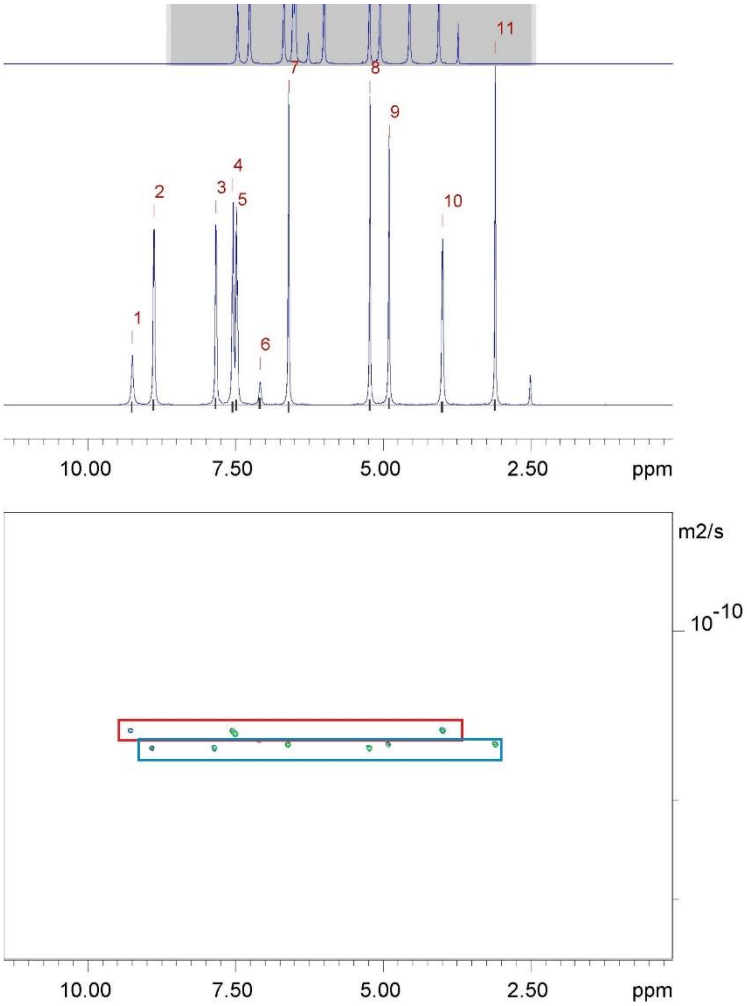

Peak name	F2 [ppm]	Io	error	D [m2/s]	error
1	9.256	4.12e+09	3.565e+05	1.51e-10	2.906e-14
2	8.888	1.58e+10	3.621e+05	1.61e-10	8.094e-15
3	7.838	1.50e+10	3.628e+05	1.62e-10	8.615e-15
4	7.550	1.80e+10	3.883e+05	1.50e-10	7.191e-15
5	7.484	1.77e+10	3.897e+05	1.52e-10	7.426e-15
6	7.091	2.72e+09	4.255e+05	1.58e-10	5.452e-14
7	6.602	1.98e+10	3.618e+05	1.60e-10	6.441e-15
8	5.225	2.05e+10	3.958e+05	1.62e-10	6.868e-15
9	4.898	1.77e+10	3.619e+05	1.60e-10	7.226e-15
10	3.997	1.82e+10	4.205e+05	1.51e-10	7.731e-15
11	3.107	1.89e+10	3.588e+05	1.58e-10	6.613e-15

Fig. S62. ^{1}H DOSY NMR spectrum of **mon3** (112 mM) in DMSO-d_6 at 298 K and a table exporting the diffusion constants calculated for each peak used to determine the hydrodynamic diameter of the anionic (dH = 1.44 nm) and cationic (dH = 1.37 nm) components of **mon3**. Peaks 1, 4 - 6, 10 correspond to the anionic component of monomer **3** while peaks 2, 3, 7- 9, 11 correspond to the cationic component of **mon3**.

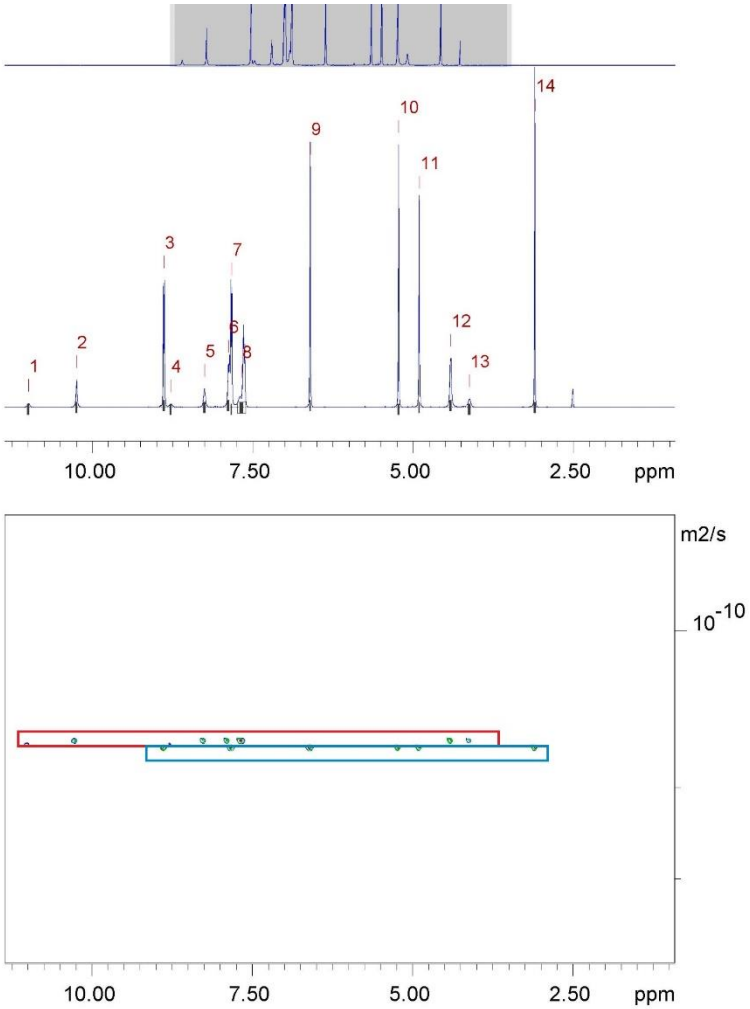

Peak name	F2 [ppm]	Io	error	D [m2/s]	error
1	10.993	5.34e+08	2.090e+05	1.64e-10	1.426e-13
2	10.246	2.42e+09	1.908e+05	1.62e-10	2.842e-14
3	8.882	1.14e+10	1.925e+05	1.68e-10	6.282e-15
4	8.778	4.52e+08	1.907e+05	1.65e-10	1.545e-13
5	8.250	2.63e+09	2.247e+05	1.63e-10	3.096e-14
6	7.876	6.14e+09	2.085e+05	1.63e-10	1.227e-14
7	7.827	1.01e+10	1.720e+05	1.68e-10	6.353e-15
8	7.672	1.49e+10	3.886e+05	1.63e-10	9.446e-15
9	6.601	1.16e+10	1.824e+05	1.67e-10	5.830e-15
10	5.225	1.14e+10	1.824e+05	1.67e-10	5.949e-15
11	4.903	9.84e+09	1.605e+05	1.67e-10	6.021e-15
12	4.414	6.52e+09	2.170e+05	1.62e-10	1.202e-14
13	4.120	1.40e+09	2.259e+05	1.64e-10	5.857e-14
14	3.101	1.21e+10	2.011e+05	1.68e-10	6.182e-15

Fig. S63. ^{1}H DOSY NMR spectrum of **mon4** (112 mM) in DMSO-d_6 at 298 K and a table exporting the diffusion constants calculated for each peak used to determine the hydrodynamic diameter of the anionic (dH = 1.34 nm) and cationic (dH = 1.31 nm) components of **mon4**. Peaks 1, 2, 4-6, 8, 12, 13 correspond to the anionic component of monomer **4** while peaks 3, 7, 9-11, 14 correspond to the cationic component of **mon4**.

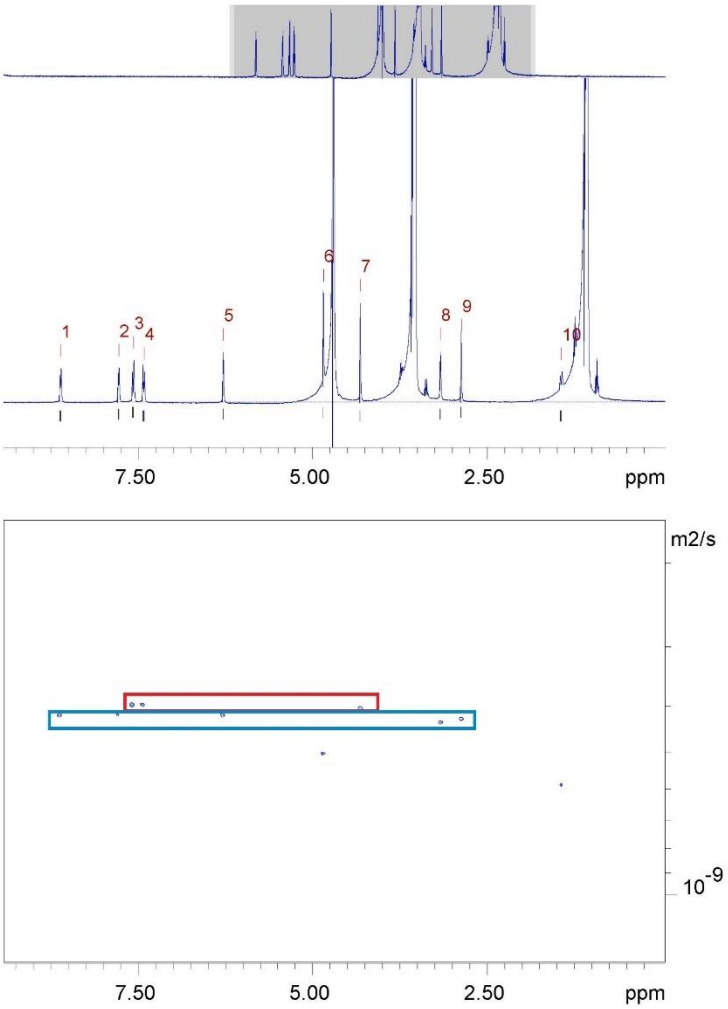

Peak name	F2 [ppm]	Io	error	D [m2/s]	error
1	8.609	7.40e+07	4.325e+04	4.20e-10	5.339e-13
2	7.776	9.04e+07	4.526e+04	4.19e-10	4.557e-13
3	7.566	1.05e+08	4.964e+04	3.96e-10	4.089e-13
4	7.414	9.42e+07	4.816e+04	3.98e-10	4.446e-13
5	6.276	8.11e+07	3.444e+04	4.15e-10	3.833e-13
6	4.842	1.10e+08	2.789e+04	5.03e-10	2.751e-13
7	4.313	9.05e+07	2.625e+04	4.07e-10	2.571e-13
8	3.166	7.92e+07	3.255e+04	4.35e-10	3.878e-13
9	2.868	8.21e+07	2.939e+04	4.26e-10	3.308e-13
10	1.439	1.02e+08	5.571e+04	5.89e-10	6.852e-13

Fig. S64. ^{1}H DOSY NMR spectrum of **mon1** (5.56 mM) in D_2O with 5 % EtOH at 298 K. Hydrodynamic diameters of the anionic and cationic components of **mon1** were calculated to be d_H = 1.10 nm and d_H = 1.04 nm respectively. Peaks 3, 4 and 7 correspond to the anionic component of **mon1** while peaks 1, 2, 5, 6 and 8 – 10 correspond to the cationic component of **mon1**.

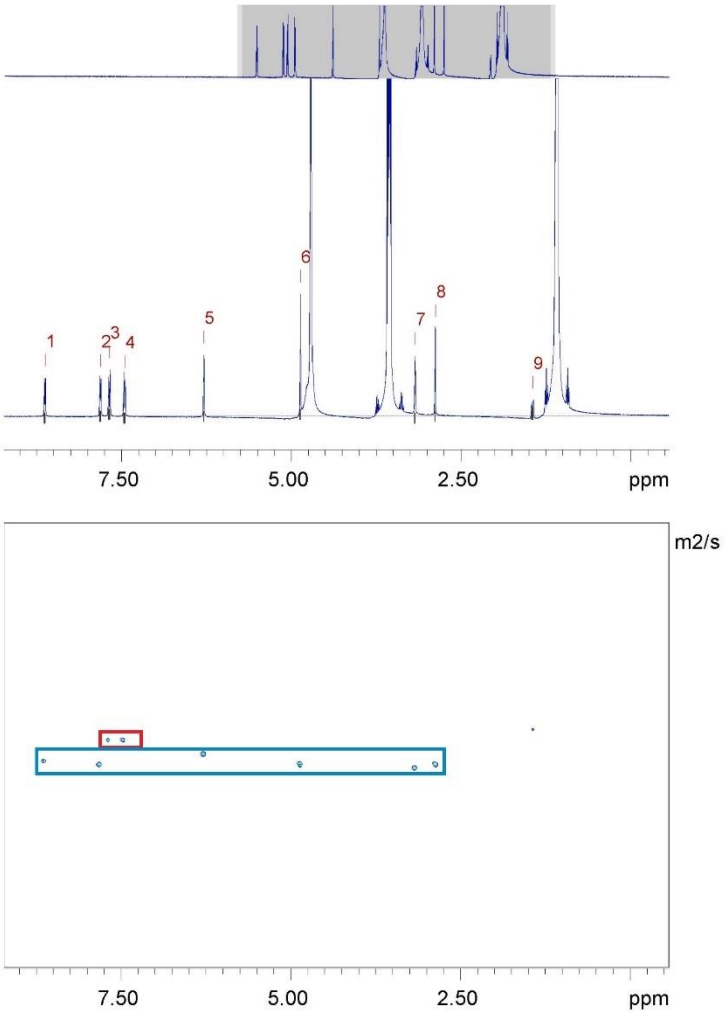

Peak name	F2 [ppm]	Io	error	D [m2/s]	error
1	8.624	1.18e+08	4.739e+04	4.42e-10	3.811e-13
2	7.807	1.33e+08	4.747e+04	4.44e-10	3.402e-13
3	7.674	1.57e+08	5.194e+04	4.03e-10	2.887e-13
4	7.451	1.46e+08	5.091e+04	4.02e-10	3.046e-13
5	6.283	1.29e+08	3.906e+04	4.29e-10	2.786e-13
6	4.861	1.85e+08	3.947e+04	4.45e-10	2.040e-13
7	3.172	1.57e+08	4.389e+04	4.53e-10	2.716e-13
8	2.875	1.43e+08	3.470e+04	4.42e-10	2.308e-13
9	1.441	6.38e+07	5.514e+04	3.82e-10	7.190e-13

Fig. S65. ^{1}H DOSY NMR spectrum of **mon2** (5.56 mM) in D_2O with 5 % EtOH at 298 K. Hydrodynamic diameters of the anionic and cationic components of **mon2** were calculated to be d_H = 1.05 nm and d_H = 0.98 nm respectively. Peaks 3 and 4 correspond to the anionic component of **mon2** while peaks 1, 2 and 5 – 9 correspond to the cationic component of **mon2**.

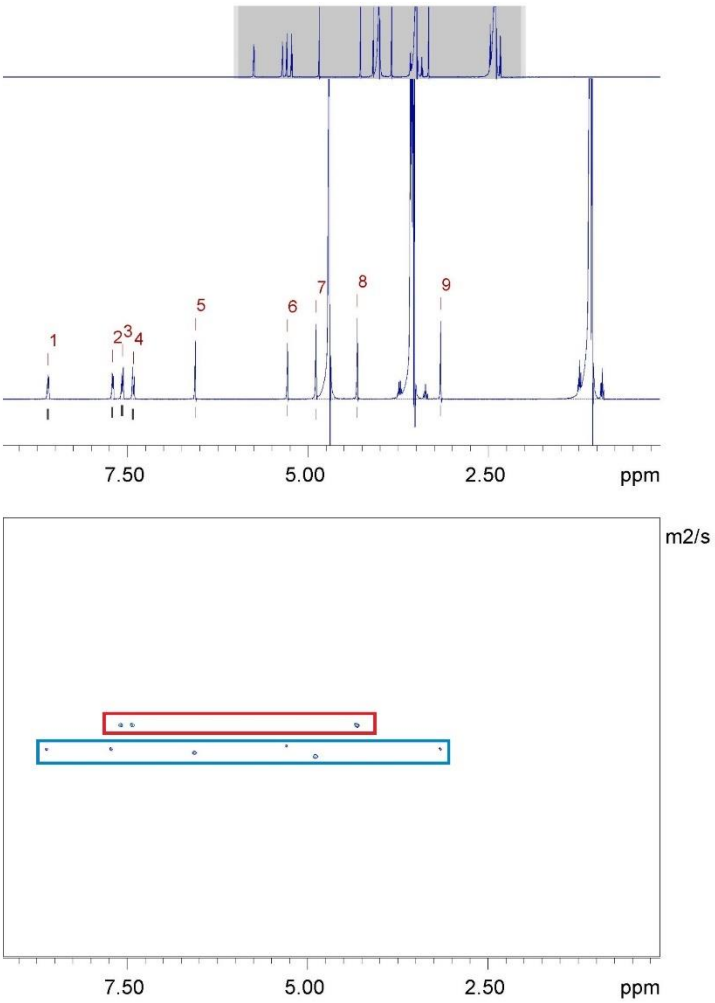

Peak name	F2 [ppm]	Io	error	D [m2/s]	error
1	8.595	9.79e+07	4.352e+04	4.43e-10	4.336e-13
2	7.703	1.01e+08	4.355e+04	4.44e-10	4.205e-13
3	7.567	1.31e+08	4.864e+04	4.00e-10	3.304e-13
4	7.417	1.27e+08	4.869e+04	4.01e-10	3.427e-13
5	6.555	1.00e+08	2.803e+04	4.46e-10	2.745e-13
6	5.283	7.40e+07	2.836e+04	4.39e-10	3.705e-13
7	4.886	1.29e+08	2.864e+04	4.55e-10	2.228e-13
8	4.314	1.21e+08	2.769e+04	4.01e-10	2.044e-13
9	3.160	8.09e+07	2.507e+04	4.39e-10	3.002e-13

Fig. S66. ^{1}H DOSY NMR spectrum of **mon3** (5.56 mM) in D_2O with 5 % EtOH at 298 K. Hydrodynamic diameters of the anionic and cationic components of **mon3** were calculated to be d_H = 1.09 nm and d_H = 0.98 nm respectively. Peaks 3, 4 and 8 correspond to the anionic component of **mon3** while peaks 1, 2, 5 – 7 and 9 correspond to the cationic component of **mon3**.

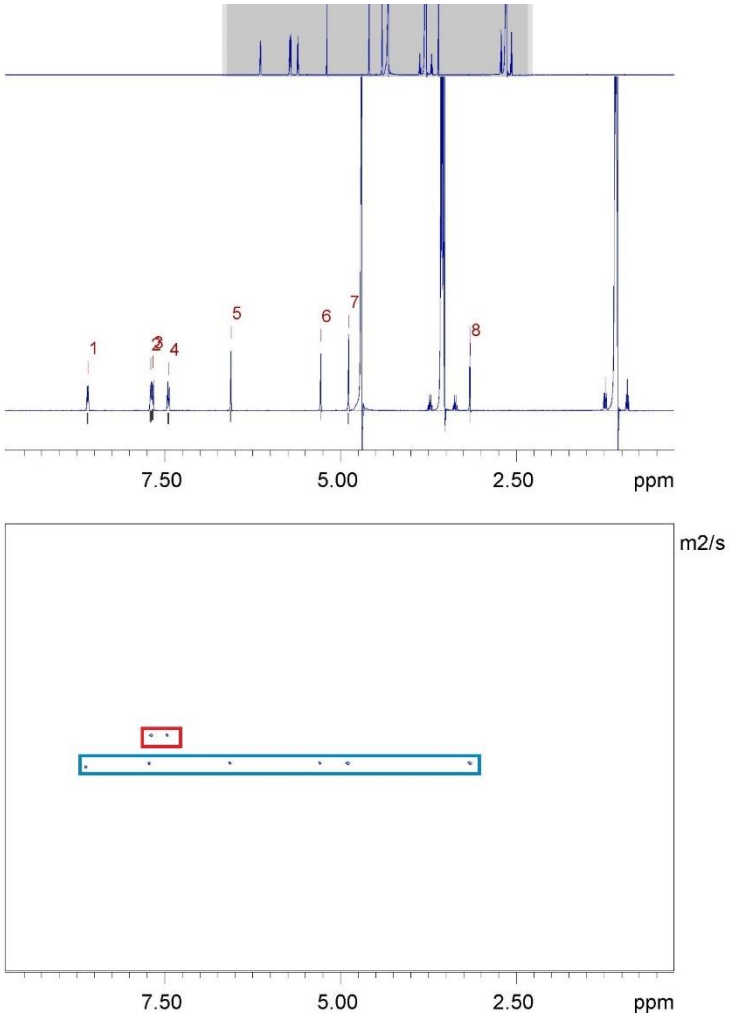

Peak name	F2 [ppm]	Io	error	D [m2/s]	error
1	8.594	1.15e+08	4.362e+04	4.49e-10	3.736e-13
2	7.697	1.26e+08	4.342e+04	4.42e-10	3.334e-13
3	7.670	1.52e+08	4.720e+04	3.95e-10	2.713e-13
4	7.445	1.32e+08	4.693e+04	3.94e-10	3.103e-13
5	6.558	1.10e+08	2.862e+04	4.45e-10	2.540e-13
6	5.279	1.14e+08	2.860e+04	4.44e-10	2.440e-13
7	4.883	1.60e+08	3.118e+04	4.45e-10	1.897e-13
8	3.157	1.24e+08	2.529e+04	4.45e-10	1.983e-13

Fig. S67. ^{1}H DOSY NMR spectrum of **mon4** (5.56 mM) in D_2O with 5 % EtOH at 298 K. Hydrodynamic diameters of the anionic and cationic components of **mon4** were calculated to be d_H = 1.11 nm and d_H = 0.98 nm respectively. Peaks 3 and 4 correspond to the anionic component of **mon4** while peaks 1, 2 and 5 – 8 correspond to the cationic component of **mon4**.

5. ^{1}H DOSY NMR experiments on polymers **poly1 – poly4**

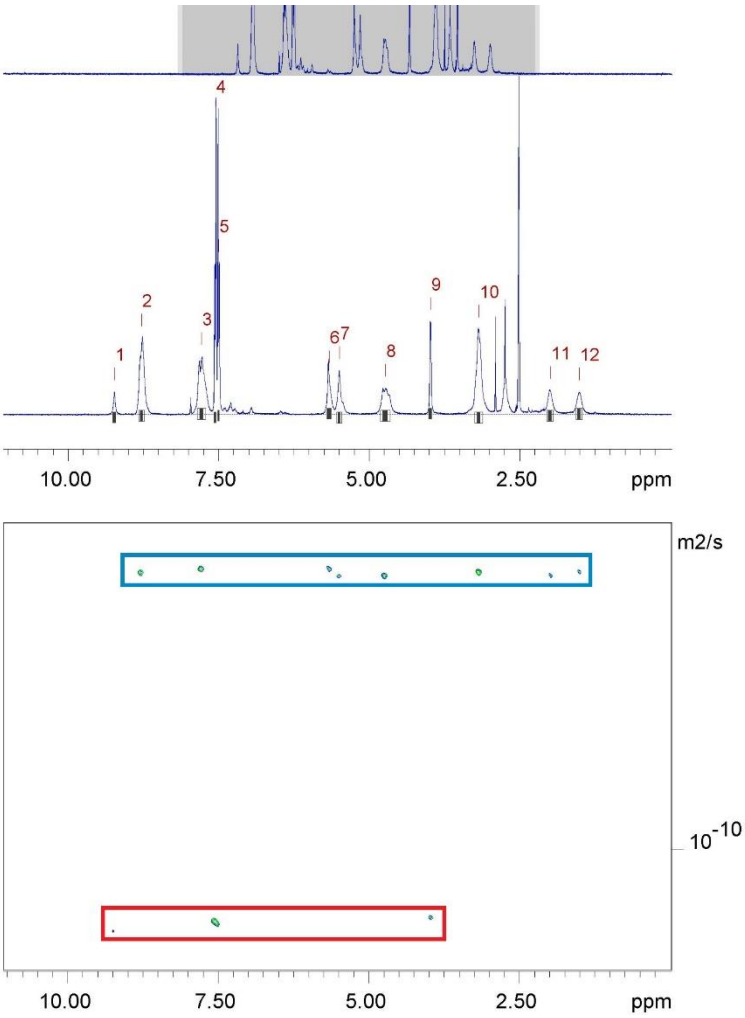

Peak name	F2 [ppm]	Io	error	D [m2/s]	error
1	9.227	1.95e+09	3.322e+06	1.43e-10	4.874e-13
2	8.778	1.49e+10	2.786e+06	2.97e-11	1.229e-14
3	7.781	1.60e+10	3.316e+06	2.95e-11	1.343e-14
4	7.551	1.38e+10	2.770e+06	1.37e-10	5.520e-14
5	7.495	1.20e+10	2.482e+06	1.38e-10	5.730e-14
6	5.659	6.81e+09	2.573e+06	2.96e-11	2.464e-14
7	5.493	5.94e+09	2.595e+06	3.04e-11	2.927e-14
8	4.728	9.14e+09	3.665e+06	3.04e-11	2.682e-14
9	3.977	7.38e+09	3.464e+06	1.34e-10	1.270e-13
10	3.179	2.05e+10	3.338e+06	3.00e-11	1.074e-14
11	1.992	5.29e+09	3.086e+06	3.03e-11	3.889e-14
12	1.513	4.65e+09	2.892e+06	3.01e-11	4.114e-14

Fig. S68. ^{1}H DOSY NMR spectrum of **poly1** (20 mg/mL) in DMSO-d_6 at 298 K. Hydrodynamic diameter of the anionic and cationic components of **poly1** were calculated to be d_H = 1.59 nm and d_H = 7.31 nm respectively. Peaks 1, 4, 5 and 9 correspond to the anionic SSA, while peaks 2, 3, 6,-8, 10-12 correspond to the cationic polymer backbone.

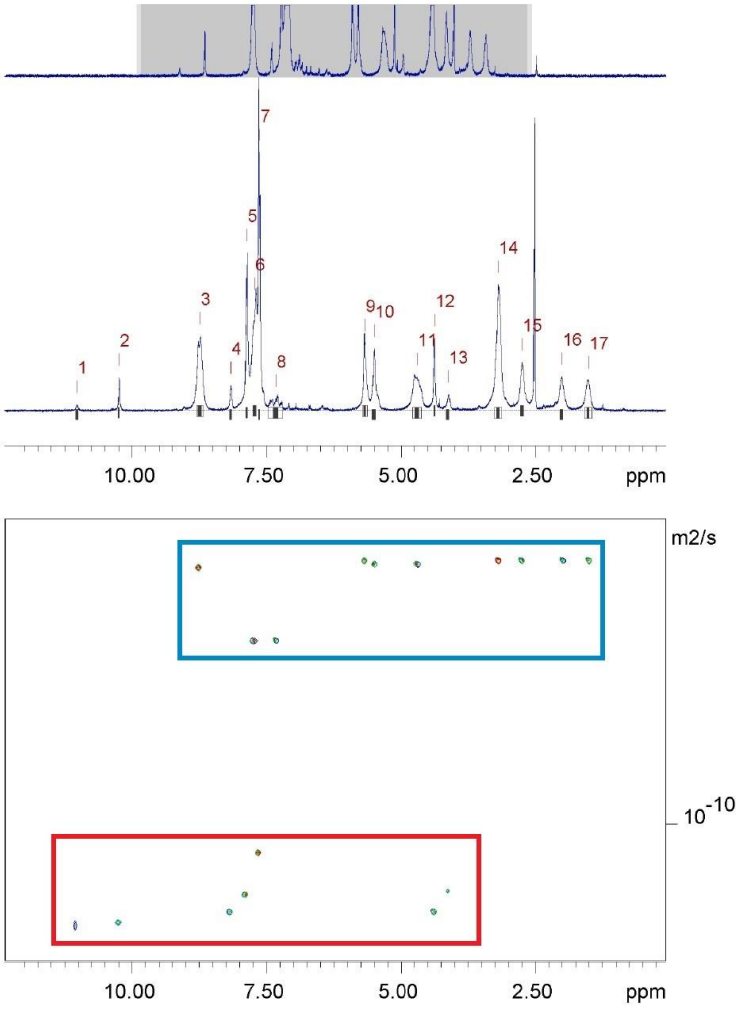

Peak name	F2 [ppm]	Io	error	D [m2/s]	error
1	11.024	5.91e+08	7.689e+06	1.66e-10	4.231e-12
2	10.243	1.92e+09	6.199e+06	1.61e-10	1.023e-12
3	8.741	2.08e+10	6.566e+06	2.81e-11	1.939e-14
4	8.165	2.27e+09	6.807e+06	1.54e-10	9.083e-13
5	7.869	1.52e+10	6.583e+06	1.42e-10	1.223e-13
6	7.721	2.02e+10	5.699e+06	4.06e-11	2.468e-14
7	7.635	2.29e+10	5.425e+06	1.14e-10	5.489e-14
8	7.330	5.87e+09	1.072e+07	4.05e-11	1.597e-13
9	5.677	1.18e+10	5.810e+06	2.70e-11	2.912e-14
10	5.504	9.28e+09	5.344e+06	2.77e-11	3.504e-14
11	4.693	1.34e+10	7.376e+06	2.78e-11	3.358e-14
12	4.369	5.88e+09	6.092e+06	1.55e-10	3.152e-13
13	4.122	2.22e+09	8.252e+06	1.39e-10	1.031e-12
14	3.188	3.28e+10	6.932e+06	2.73e-11	1.266e-14
15	2.744	8.22e+09	5.046e+06	2.72e-11	3.668e-14
16	2.003	5.03e+09	4.461e+06	2.72e-11	5.301e-14
17	1.514	8.18e+09	6.732e+06	2.74e-11	4.952e-14

Fig. S69. ^{1}H DOSY NMR spectrum of **poly2** (20 mg/mL) in DMSO-d_6 at 298 K. Hydrodynamic diameter of the anionic and cationic components of **poly2** were calculated to be d_H = 1.49 nm and d_H = 7.29 nm respectively. Peaks 1, 2, 4, 5, 7, 12, 13 correspond to the anionic SSA, while peaks 3, 6, 8, 9 - 11, 14 -17 correspond to the cationic polymer backbone.

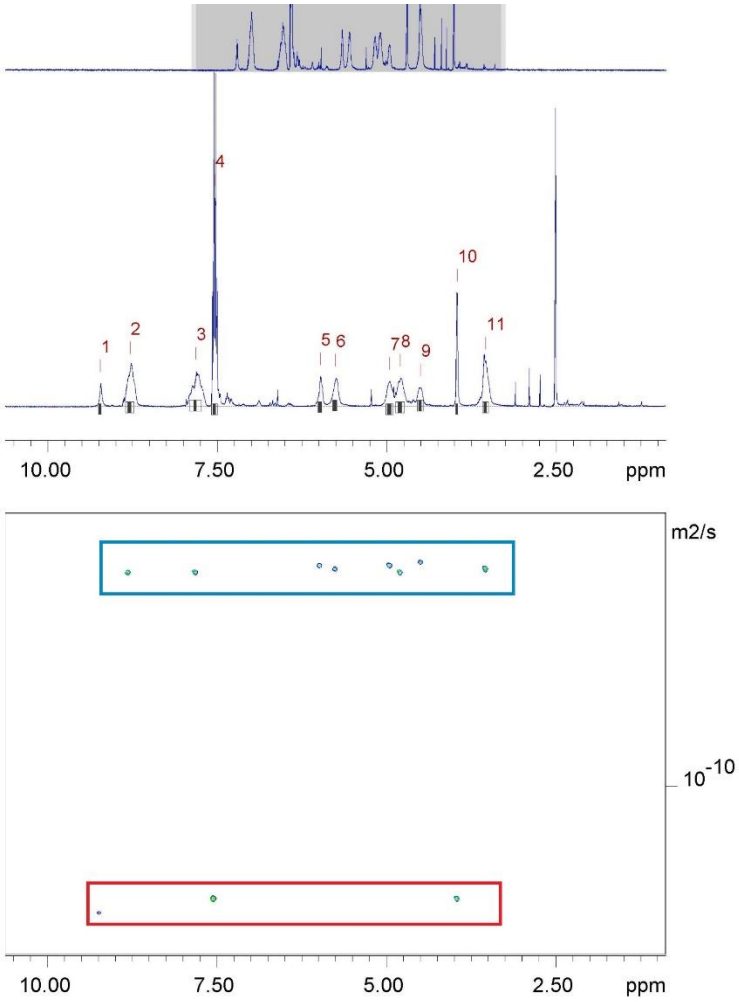

Peak name	F2 [ppm]	Io	error	D [m2/s]	error
1	9.226	2.79e+09	3.036e+06	1.63e-10	3.650e-13
2	8.791	1.49e+10	3.230e+06	4.32e-11	2.068e-14
3	7.822	1.55e+10	3.725e+06	4.32e-11	2.293e-14
4	7.542	3.92e+10	3.951e+06	1.55e-10	3.244e-14
5	5.980	4.91e+09	2.213e+06	4.22e-11	4.201e-14
6	5.761	6.38e+09	2.431e+06	4.26e-11	3.585e-14
7	4.959	7.67e+09	2.807e+06	4.26e-11	3.437e-14
8	4.804	1.08e+10	3.234e+06	4.34e-11	2.852e-14
9	4.506	5.55e+09	2.705e+06	4.20e-11	4.520e-14
10	3.962	1.10e+10	2.600e+06	1.56e-10	7.646e-14
11	3.543	1.31e+10	2.626e+06	4.26e-11	1.887e-14

Fig. S70. ^{1}H DOSY NMR spectrum of **poly3** (20 mg/mL) in DMSO-d_6 at 298 K. Hydrodynamic diameter of the anionic and cationic components of **poly3** were calculated to be d_H = 1.39 nm and d_H = 4.99 nm respectively. Peaks 1, 4, 10 correspond to the anionic SSA, while peaks 2, 3, 5 – 9, 11 correspond to the cationic polymer backbone.

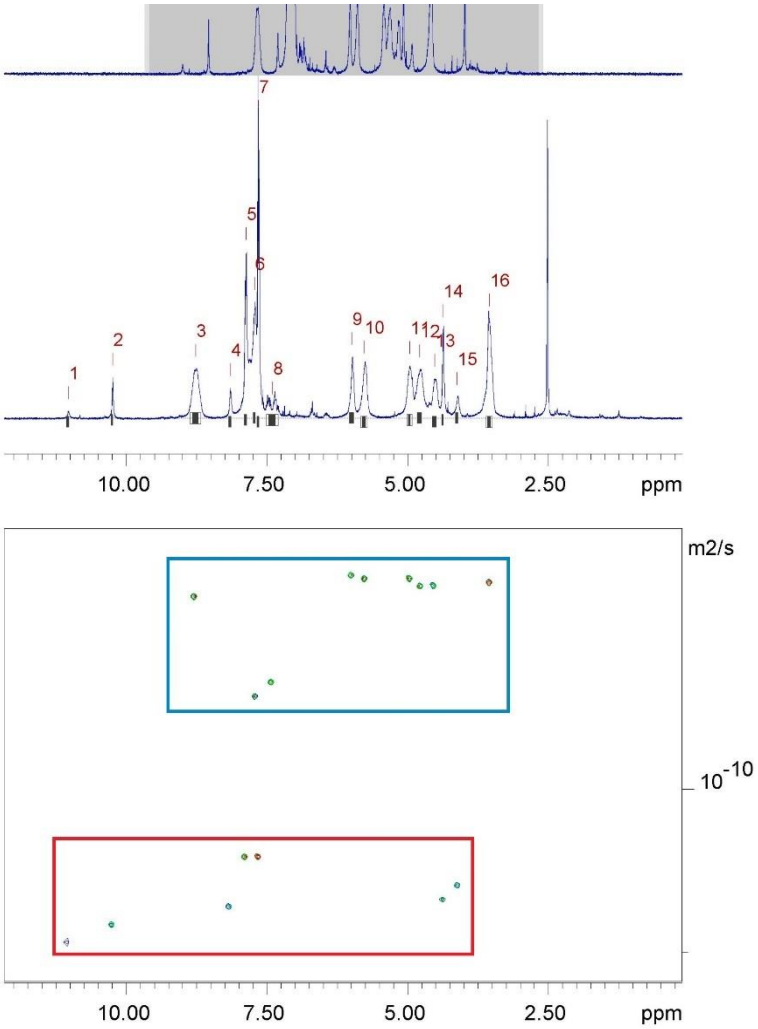

Peak name	F2 [ppm]	Io	error	D [m2/s]	error
1	11.031	7.84e+08	6.757e+06	1.92e-10	3.285e-12
2	10.244	2.87e+09	5.996e+06	1.78e-10	7.422e-13
3	8.766	2.28e+10	8.331e+06	4.37e-11	3.466e-14
4	8.150	3.25e+09	6.354e+06	1.64e-10	6.471e-13
5	7.874	1.91e+10	5.898e+06	1.34e-10	8.446e-14
6	7.717	1.52e+10	4.674e+06	6.72e-11	4.392e-14
7	7.650	3.12e+10	5.911e+06	1.33e-10	5.165e-14
8	7.404	1.01e+10	9.867e+06	6.29e-11	1.310e-13
9	5.990	1.10e+10	5.389e+06	4.01e-11	4.304e-14
10	5.773	1.52e+10	6.320e+06	4.05e-11	3.674e-14
11	4.963	1.36e+10	5.662e+06	4.07e-11	3.706e-14
12	4.784	1.37e+10	5.703e+06	4.17e-11	3.765e-14
13	4.523	8.58e+09	5.219e+06	4.21e-11	5.566e-14
14	4.374	6.42e+09	5.164e+06	1.60e-10	2.596e-13
15	4.124	2.85e+09	6.629e+06	1.49e-10	7.040e-13
16	3.549	2.75e+10	6.359e+06	4.13e-11	2.079e-14

Fig. S71. ^{1}H DOSY NMR spectrum of **poly4** (20 mg/mL) in DMSO-d_6 at 298 K. Hydrodynamic diameter of the anionic and cationic components of **poly4** were calculated to be d_H = 1.30 nm and d_H = 4.69 nm respectively. Peaks 1, 2, 4, 5, 7, 14, 15 correspond to the anionic SSA, while peaks 3, 6, 8 - 13, 16 correspond to the cationic polymer backbone.

Table S1. Overview of diffusion coefficients and hydrodynamic diameter for monomers **mon1 - mon4** and polymers **poly1 – poly4** in DMSO-d_6 and D_2O at 298 K. Errors for diffusion constants are no greater than ± 1 x 10-13 m^2/s.

Compound	Solvent	Cation		Anion	
		D (m^2/s)	d_H (nm)	D (m^2/s)	d_H (nm)
Mon 1	DMSO-d_6	1.67×10^{-10}	1.31	1.55×10^{-10}	1.41
Mon 2	DMSO-d_6	1.71×10^{-10}	1.28	1.64×10^{-10}	1.34
Mon 3	DMSO-d_6	1.61×10^{-10}	1.37	1.52×10^{-10}	1.44
Mon 4	DMSO-d_6	1.68×10^{-10}	1.31	1.63×10^{-10}	1.34
Mon 1	D_2O	4.18×10^{-10}	1.04	3.97×10^{-10}	1.10
Mon 2	D_2O	4.45×10^{-10}	0.98	4.17×10^{-10}	1.05
Mon 3	D_2O	4.44×10^{-10}	0.98	4.0×10^{-10}	1.09
Mon 4	D_2O	4.46×10^{-10}	0.98	3.94×10^{-10}	1.11
Poly1	DMSO-d_6	3.0×10^{-11}	7.31	1.38×10^{-10}	1.59
Poly2	DMSO-d_6	3.0×10^{-11}	7.29	1.47×10^{-10}	1.49
Poly3	DMSO-d_6	4.39×10^{-11}	4.99	1.58×10^{-10}	1.39
Poly4	DMSO-d_6	4.67×10^{-11}	4.69	1.69×10^{-10}	1.30

6. Quantitative ^{1}H NMR experiments on monomers **mon1 – mon4**

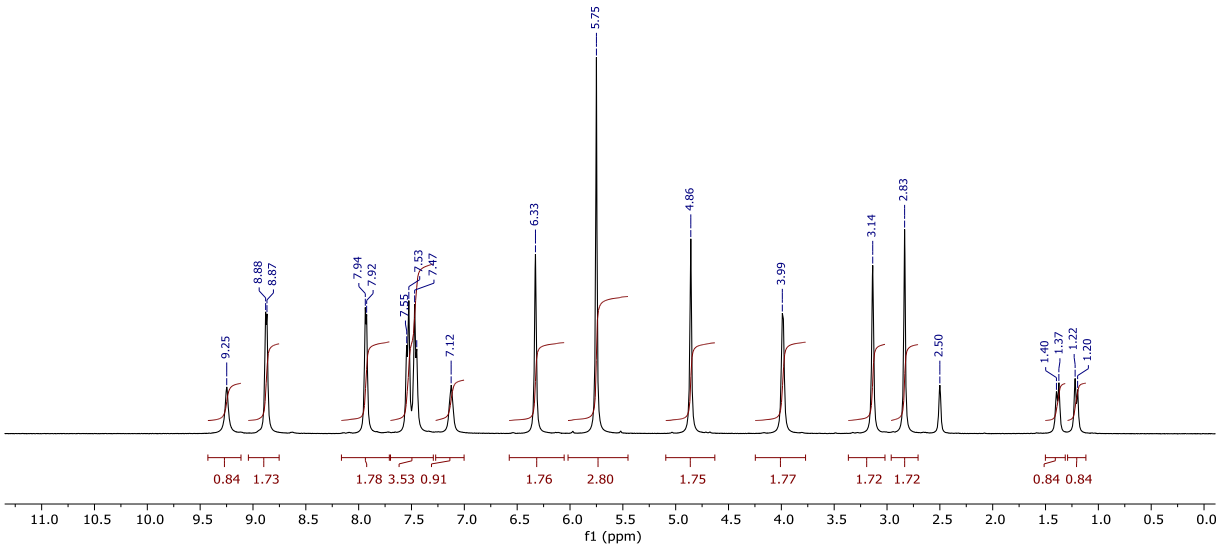

Fig. S72. ^{1}H NMR spectrum with a delay (d_1 = 60 s) of **mon1** (112 mM) in DMSO-d_6/ 1.0 % DCM. Comparative integration indicated that 12 % of both cationic and anionic components of the sample have become NMR silent.

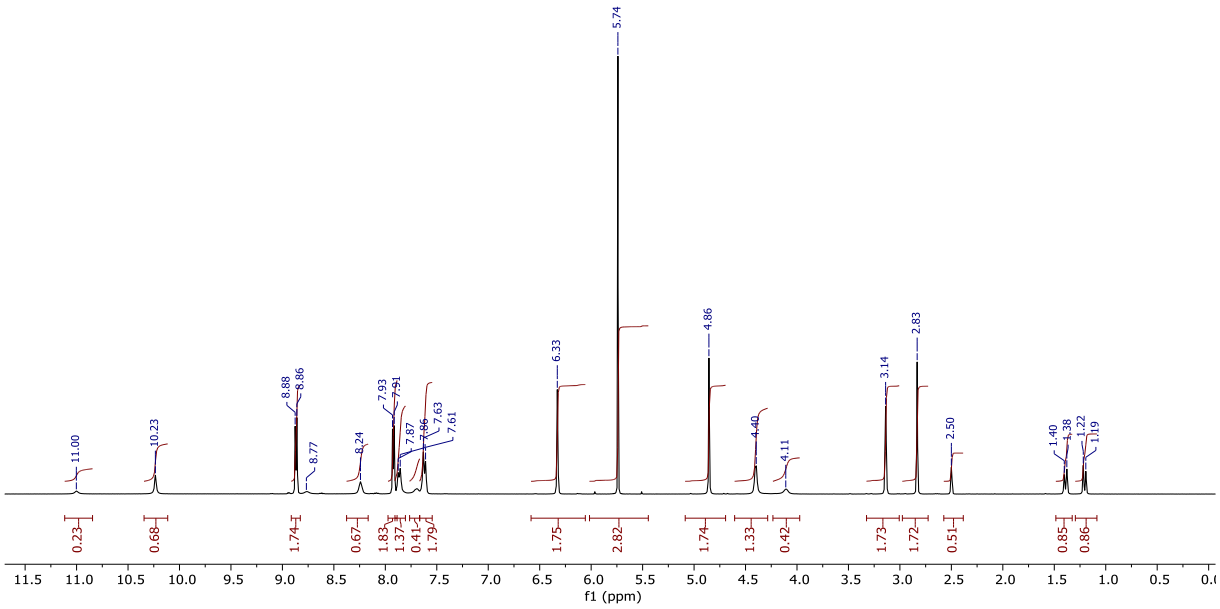

Fig. S73. ^{1}H NMR spectrum with a delay (d_1 = 60 s) of **mon2** (112 mM) in DMSO-d_6/ 1.0 % DCM. Comparative integration indicated respectively that 12.5 % and 10.5 % of the cationic and anionic components of the sample have become NMR silent.

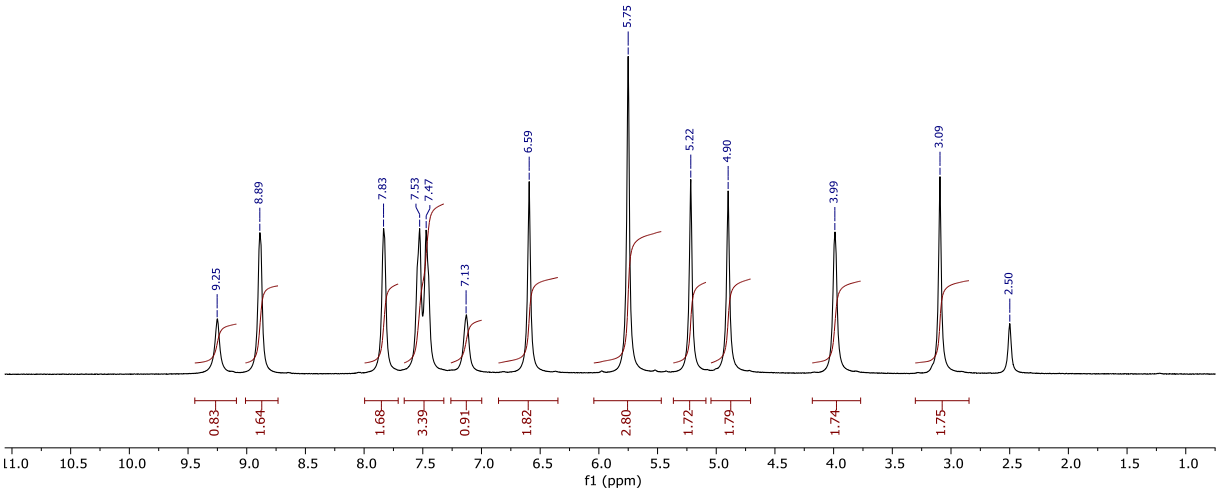

Fig. S74. ^{1}H NMR spectrum with a delay (d_1 = 60 s) of monomer **3** (112 mM) in DMSO-d_6/ 1.0 % DCM. Comparative integration indicated respectively that 9 % and 15 % of the cationic and anionic components of the sample have become NMR silent.

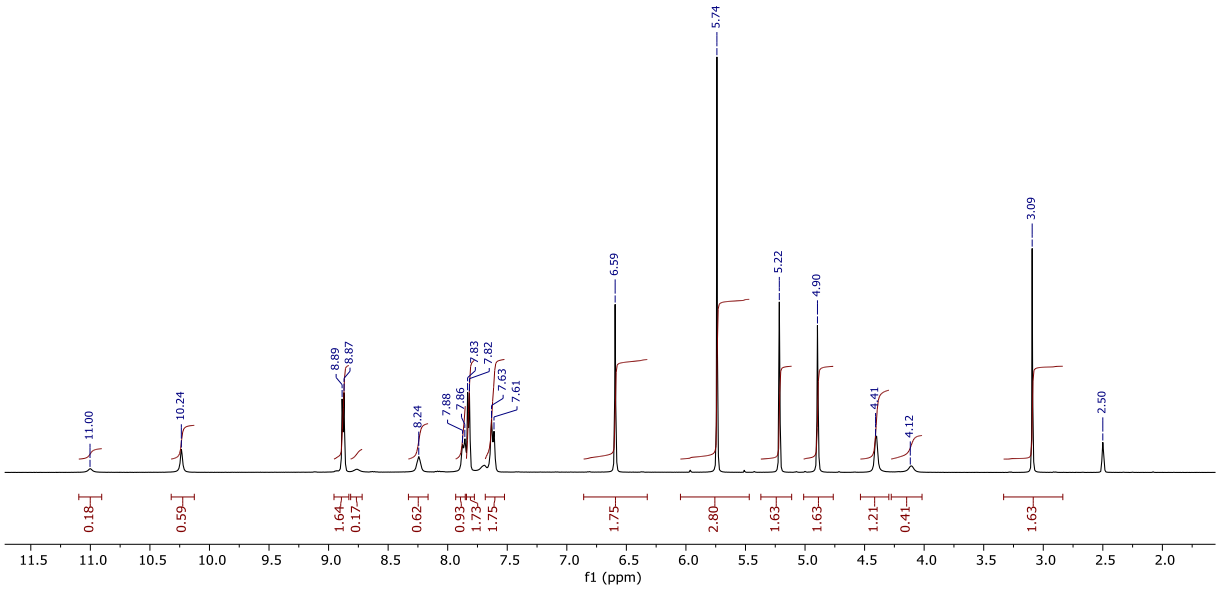

Fig. S75. ^{1}H NMR spectrum with a delay (d_1 = 60 s) of **mon4** (112 mM) in DMSO-d_6/ 1.0 % DCM. Comparative integration indicated that 12.5 % of both cationic and anionic components of the sample have become NMR silent.

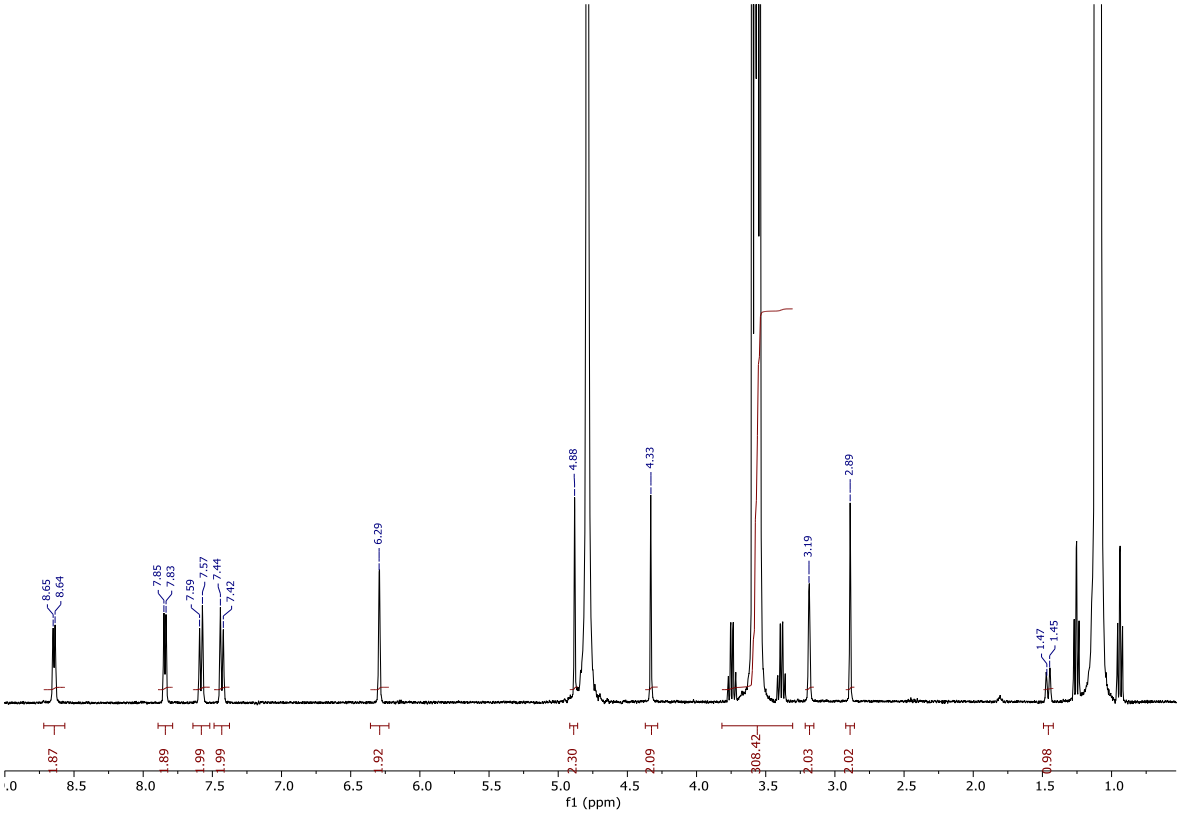

Fig. S76. ^{1}H NMR spectrum with a delay (d_1 = 60 s) of **mon1** (5.56 mM) in D_2O/ 5.0 % EtOH. Comparative integration indicated 4 % of the anionic component and 0.5 % of the cation component has become NMR silent, concluding that no apparent loss is present in this sample.

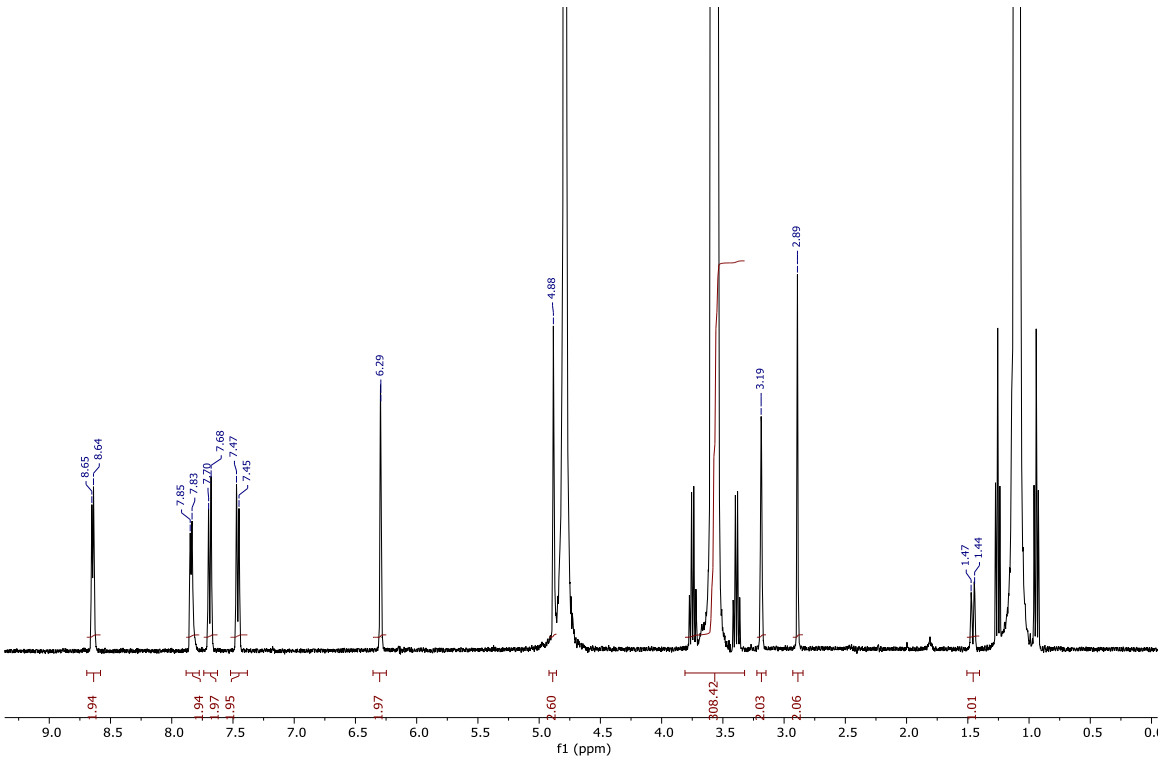

Fig. S77. ^{1}H NMR spectrum with a delay (d_1 = 60 s) of **mon2** (5.56 mM) in D_2O/ 5.0 % EtOH. Comparative integration indicated 1.5 % of the anionic and the cation components have become NMR silent, concluding that no loss is present in this sample.

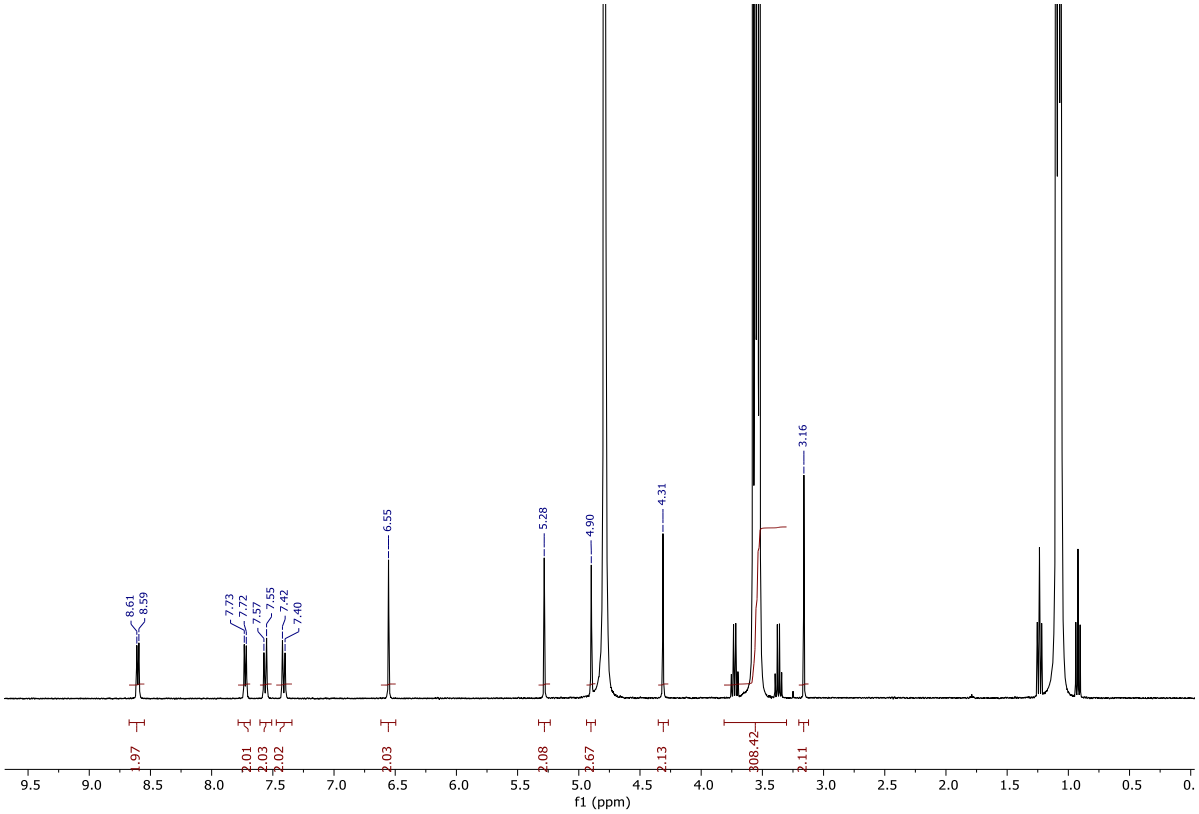

Fig. S78. ^{1}H NMR spectrum with a delay (d_1 = 60 s) of monomer **3** (5.56 mM) in D_2O/ 5.0 % EtOH. Comparative integration indicated that no loss is present for both the anionic and the cation components of the sample.

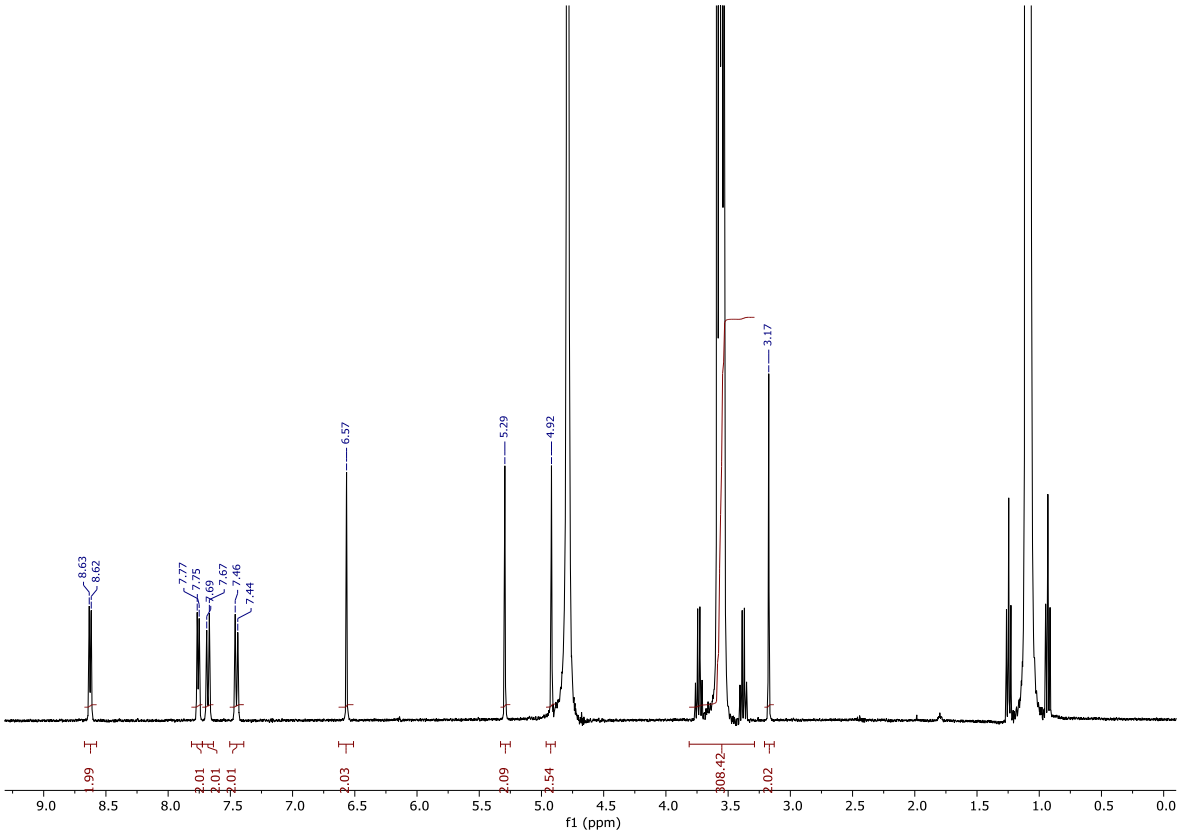

Fig. S79. ^{1}H NMR spectrum with a delay (d_1 = 60 s) of **mon4** (5.56 mM) in D_2O/ 5.0 % EtOH. Comparative integration indicated that no loss is present for both the anionic and the cation components of the sample.

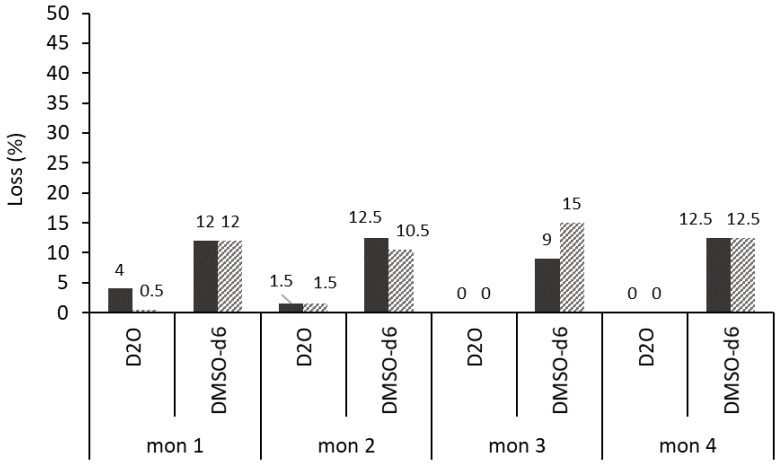

Fig. S80. Overview of the results from quantitative ^{1}H NMR studies obtained from DMSO-d_6, standardised with 1.0% DCM at 112 mM and D_2O standardised with 5.0% ethanol at 5.56 mM. The graph shows the proportion, as percentage, of cation (solid fill) and anion (pattern fill) in **mon1 - mon4** to become NMR silent. All quantitative ^{1}H NMR experiments were conducted with a delay time (d_1) of 60 s at 298 K.

7. Relative quantitative ^{1}H NMR studies on polymers, poly1 – poly4

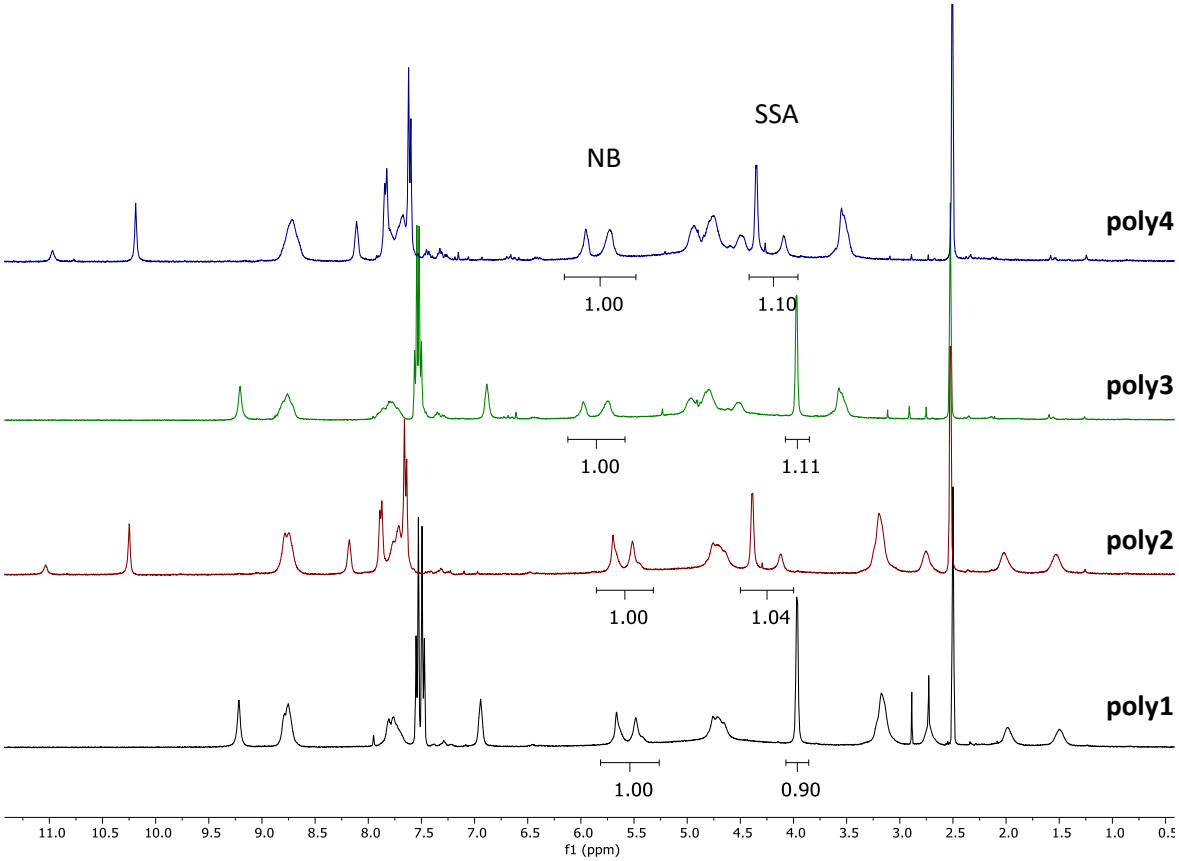

Fig. S81. Relative qNMR on **poly1 – poly4** with relaxation delay of 90 seconds. Comparative integration of integrals of interests affords the ratio between the cation (NB polymer) and anion (SSA) within the polymer backbone.

8. ^{1}H NMR self-association studies on **mon1 – mon4**

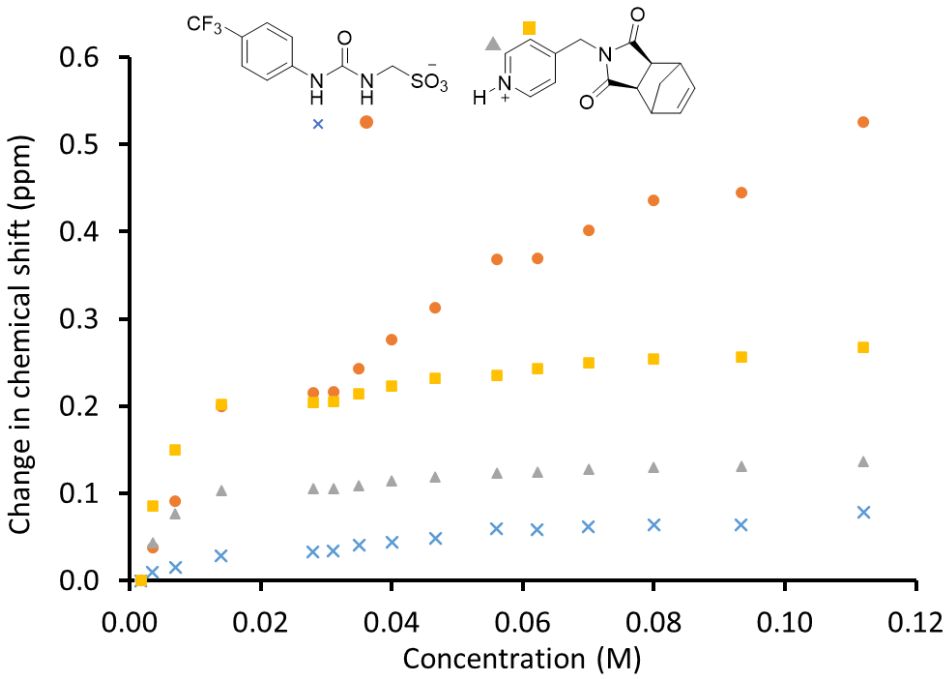

Fig. S82. Graph illustrating the ^{1}H NMR down-field change in chemical shift of protons with increasing concentration of **mon1** in DMSO- d_6 0.5% H_2O (298 K).

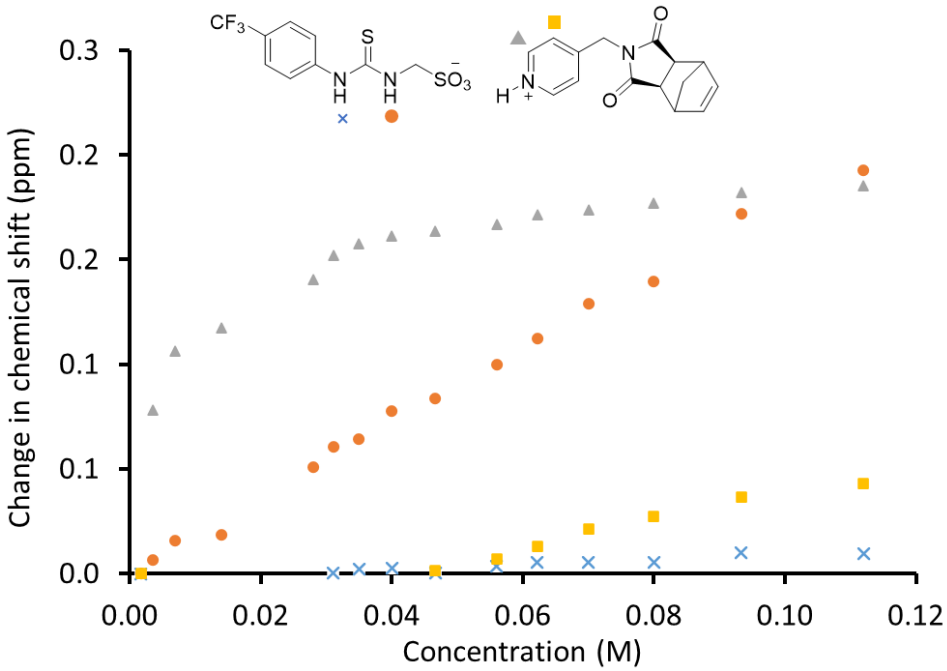

Fig. S83. Graph illustrating the ^{1}H NMR down-field change in chemical shift of protons with increasing concentration of **mon2** in DMSO- d_6 0.5% H_2O (298 K).

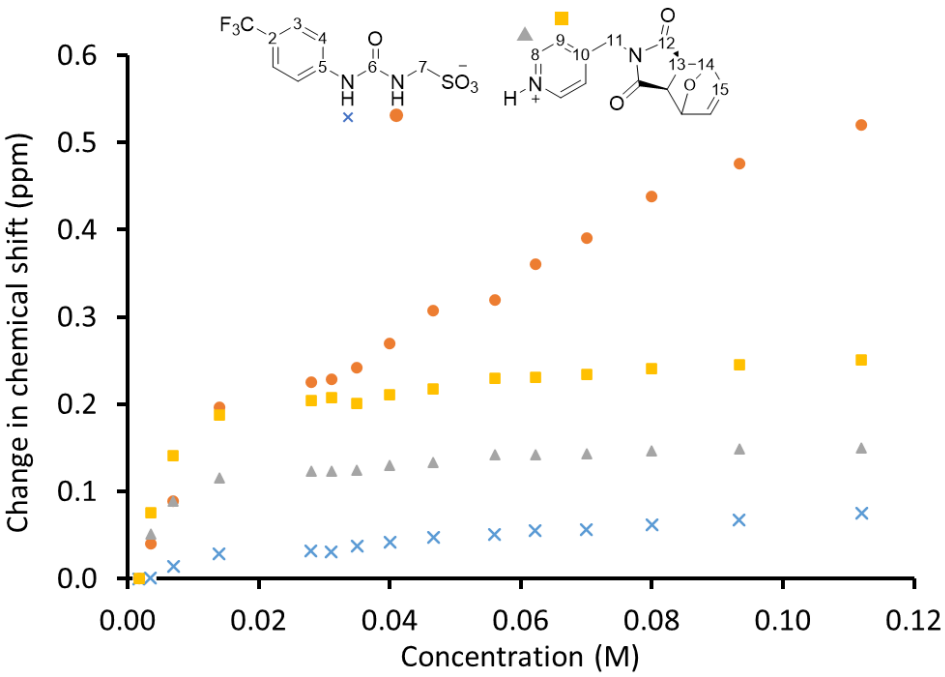

Fig. S84. Graph illustrating the ^{1}H NMR down-field change in chemical shift of protons with increasing concentration of **mon3** in DMSO- d_6 0.5% H_2O (298 K).

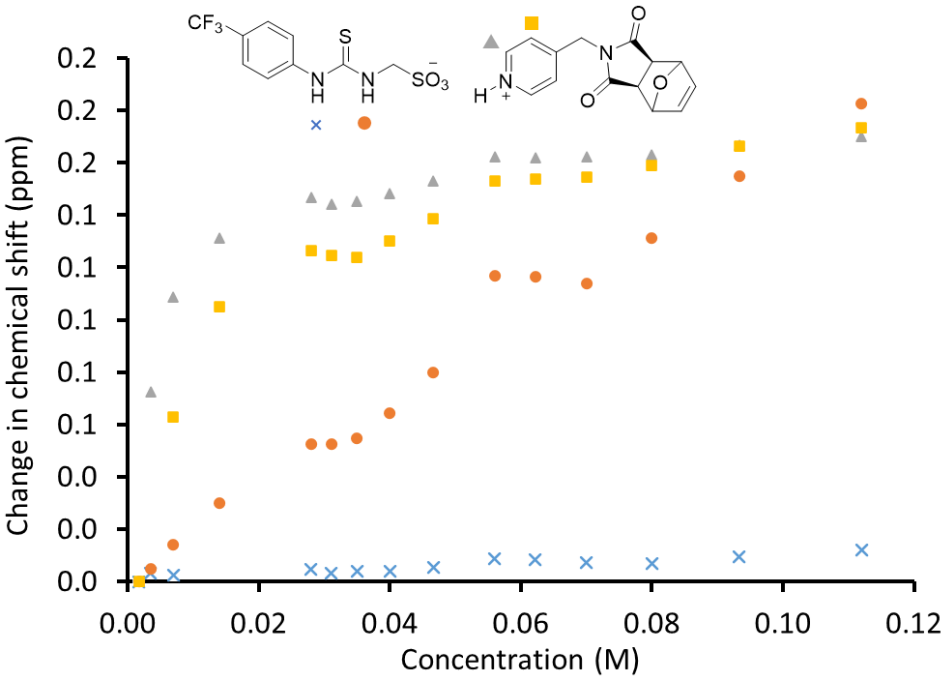

Fig. S85. Graph illustrating the ^{1}H NMR down-field change in chemical shift of protons with increasing concentration of **mon4** in DMSO- d_6 0.5% H_2O (298 K).

9. Dynamic light scattering of mon1 - mon4 and poly1 – poly4

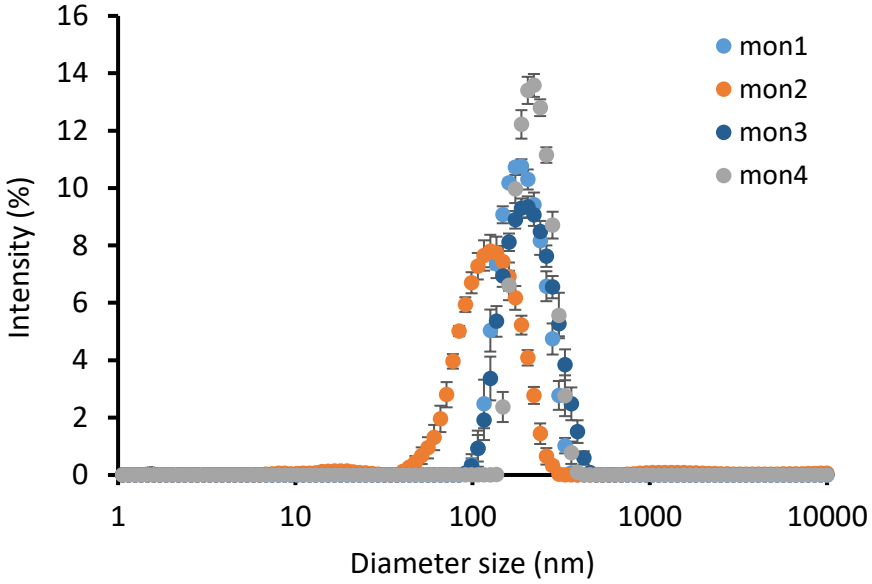

Fig. S86. Average intensity size distribution of **mon1 – mon4** measured at a concentration of 5.56 mM in a solution of H_2O with 5.0% EtOH at 298 K (10 DLS measurements were run).

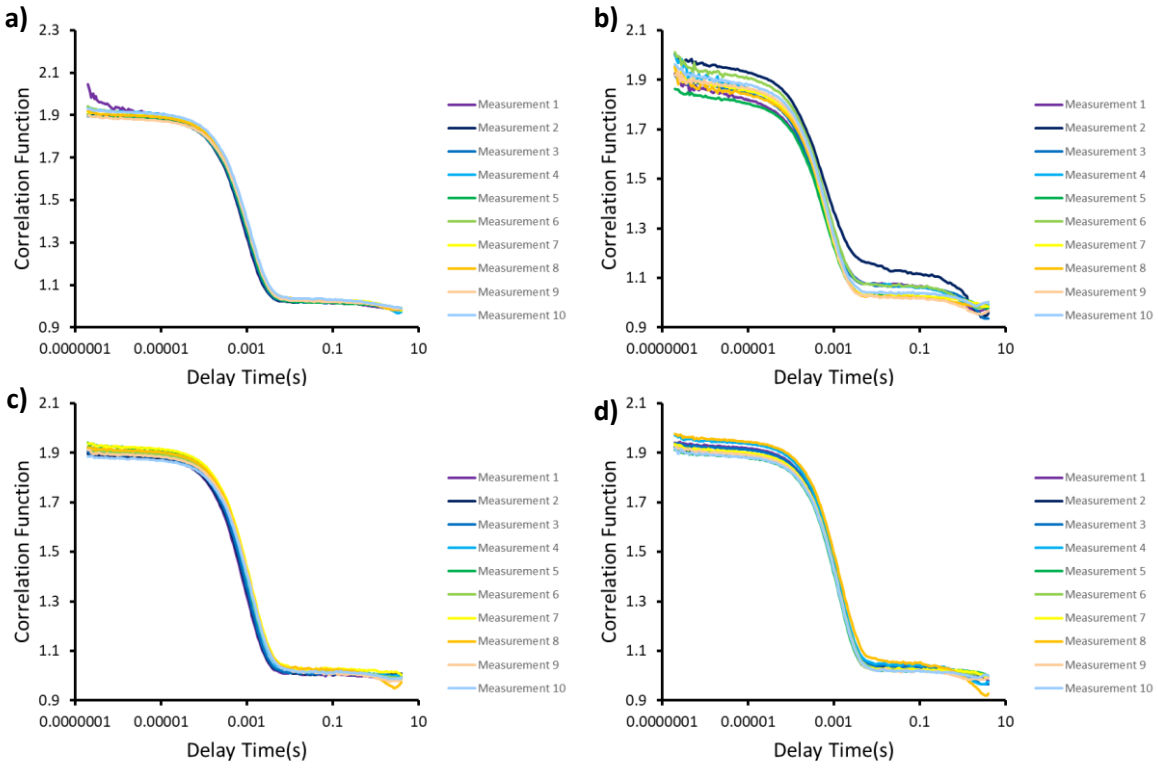

Fig. S87. Correlation function of (a) **mon1**, (b) **mon2**, (c) **mon3 and** (d) **mon4** measured at a concentration of 5.56 mM in a solution of H_2O with 5.0% EtOH at 298 K.

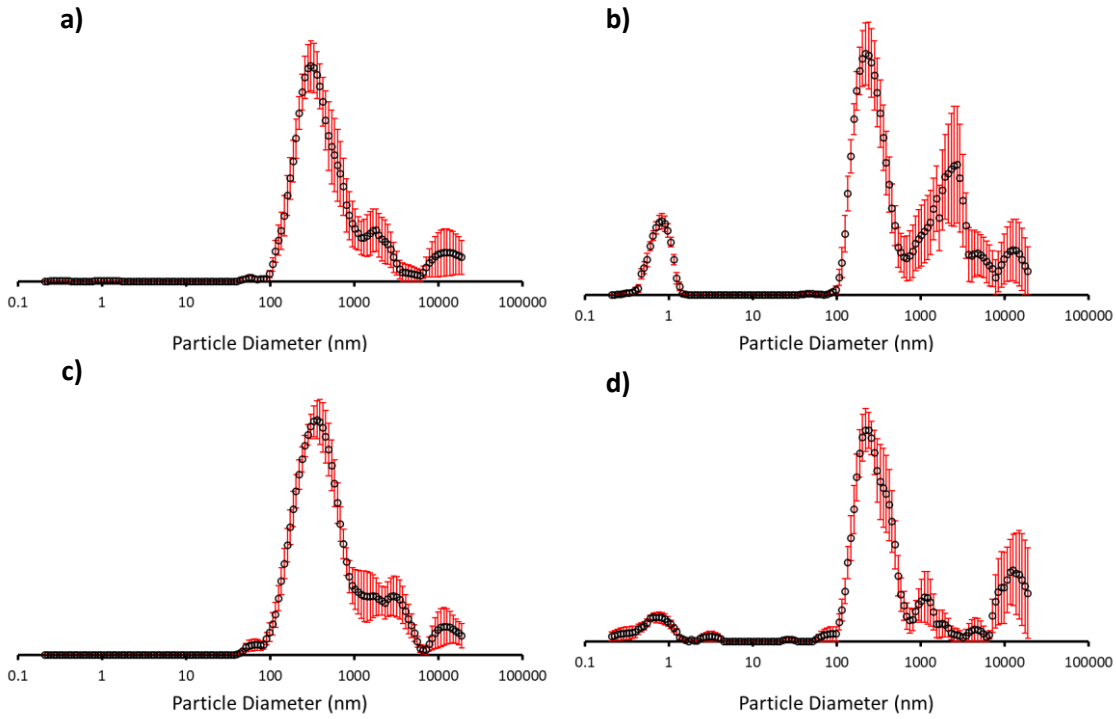

Fig. S88. Average intensity size distribution of **mon1 – mon4** measured at a concentration of 112 mM in DMSO at 298 K (10 DLS measurements were run).

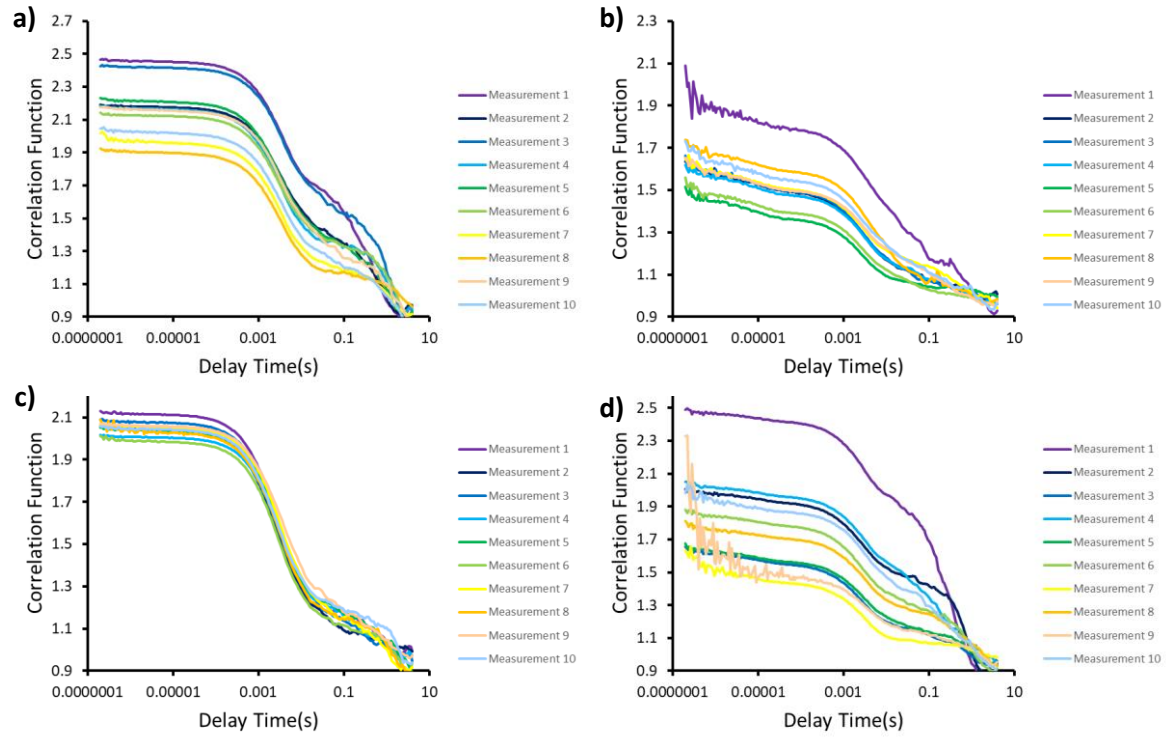

Fig. S89. Correlation function of (a) **mon1**, (b) **mon2**, (c) **mon3 and** (d) **mon4** measured at a concentration of 112 mM in DMSO at 298 K.

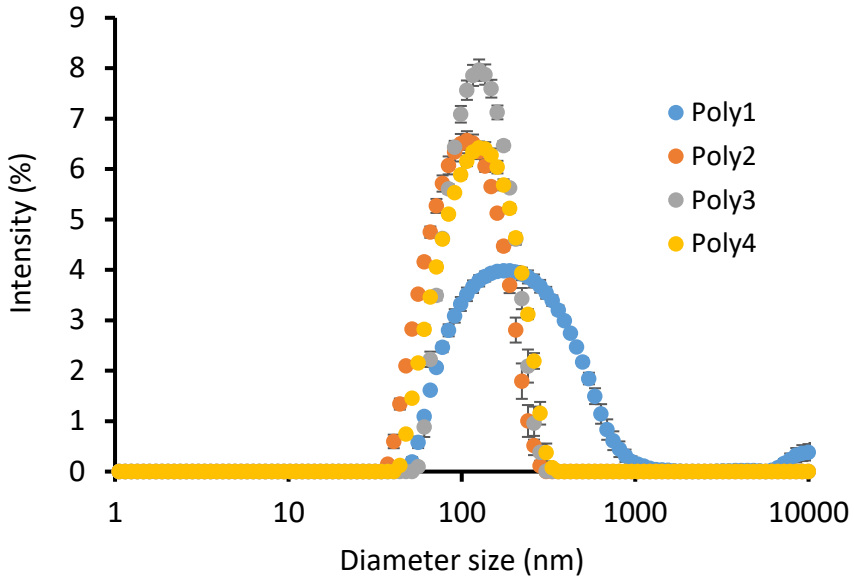

Fig. S90. Average intensity size distribution of polymers **poly1 – poly4** measured at a concentration of 1 mg/mL in a solution of H_2O with 1.0% DMSO at 298 K.

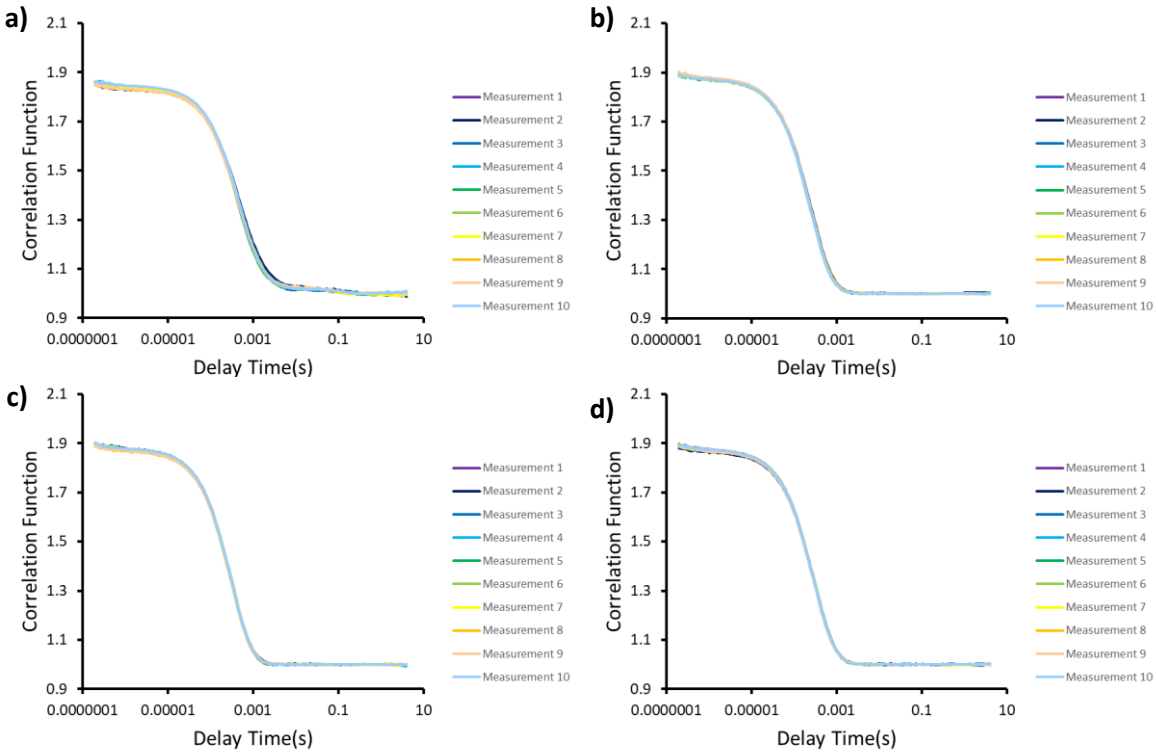

Fig. S91. Correlation function of polymers **poly1 – poly4** measured at a concentration of 1 mg/mL in a solution of H_2O with 1.0% DMSO at 298 K.

Table S2. Overview of average DLS intensity particle size distribution, zeta potential and CMC measurements obtained for **mon1 – mon4** at a concentration of 5.56 mM in H_2O/5.0% EtOH solution and for polymers **poly1 – poly4** at a concentration of 1 mg/mL in H_2O/1.0% DMSO solution at 298 K. a = CMC of polymers could not be measured as above the solubility limit.

	Solvent system	Concentration	DH (nm)	Polydispersity (%)	Zeta potential (mV)	CMC
mon 1	H2O/5% EtOH	5.56 mM	194	15 (± 1.49)	- 11	10.11 mM
mon 2	H2O/5% EtOH	5.56 mM	131	21 (± 1.42)	- 11	5.33 mM
mon 3	H2O/5% EtOH	5.56 mM	216	17 (± 1.54)	- 3	n.a.
mon 4	H2O/5% EtOH	5.56 mM	226	10 (± 2.25)	- 10	7.84 mM
Poly 1	1% DMSO	1 mg/mL	246	27 (± 0.37)	+ 32	a
Poly 2	1% DMSO	1 mg/mL	112	21 (± 0.32)	+ 49	a
Poly 3	1% DMSO	1 mg/mL	134	21 (± 0.31)	+ 54	a
Poly 4	1% DMSO	1 mg/mL	134	17 (± 0.6)	+ 52	a

10. Antibacterial activity studies of mon1 – mon4 and poly1 – poly 4

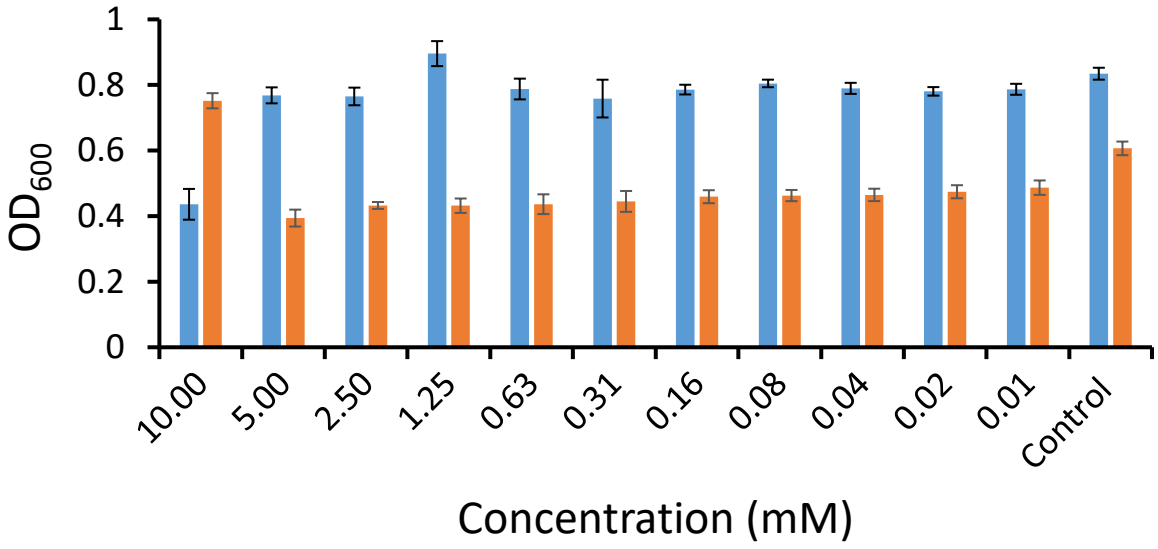

Fig. S92. Optical Density measured at different concentrations for **mon1** against MRSA (orange) and *E. coli* (blue).

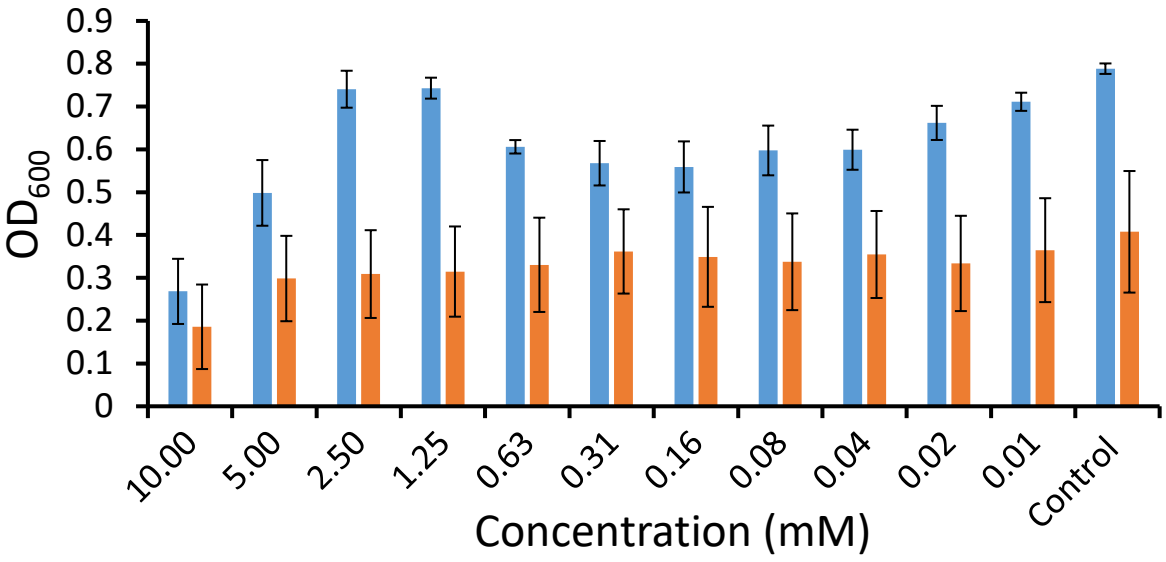

Fig. S93. Optical Density measured at different concentrations for **mon2** against MRSA (orange) and *E. coli* (blue).

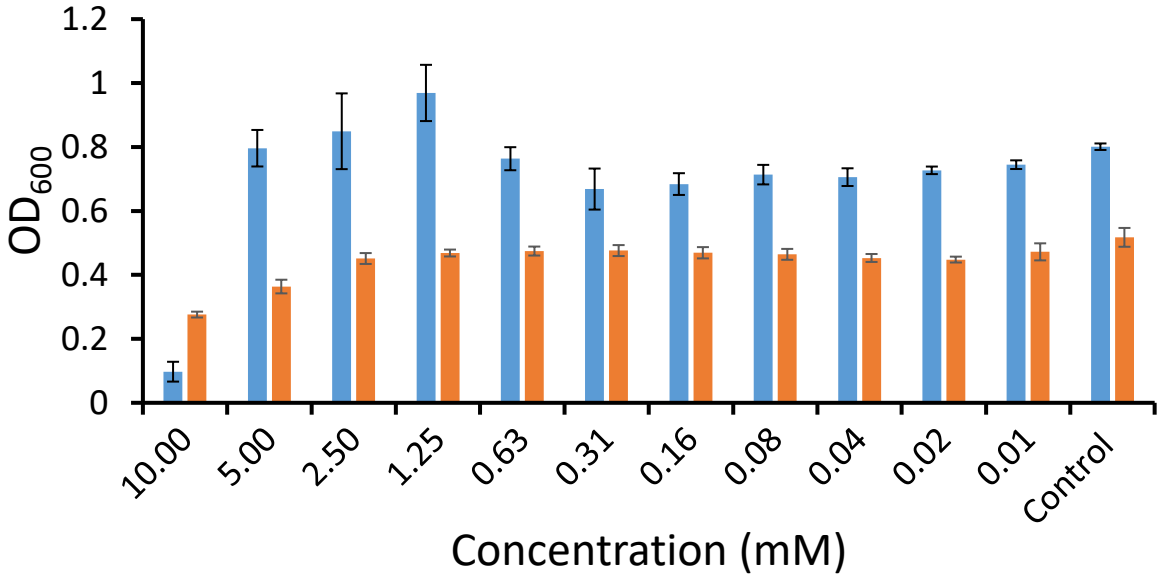

Fig. S94. Optical Density measured at different concentrations for **mon4** against MRSA (orange) and *E. coli* (blue).

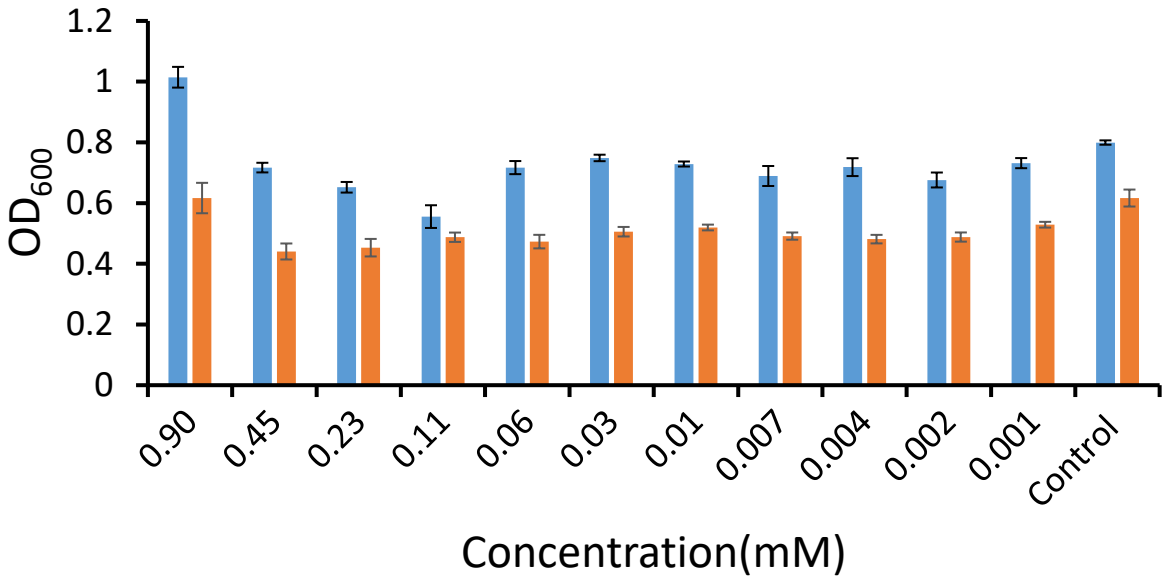

Fig. S95. Optical Density measured at different concentrations for **poly1** against MRSA (orange) and *E. coli* (blue).

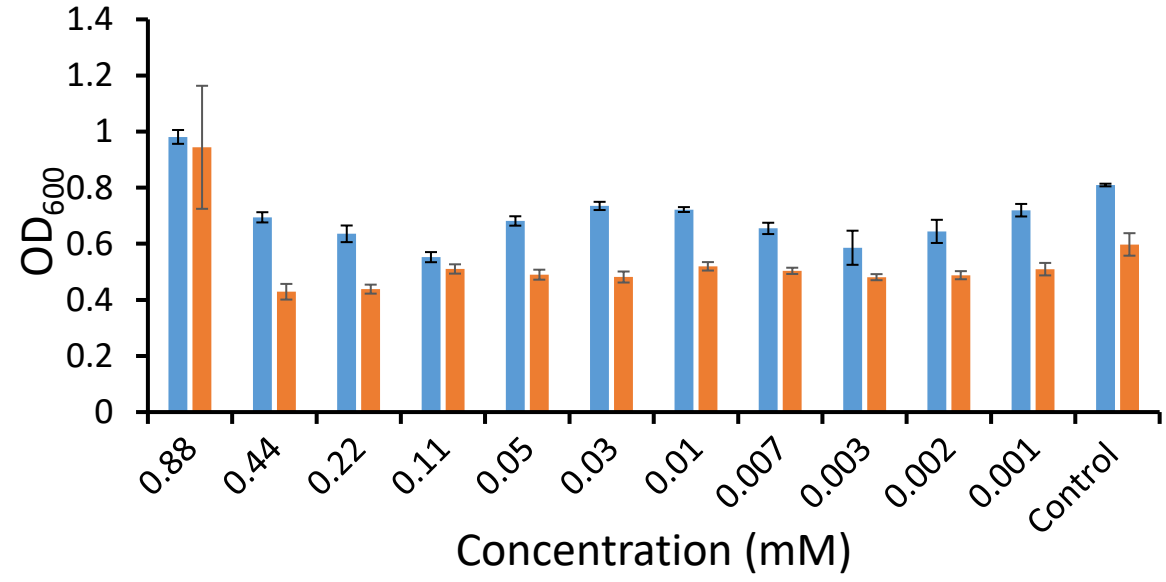

Fig. S96. Optical Density measured at different concentrations for **poly2** against MRSA (orange) and *E. coli* (blue).

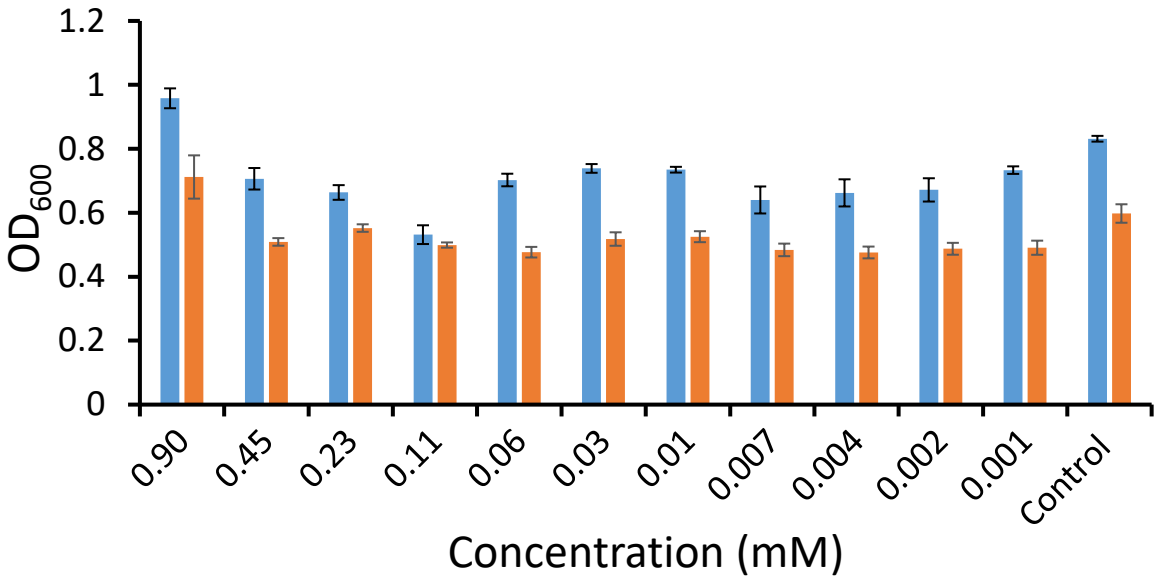

Fig. S97. Optical Density measured at different concentrations for **poly3** against MRSA (orange) and *E. coli* (blue).

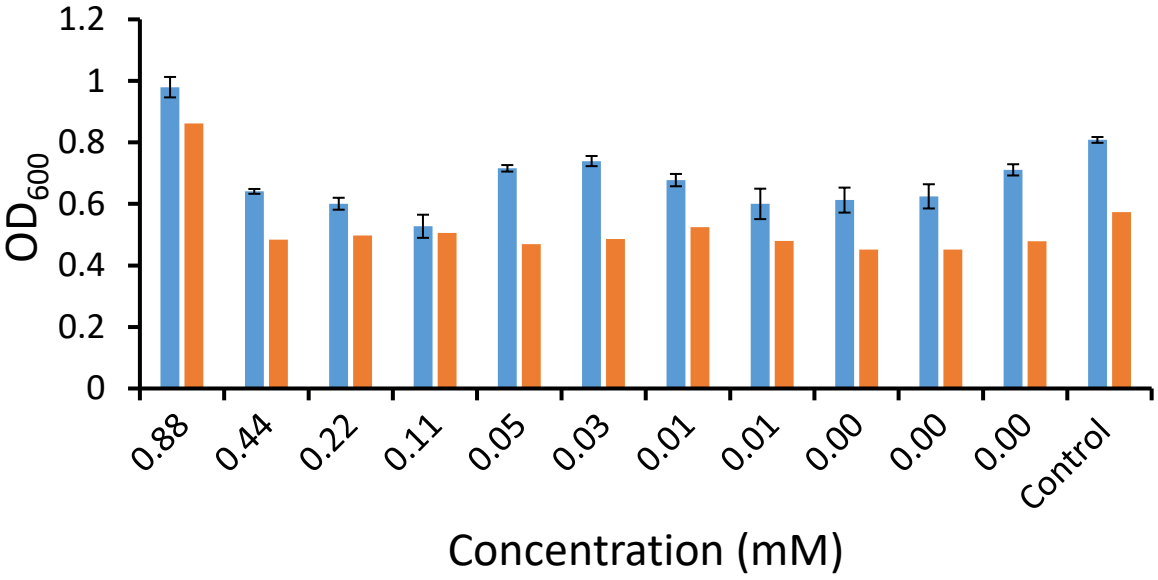

Fig. S98. Optical Density measured at different concentrations for **poly4** against MRSA (orange) and *E. coli* (blue).

11. Single crystal X-Ray diffraction of mon1 and mon2

Table S3. Single crystal X-Ray values obtained for **mon1** and **mon2**.

Compound	mon1	mon2
Empirical formula	$C_{24}H_{23}N_4O_6F_3S$	$C_{24}H_{23}F_3N_4O_5S_2$
Formula weight	552.52	568.58
Temperature/K	99.99(11)	100.00(12)
Crystal system	monoclinic	monoclinic
Space group	$P2_1/c$	C2/c
a/Å	23.527(3)	40.110(14)
b/Å	5.5052(6)	7.8300(15)
c/Å	20.755(3)	15.943(4)
α/°	90	90
β/°	114.673(16)	98.50(3)
γ/°	90	90
Volume/Å^3	2442.7(6)	4952(2)
Z	4	8
ρ_{calc}g/cm^3	1.502	1.525
μ/mm^{-1}	1.826	2.555
F(000)	1144.0	2352.0
Crystal size/mm^3	0.159 × 0.065 × 0.042	0.13 × 0.079 × 0.01
Radiation	Cu Kα (λ = 1.54184)	Cu Kα (λ = 1.54184)
2Θ range for data collection/°	8.272 to 142.346	8.916 to 133.192
Index ranges	-28 ≤ h ≤ 28, -6 ≤ k ≤ 6, -25 ≤ l ≤ 22	-47 ≤ h ≤ 47, -9 ≤ k ≤ 8, -18 ≤ l ≤ 18
Reflections collected	11709	17086
Independent reflections	4657 [R_{int} = 0.1170, R_{sigma} = 0.1415]	4378 [R_{int} = 0.3577, R_{sigma} = 0.2217]
Data/restraints/parameters	4657/55/275	4378/0/343
Goodness-of-fit on F^2	1.002	1.055
Final R indexes [I>=2σ (I)]	R_1 = 0.0995, wR_2 = 0.2473	R_1 = 0.1771, wR_2 = 0.4022
Final R indexes [all data]	R_1 = 0.1522, wR_2 = 0.2930	R_1 = 0.2798, wR_2 = 0.5056
Largest diff. peak/hole / e Å^{-3}	0.81/-0.61	0.52/-0.83

12. Solubility studies of poly1 – poly4

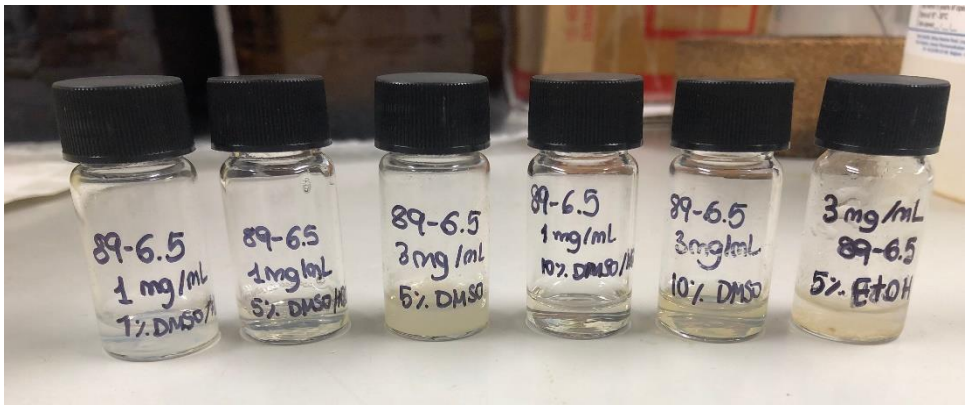

Fig. S99. Solubility studies of **poly1** at different concentrations (1 mg/mL and 3 mg/mL) and different percentages of DMSO in water (1 %, 5 % and 10 %) and in 5 % MeOH in water at a concentration of 3 mg/mL.

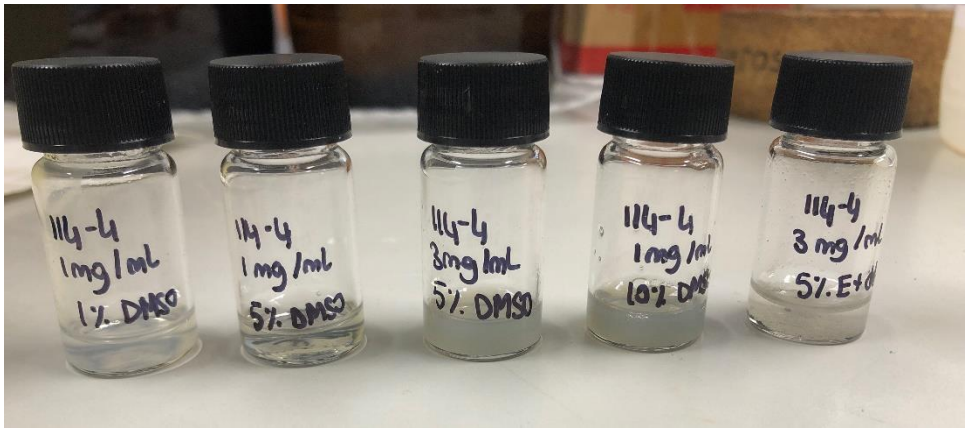

Fig. S100. Solubility studies of **poly2** at different concentrations (1 mg/mL and 3 mg/mL) and different percentages of DMSO in water (1 %, 5 % and 10 %) and in 5 % MeOH in water at a concentration of 3 mg/mL.

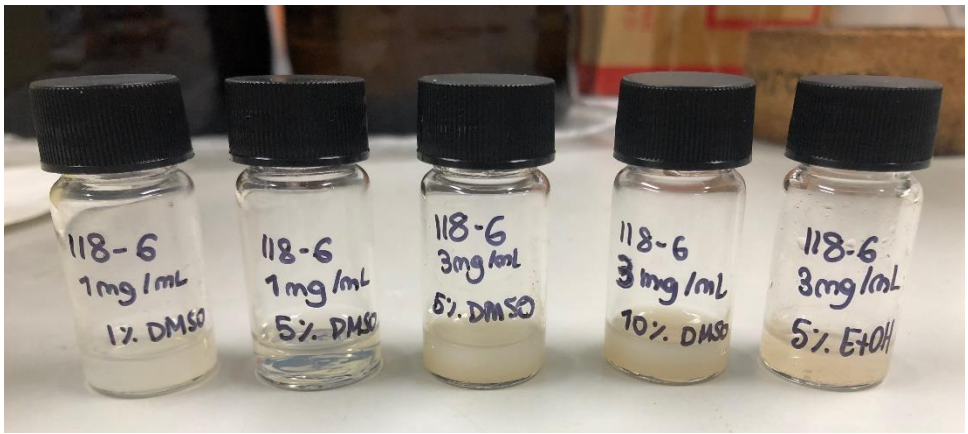

Fig. S101. Solubility studies of **poly3** at different concentrations (1 mg/mL and 3 mg/mL) and different percentages of DMSO in water (1 %, 5 % and 10 %) and in 5 % MeOH in water at a concentration of 3 mg/mL.

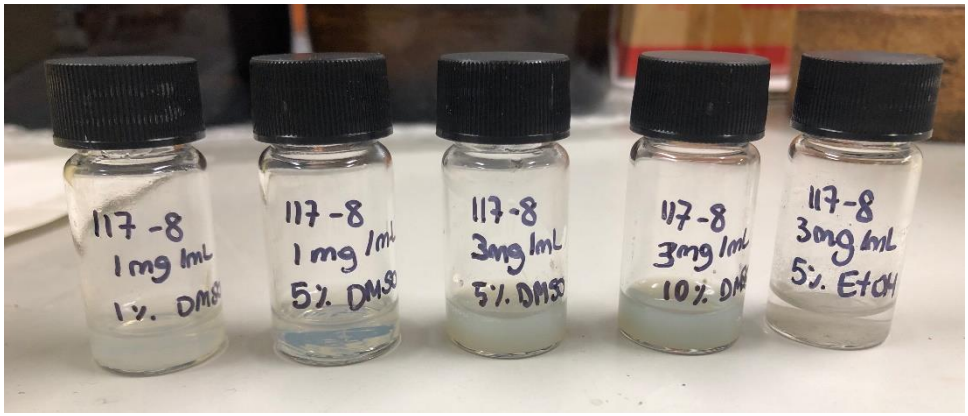

Fig. S102. Solubility studies of **poly4** at different concentrations (1 mg/mL and 3 mg/mL) and different percentages of DMSO in water (1 %, 5 % and 10 %) and in 5 % MeOH in water at a concentration of 3 mg/mL.